The Abdus Salam International Centre for Theoretical Physics

United Nations Educational, Scientific and Cultural Organization

IAEA International Atomic Energy Agency

2064-7

Joint ICTP/IAEA Advanced School on in-situ X-ray Fluorescence and Gamma Ray Spectrometry

26 - 30 October 2009

Portable XRF instrumentaton (including excitation sources, detectors, electronics, software)

R. Cesareo

Universita'degli Studi di Sassari
Italy

ROBERTO CESAREO
Universita´ di Sassari, ITALIA

ENERGY–DISPERSIVE X-RAY FLUORESCENCE : PHYSICAL BACKGROUND

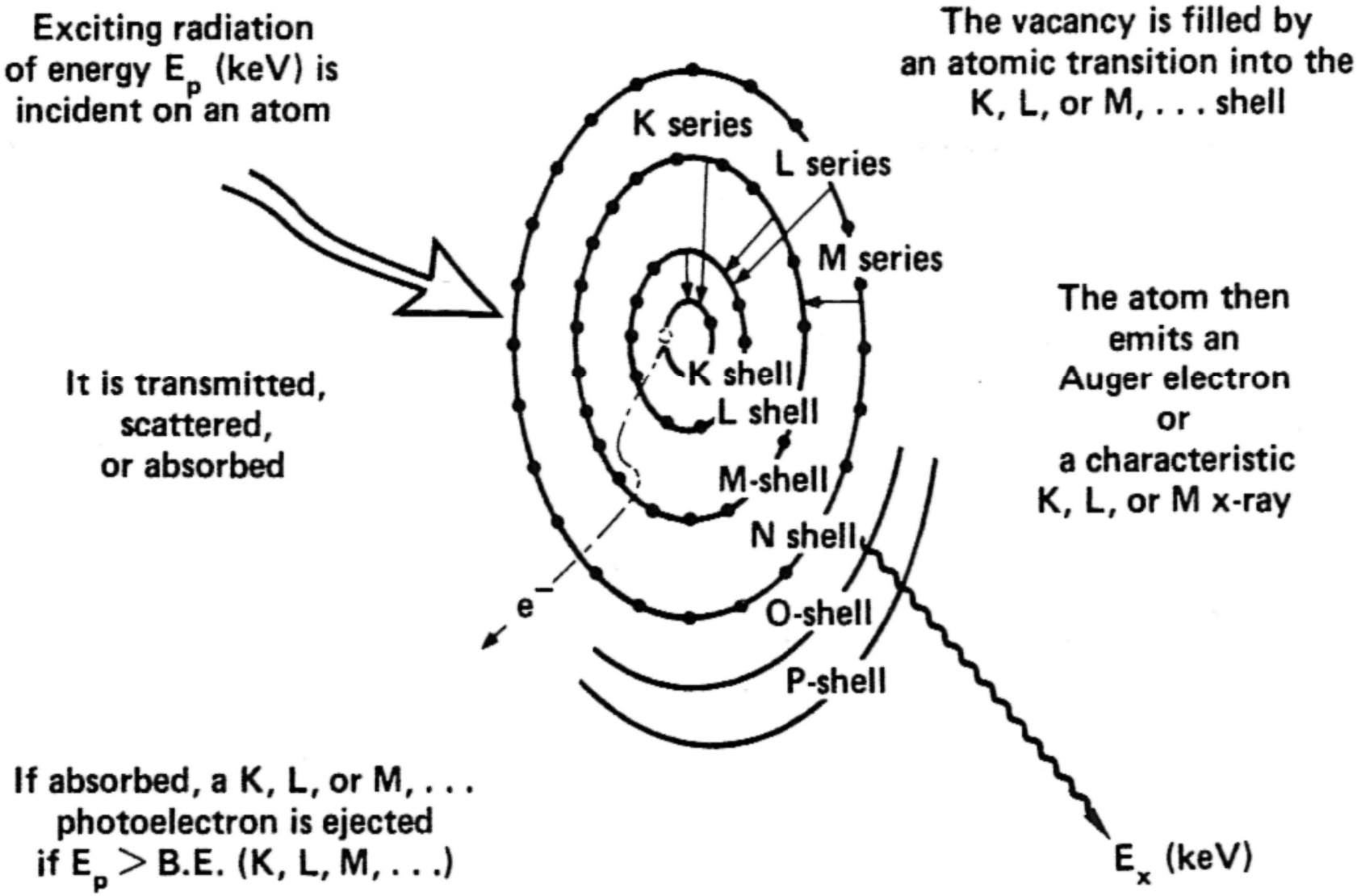
Exciting radiation of energy E_p (keV) is incident on an atom
The vacancy is filled by an atomic transition into the K, L, or M, . . . shell
K series
L series
M series
K shell
L shell
M-shell
N shell
O-shell
P-shell
It is transmitted, scattered, or absorbed
The atom then emits an Auger electron or a characteristic K, L, or M x-ray
e^-
If absorbed, a K, L, or M, . . . photoelectron is ejected if $E_p >$ B.E. (K, L, M, . . .)
E_x (keV)

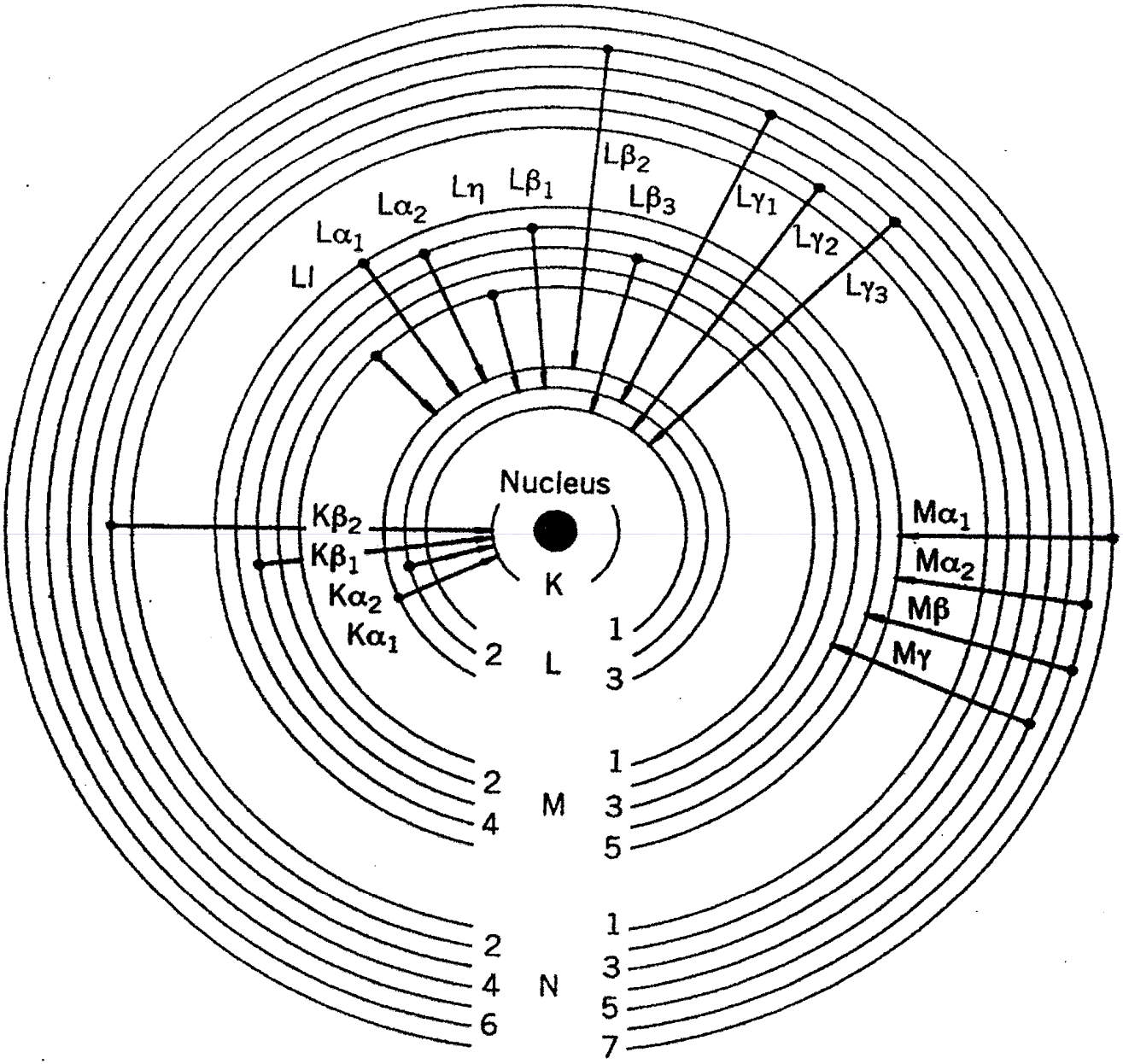
Nucleus
K
L
M
N
Kβ2
Kβ1
Kα2
Kα1
Ll
Lα1
Lα2
Lη
Lβ1
Lβ2
Lβ3
Lγ1
Lγ2
Lγ3
Mα1
Mα2
Mβ
Mγ
1
2
3
1
2
3
4
5
1
2
3
4
5
6
7

PRINCIPALI RAGGI X

ELEMENTO	Kα	Kβ	Lα	Lβ	Lγ
SODIO	1.04				
MAGNESIO	1.25				
ALLUMINIO	1.49				
SILICIO	1.74				
FOSFORO	2.01				
ZOLFO	2.31				
CLORO	2.62	2.81			
ARGON	2.96	3.2			
POTASSIO	3.31	3.6			
CALCIO	3.69	4.0			
TITANIO	4.51	4.93			
CROMO	5.41	5.95			
MANGANESE	5.90	6.5			
FERRO	6.40	7.06			
COBALTO	6.93	7.65			
NICHEL	7.48	8.26			
RAME	8.05	8.9			
ZINCO	8.64	9.6			
ARSENICO	10.54	11.7			
SELENIO	11.22	12.5			
BROMO	11.92	13.3			
RUBIDIO	13.39	15.0	1.7		
STRONZIO	14.16	15.8	1.8		
ITTRIO	14.96	16.7	1.92		
ZIRCONIO	15.77	17.7	2.04		
NIOBIO	16.61	18.6	2.16		
MOLIBDENO	17.5	19.6	2.3	2.5	
ARGENTO	22.2	24.9	2.98	3.2	
CADMIO	23.2	26.1	3.13	3.45	
STAGNO	25.3	28.5	3.4	3.8	
ANTIMONIO	26.4	29.7	3.6	4.0	
BARIO	32.2	36.4	4.45	5.0	
TUNGSTENO	59.3	67.2	8.4	9.9	
ORO	68.8	78.0	9.7	11.5	
MERCURIO	70.8	80.3	9.95	11.9	
PIOMBO	75	84.9	10.5	12.6	
URANIO	98.4	111.3	13.5	17.5	

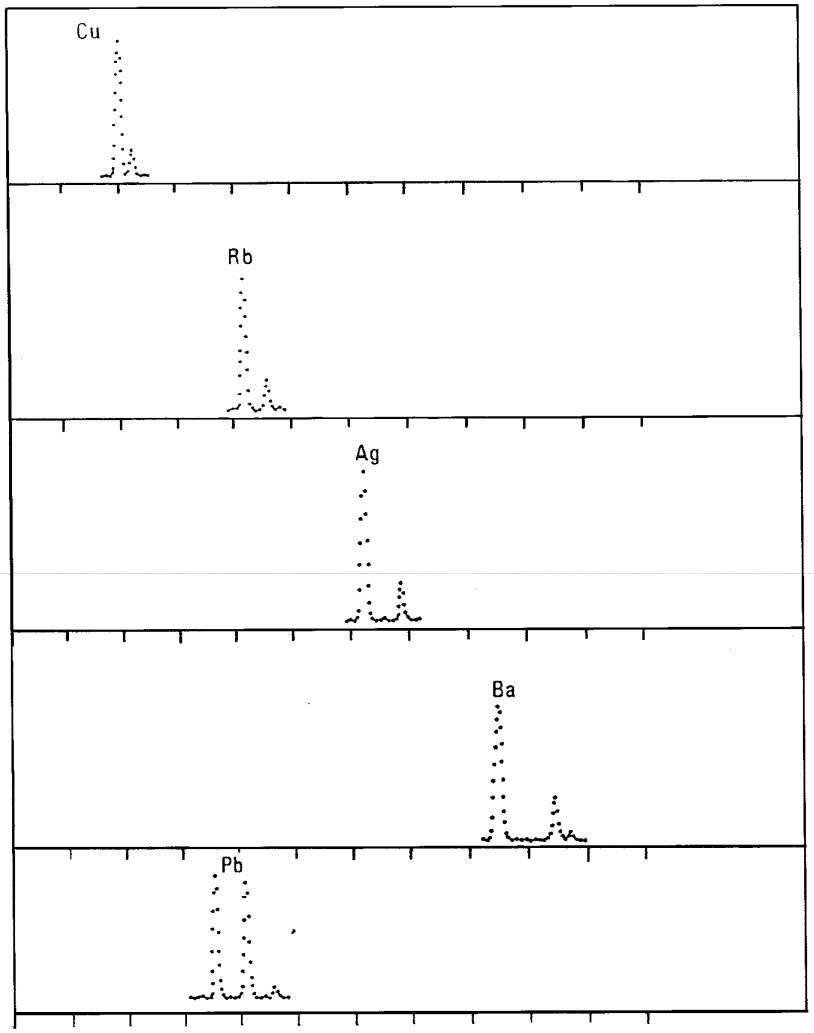

Fig. **2**.4. – X-ray fluorescence spectra of some typical pure elements collected with a HpG semiconductor detector. From the top X_K-rays of Cu (8.04 and 8.94 keV), Rb (13.36 an 15.1 keV), Ag (22.1 and 25.2 keV) and Ba (32.0 and 36.8 keV), and X_L-rays of Pb (10.5 an 12.615 keV).

THE INTERNAL RATIO OF THE X-LINES IS GENERALLY FIXED:

FOR EXAMPLE THE RATIO Kalfa TO Kbeta OF COPPER IS 6.4

THE RATIO Lalfa TO Lbeta OF LEAD IS 1.

HOWEVER THIS RATIO MAY CHANGE IF THE LINES ARE DIFFERENTLY ABSORBED

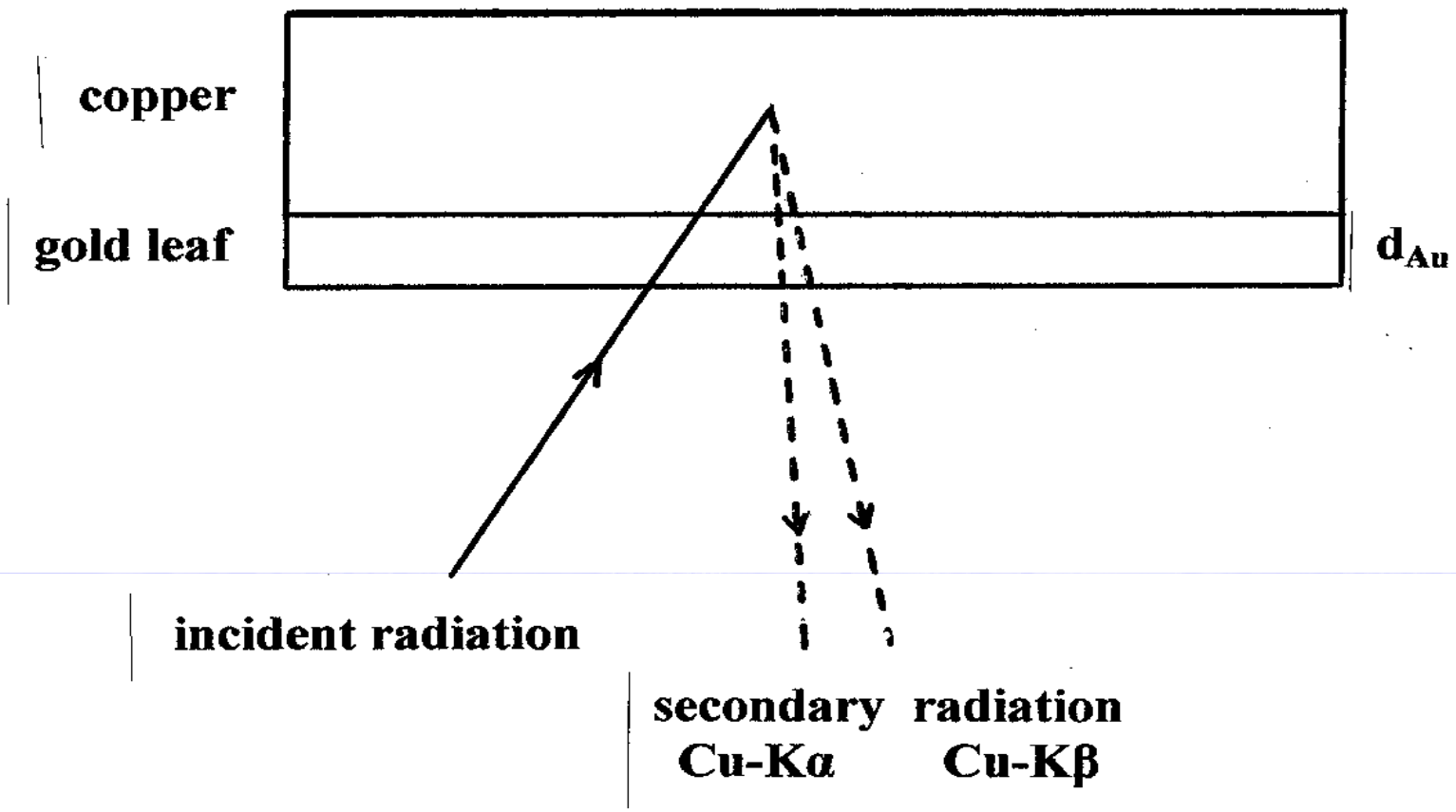
copper
gold leaf
d_{Au}
incident radiation
secondary radiation
Cu-Kα
Cu-Kβ

When a sample containing an element a with a concentration $\mathbf{c_a}$ i Is irradiated by a beam of X-rays having an energy $\mathbf{E_0}$ and intensity of $\mathbf{N_0}$ photons/s, the number N_a of fluorescent X-rays emitted by the element a , is approximately given by:

$$\mathbf{N_a = N_0\ k\ \omega_a\ J_a\ \sigma_a\ c_a\ M}$$

where:

-**k** is an overall geometrical factor;

-$\boldsymbol{\omega_a}$ is the fluorescent yield of the element a in the shell of interest (i.e. percent probability of a fluorescence effect compared with an Auger effect));

-$\boldsymbol{\sigma_a}$ (cross section in cm^2) is related to the probability for fluorescent effect of element a ;

-$\mathbf{J_a}$ is the branching ratio, i.e. the intensity of the X-line of interest -over the total X-ray intensity;

-**M** is a matrix term (i.e. depending on the sample) , related to the attenuation of incident and secondary fluorescent radiation and on the sample composition.

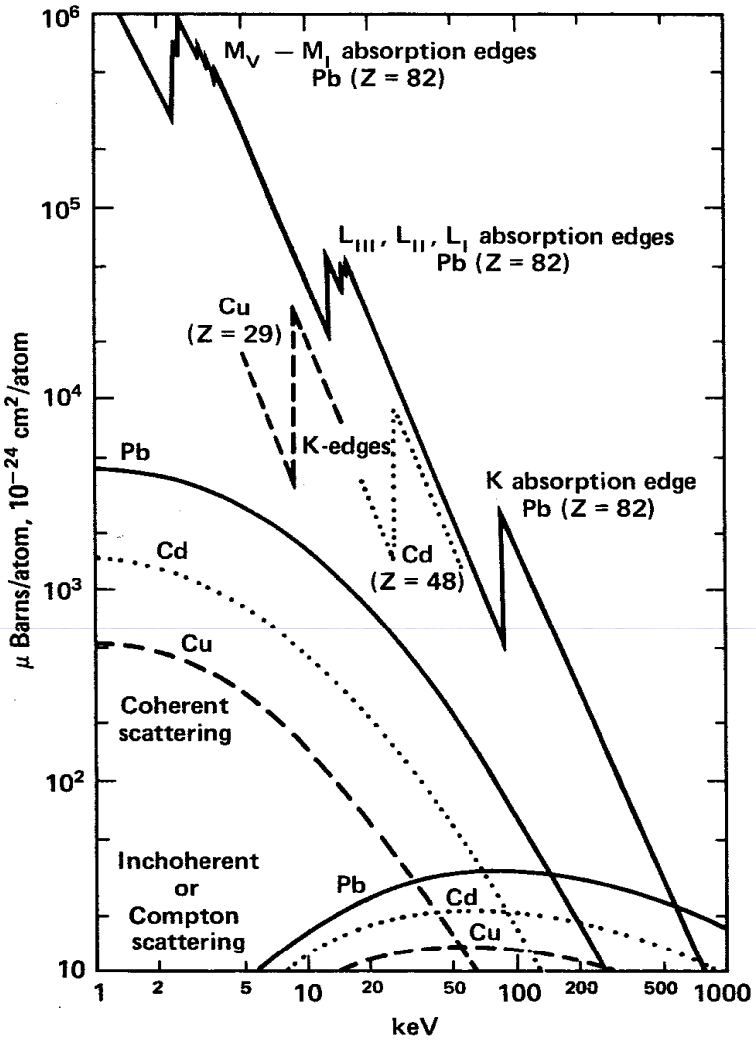

FIGURE 4. The atomic absorption and scattering cross-sections in barns (10^{-24}cm^2) per atom as a function of energy for lead (Z = 82), cadmium (Z = 48), and copper (Z = 29). The L-absorption edge positions for copper and cadmium are not shown. Barns/atom can be converted into cm^2/g via the multiplicative constants of 2.91×10^{-3} for cadmium, and 9.48×10^{-3} for copper.

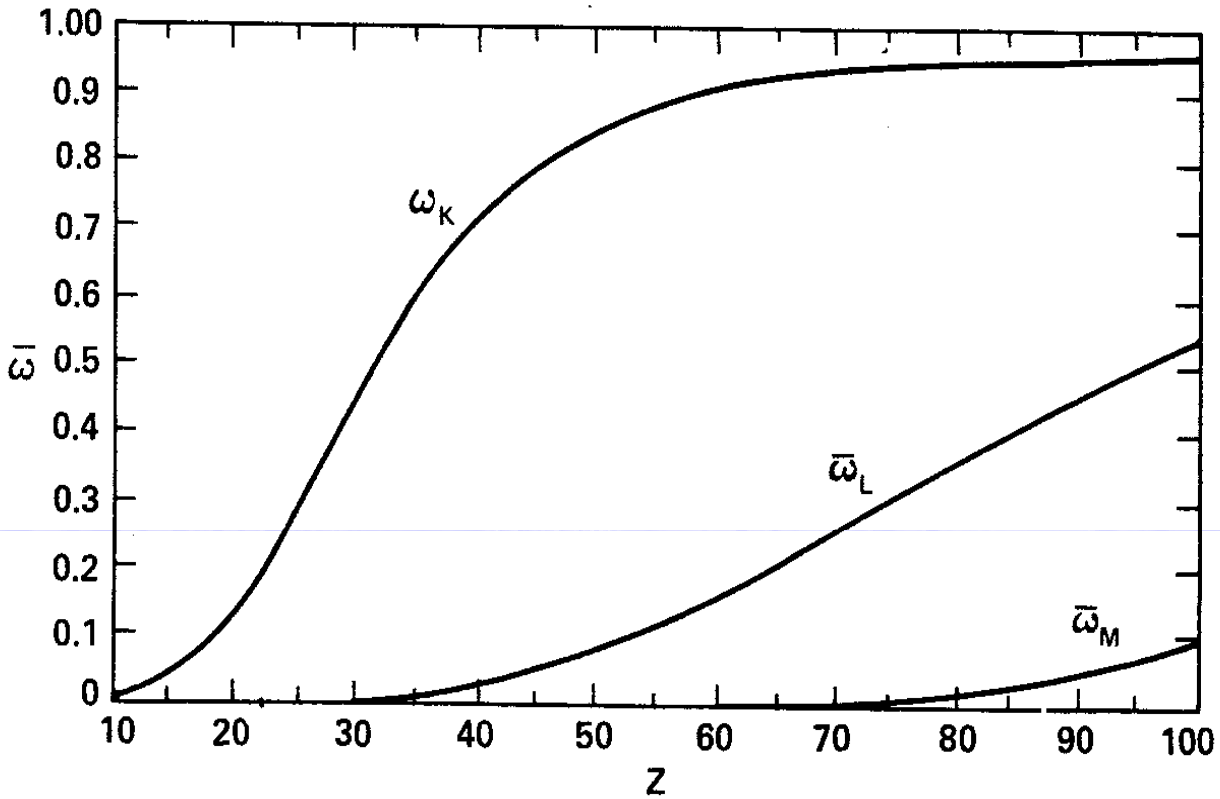

FIGURE 3. Fluorescence yields as a function of atomic number. Only mean yields can be given for the L and M shells. Exact yields depend on how the initial electron vacancy distribution is formed and filled.

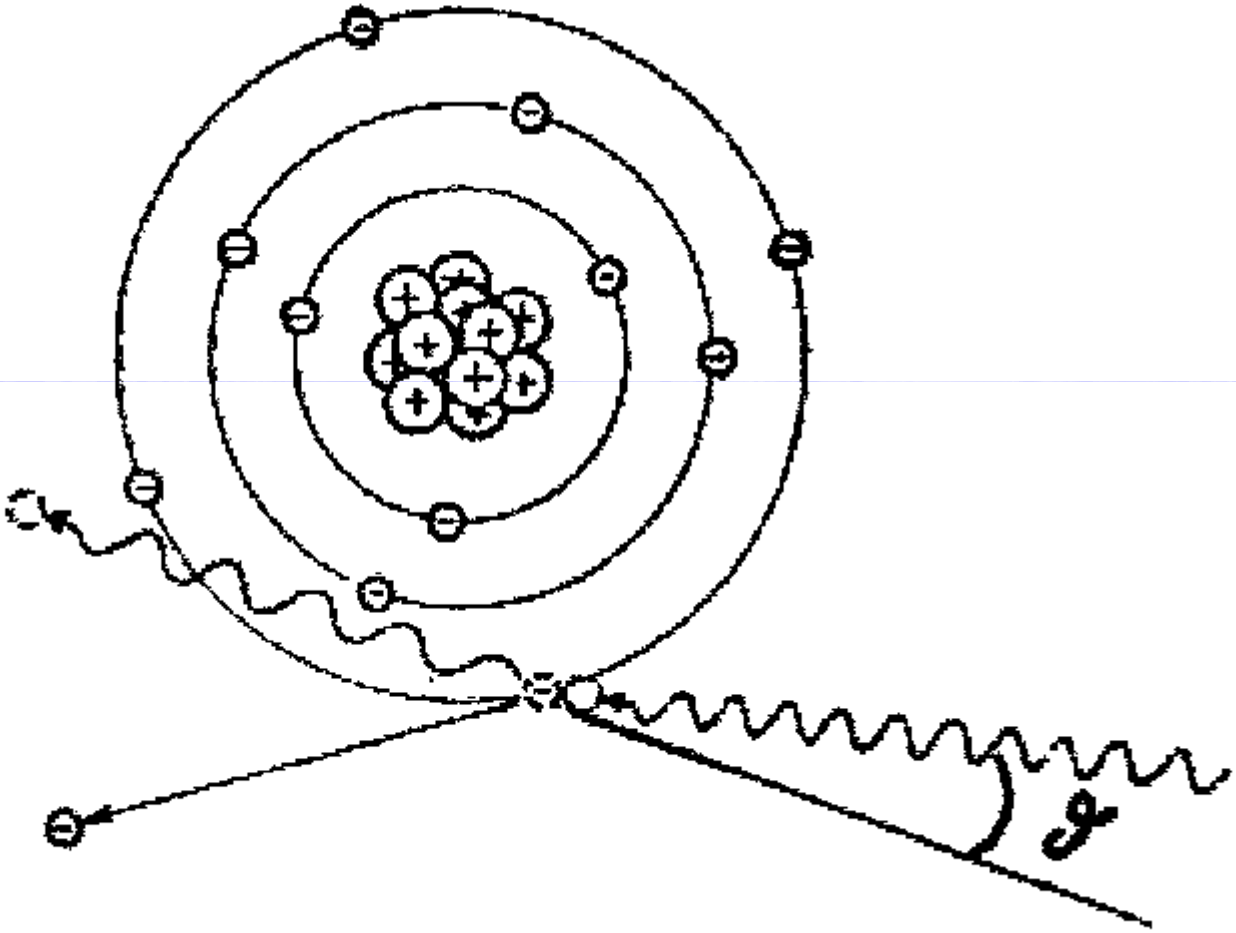
γ

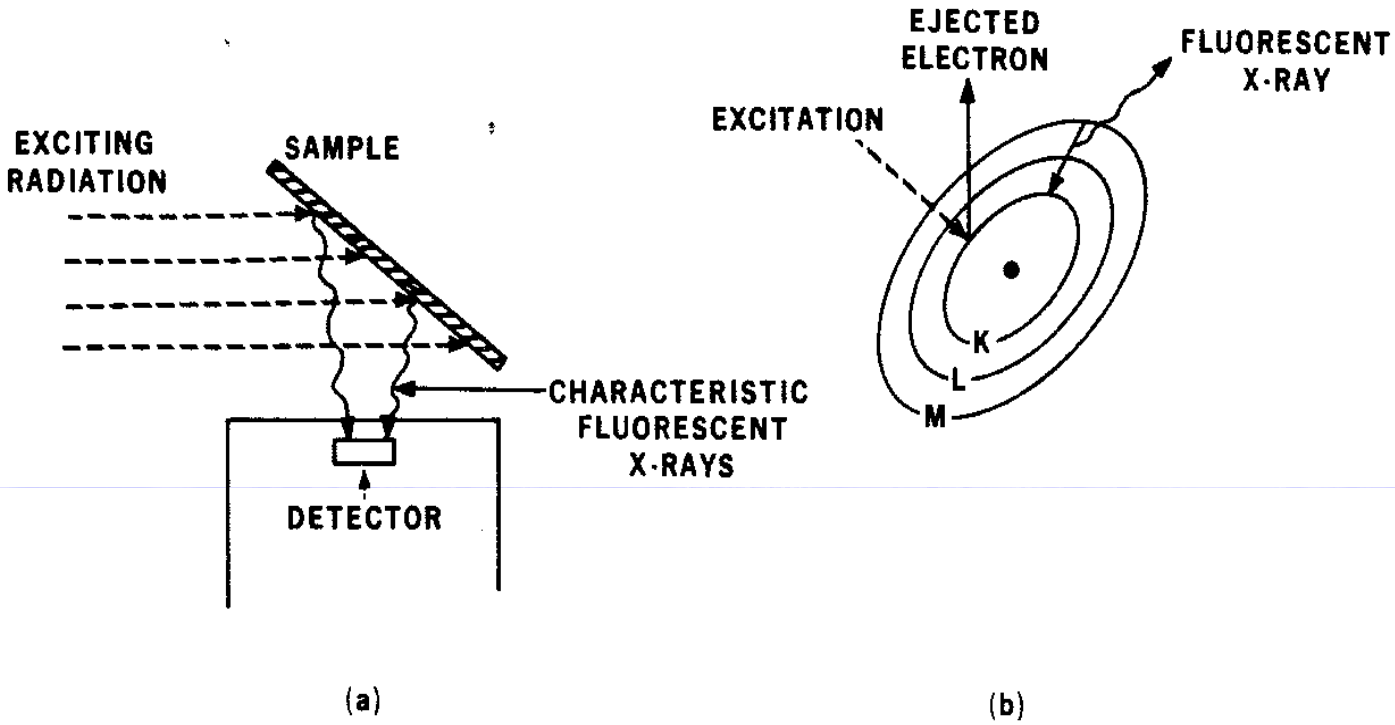

FIGURE 1. Schematic diagram of the energy dispersive X-ray fluorescence method. Figure 1a shows geometry of excitation, sample, and detector; Figure 1b illustrates a simplified picture of the fluorescence process.

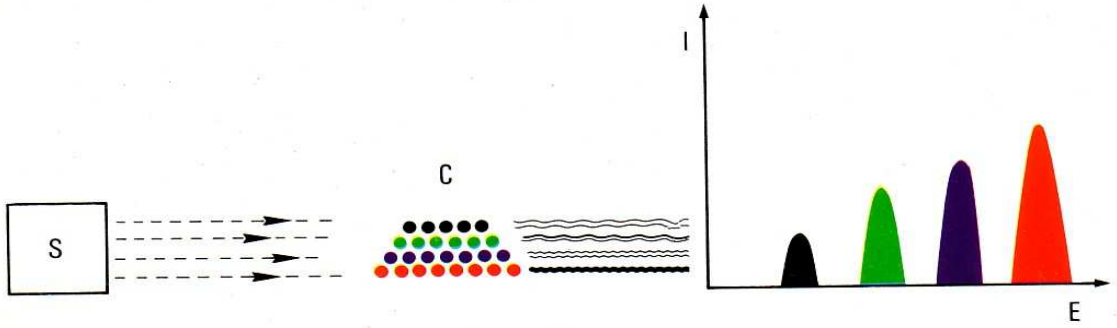

Fig. 1 – Schema di principio di un sistema di analisi basato su tecniche nucleari. Esso comprende: una sorgente S di radiazioni o di particelle cariche o di neutroni; un campione, nel quale vi sono per esempio 4 elementi in tracce di concentrazione crescente, indicati schematicamente con 4 diversi colori, il quale, investito dalla radiazione emessa dalla sorgente, emette a sua volta radiazioni caratteristiche; un rivelatore delle radiazioni emesse dai 4 elementi, caratterizzate, sulla Figura, con 4 righe di colore corrispondente a quello degli elementi, le quali consentono la valutazione qualitativa e quantitativa degli stessi

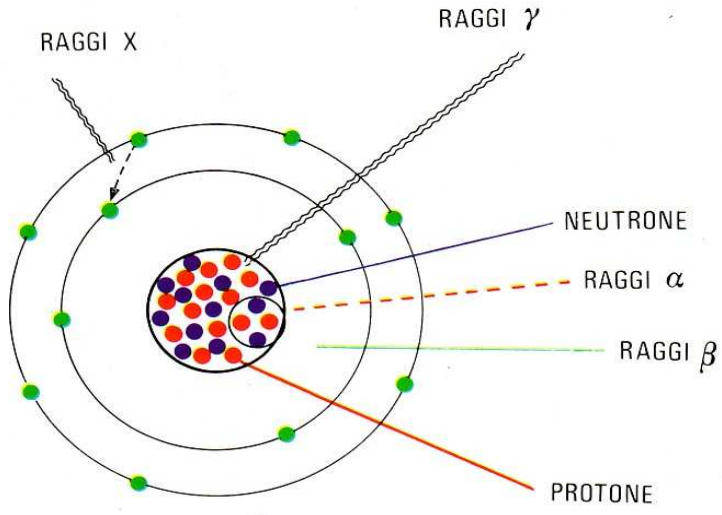

Fig. 2 – Modello dell'atomo e del suo nucleo

In the case of thin samples, primary and secondary X-rays are characterized by a penetration depth much larger than the sample thickness. In this case the matrix term of previous Eq. is approximately equal to 1, and following Eq. is valid:

$$N_a = N_0\, k\, \omega_a\, J_a\, \sigma_a\, c_a$$

i.e. counts of element a are linearly proportional to its concentration .

Intensity N_{sc} of scattered photons in the case of thin samples (mainly due to Compton scattering) is approximately given by:

$$N_{sc} \approx N_0\, k\, \mu_{sc}(E_0)\, m$$

where m (in g/cm^2) is the mass per unit area of the sample.

Artifacts like statues, columns, alloys and etc., generally appear to EDXRF analysis as "infinitely thick samples", in the sense that the thickness of the objects is much greater than the "radiation penetration" .

When a generic element a with concentration c_a , in an infinitely thick and homogeneous sample is irradiated with N_0 incident photons, the secondary fluorescent X-ray intensity N_a is given by :

$$N_a = N_o\, k\, \omega_a J_a\, c_a\, [\mu_{ph.a}(E_0) / \mu_t(E_0) + \mu_t(E_a)]$$

where:

$\mu_{ph.a}(E_o)$ represents the photoelectric attenuation coefficient of element a at incident energy E_o ; $\mu_t(E_o)$ and $\mu_t(E_a)$ represent the total attenuation coefficient of the sample at incident and fluorescent energies (E_0 and E_a) respectively .

AN EQUIPMENT FOR EDXRF-ANALYSIS IS, THEREFORE COMPOSED OF :

-A SOURCE OF X-RAYS, OR GAMMA RAYS

-A X-RAY DETECTOR

-AN ELECTRONIC CIRCUIT

-A PULSE HEIGHT ANALYZER (MULTI-CHANNEL ANALYZER

SOURCES OF EXCITATION :

-RADIOACTIVE SOURCES

-MINI-X RAY TUBES

-SYNCHROTRON RADIATION

THE IDEAL SOURCE SHOULD BE :

-MONOENERGETIC WITH AN ENERGY CLOSE (BUT NOT TOO MUCH TO THE PHOTOELECTRIC DISCONTINUITY OF THE ELEMENT UNDER STUDY;

-OF ADEQUATE INTENSITY

Table 8 – Radioactive sources for portable EDXRF equipments [44]

Source	Principal photon energies (keV)	Intensity (ph/s sr mCi)	Half-life	Elements that can be analyzed
Fe-55	5.9	2×10^6	2.7 y	$Z < 23$ (K-lines)
Cd-109	22 , 88	8×10^6	453 d	$Z < 42$ (K-lines) $Z = 50\text{-}92$ (L-lines)
Am-241	59.5	3×10^6	433 y	$Z < 69$ (K-lines) $Z = 70\text{-}92$ (L-lines)
Co-57	122	8×10^6	270 d	$Z \approx 50\text{-}92$ (K-lines)

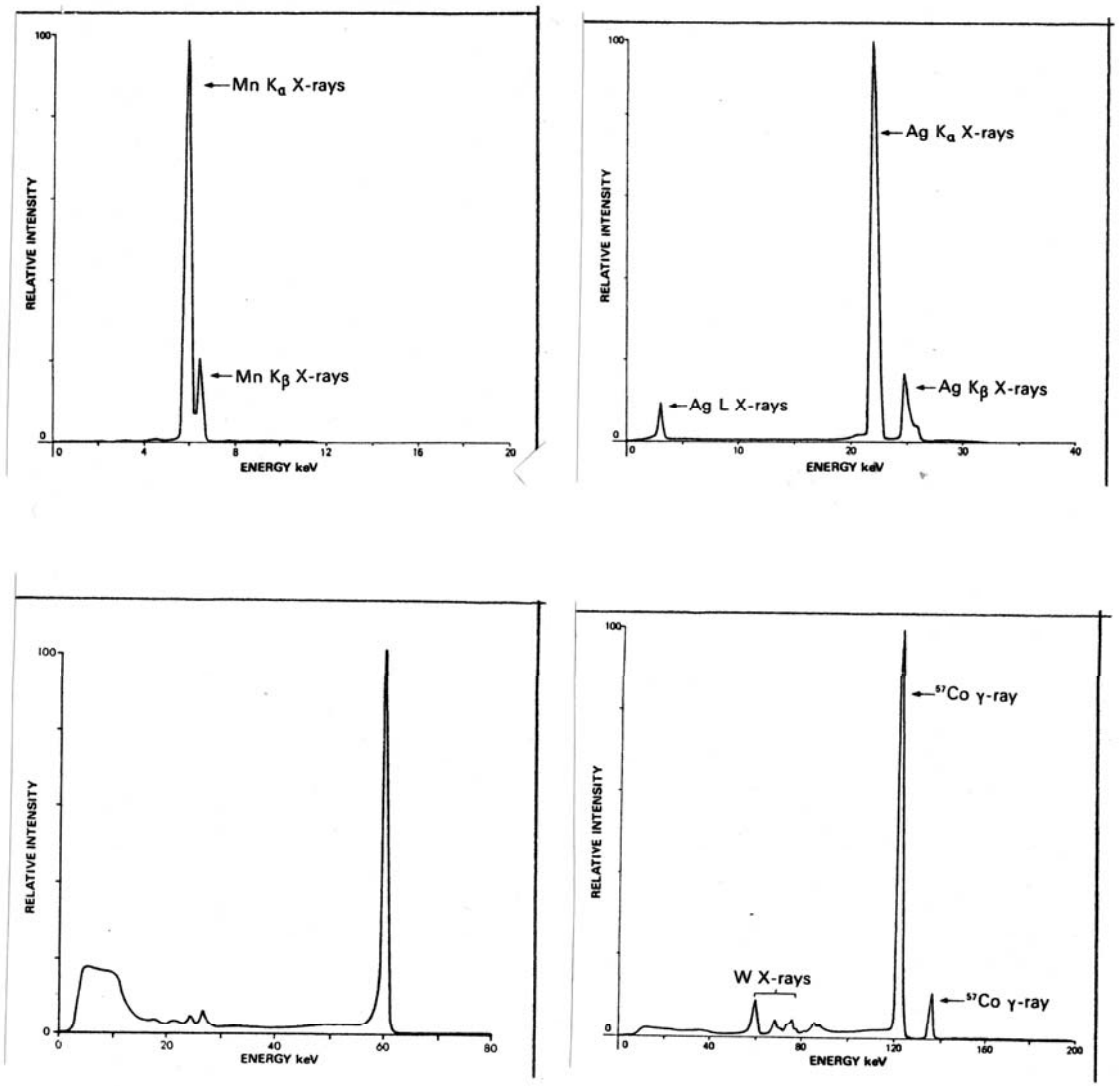

Figure 13 – Size (measures in mm) of typical radioactive sources employed for EDXRF-analysis, and emission spectra of Fe^{55}, Cd^{109}, Am^{241} and Co^{57}.

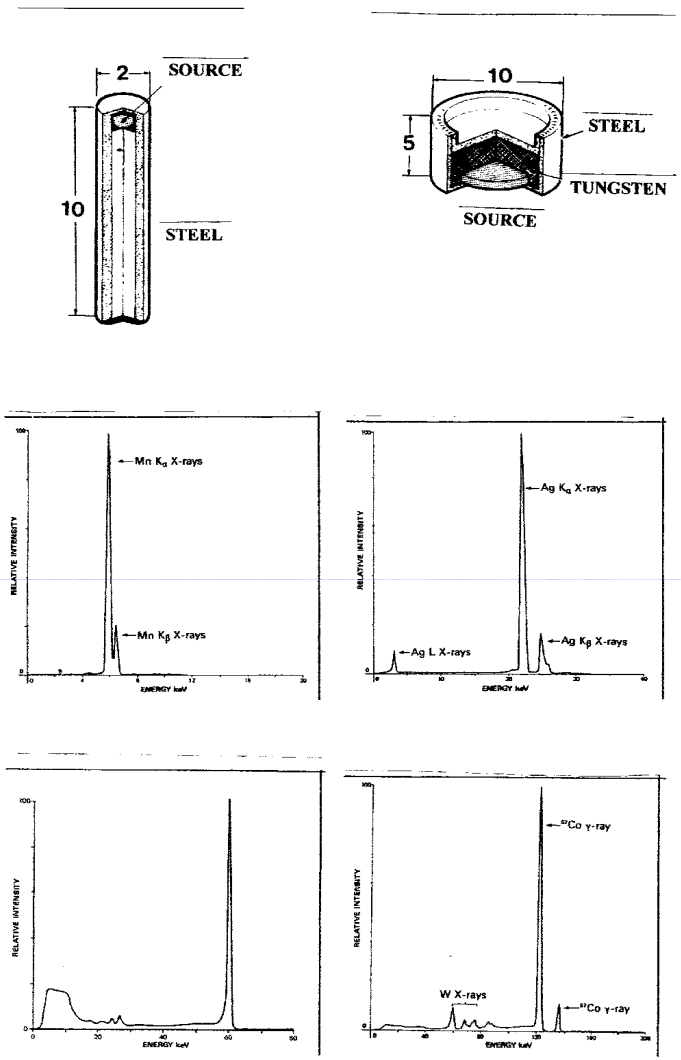

Figure 13 – Size (measures in mm) of typical radioactive sources employed for EDXRF-analysis, and emission spectra of Fe^{55}, Cd^{109}, Am^{241} and Co^{57}.

X-RAY TUBES

-ARE EMITTING RADIATION ONLY WHEN NEEDED

-ARE EMITTING BREMSSTRAHLUNG (NON MONO-ENERGETIC RADIATION)

-ARE EMITTING RADIATION OF ADEQUATE INTENSITY

-ARE OF SMALL SIZE

-MAY BE DEDICATED

-X-RAY TUBES ARE AVAILABLE OF ANY HIGH VOLTAGE, INTENSITY AND ANODE

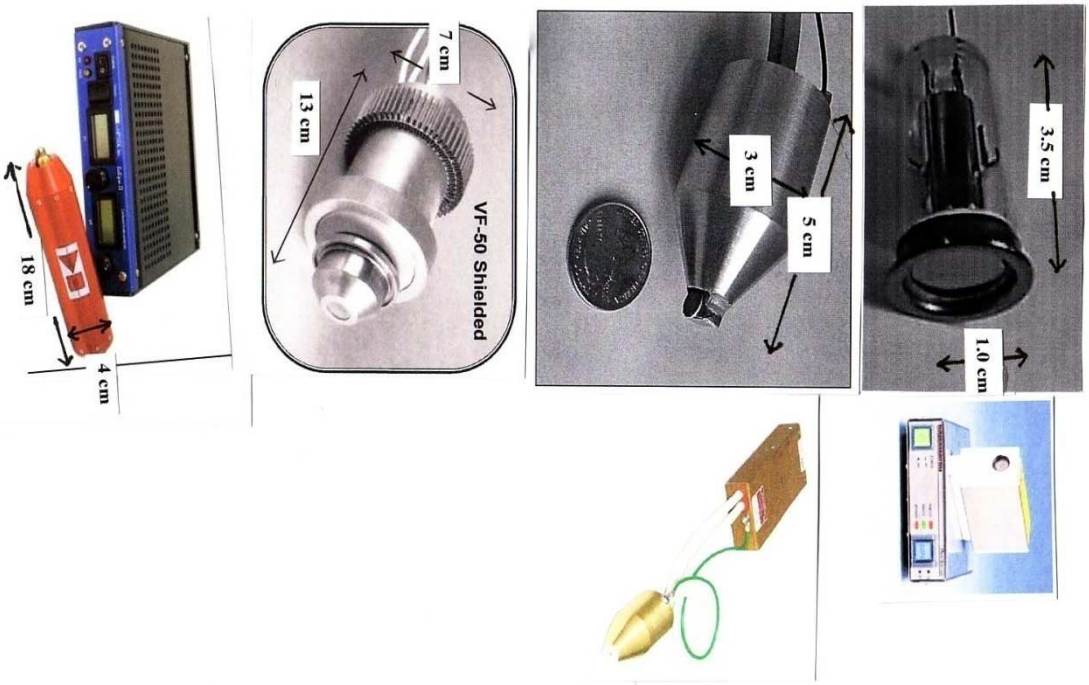

Figure 14 – Small-size X-ray tubes for EDXRF-analysis and related X-ray spectra; From top a Hamamatsu L9490 X-ray tube (W-anode, 9.5 kV and 0.18 mA maximum voltage and current; 350 g), www.hamamatsu.com; a Moxtek X-ray tube (Pd-or Ag anode in transmission or side-window, 35 kV and 0.1 mA maximum voltage and current; 450 g), www.moxtek.com ; a Varian VF-50 X-ray tube (Rh, Pd, W, Ti, Mo-anode, 50 kV and 1 mA maximum voltage and current; 500 g), www.varian.com and a Eclipse II X-ray tube by Oxford-AMPTEK (Ag-anode in transmission mode, 30 kV and 0.1 mA maximum voltage and current; 300 g), www.amptek.com .

X-RAY Sources

50kV MAGNUM®
X-ray Tubes

NEW!

The MAGNUM® x-ray tube is now available in a 50kV package. The MAGNUM 50kV x-ray tube is a low power, miniature x-ray tube used for a variety of applications including handheld and benchtop instrumentation. MAGNUM x-ray tubes are small, lightweight, and can be packaged into custom enclosures.

Features	Benefits
Small, compact design	Close coupling of source to detector
Lightweight	Portable, versatile
Close coupling of collimator & target	Efficient utilization of x-rays
Stable output	Low detection limit
Low power consumption	Long battery life
Low spectral contamination	No unwanted peaks
High x-ray output	Short sampling time
Customizable configurations	Flexible form factor

Applications

Portable XRF
- RoHS/WEEE
- Alloy sorting
- Soil analysis
- Environmental
- Lead in paint
- Plastics analysis
- Material ID
- Security

Handheld Imaging
- Medical/Dental
- Material ID
- Security

Bench top EDXRF

Instrument Calibration

Micro-Fluorescence

Micro-Diffraction

Standard Package Includes:
- Transmission Target (End Window)
- MAGNUM tube potted in a brass shield
- High voltage power supply
- High voltage wire length is 11.5 inches

Customizable Options:
- Target materials and thickness
- Tube shield design
- Power supply packaging
- High voltage wiring length
- Integrated tube and power supply

MOXTEK®
452 West 1260 North
Orem, UT 84057
P 801.225.0930
F 801.221.1121
www.moxtek.com

VARIAN medical systems | X-RAY PRODUCTS

VF-50J
Industrial X-Ray Tube

APPLICATION

The VF-50 series x-ray tube is a beryllium window x-ray tube designed for use as a radiation source for x-ray fluorescence systems.

CONSTRUCTION

The beryllium x-ray window is located at the end of the tube and the beam is projected along the longitudinal axis of the tube. The cathode operates at ground potential and the envelope is ceramic with the high voltage section potted to increase the high voltage stand off.

Specification

Envelope	Ceramic
Be Window	.003" (.076 mm) Thick
Anode	Copper body with the target material attached
Standard Target Materials	Rhodium, Palladium, Tungsten, Titanium, Moly, Copper, Silver, Chrome
Target Angle	90° from the central ray
Focal Spot	1 mm x 1 mm square
Maximum Anode Dissipation with 10 cfm forced air cooling	50 Watts Titanium - 20 Watts Chrome - 40 Watts
Filament Characteristics	3.3 Amps and 2.5 Volts maximum
Maximum Anode Potential	50 kVp Maximum D.C. (Titanium - 20 kV)
Maximum Tube Current	Refer to Emission and Rating Chart
Cooling Method	Forced air convection
Weight	2 lbs (1.2 kg)

6128 Rev E 01/06 Manufactured by Varian Medical Systems Specifications subject to change without notice.

Modern Handheld, Portable XRF Analyzer

Main Features

- ***Ergonomically designed, ideal form factor***
- ***Silicon "p-i-n" detector, < 200 eV***
- ***40 kV, 50 uA transmission anode***
  low power x-ray source
- *Lightweight*
  - 3 lbs (1.36 kg)
- ***Long, 12+ hours battery use***
- ***Large touch screen LC display***
  - 2.25" x 3" (57 mm x 76 mm)
- ***4096 channels MCA***
- ***optimized for speed ASIC based DSP***
- ***Integrated touch screen***
- ***Integrated bar code scanner***
- ***Integrated wireless communication link***
- ***Fastest FP***
- ***FP not sensitive to shape and surface irregularities***
- ***No transport restrictions***

EDXRF-equipment at work in the Museum of Sipan

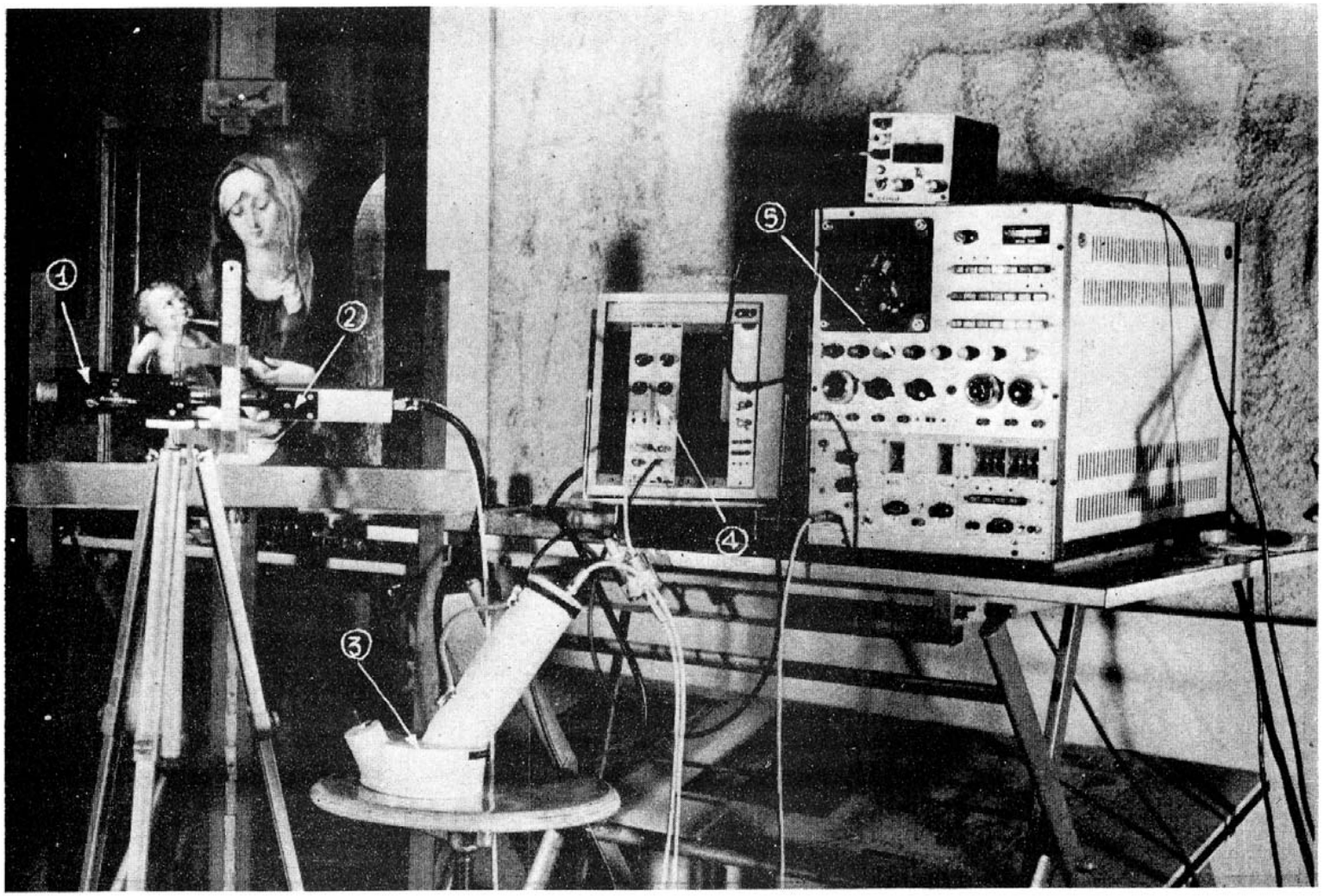

Plate 1 *Experimental layout.* (1) *measuring head* (*gas counter*), (2) *preamplifier*, (3) *measuring head* (*NaI*(*Tl*) *counter*), (4) *amplifier*, (5) *pulse height analyser.*

X-RAY TUBES MUST BE COLLIMATED. IN MANY CASES THE TUBE MUST BE ALSO FILTERED TO SELECT AN OUTPUT BEAM OF PROPER ENERGY AND INTENSITY, TO EXCITE A GIVEN ELEMENT WITH GIVEN CONCENTRATION AND IN A GIVEN MATRIX

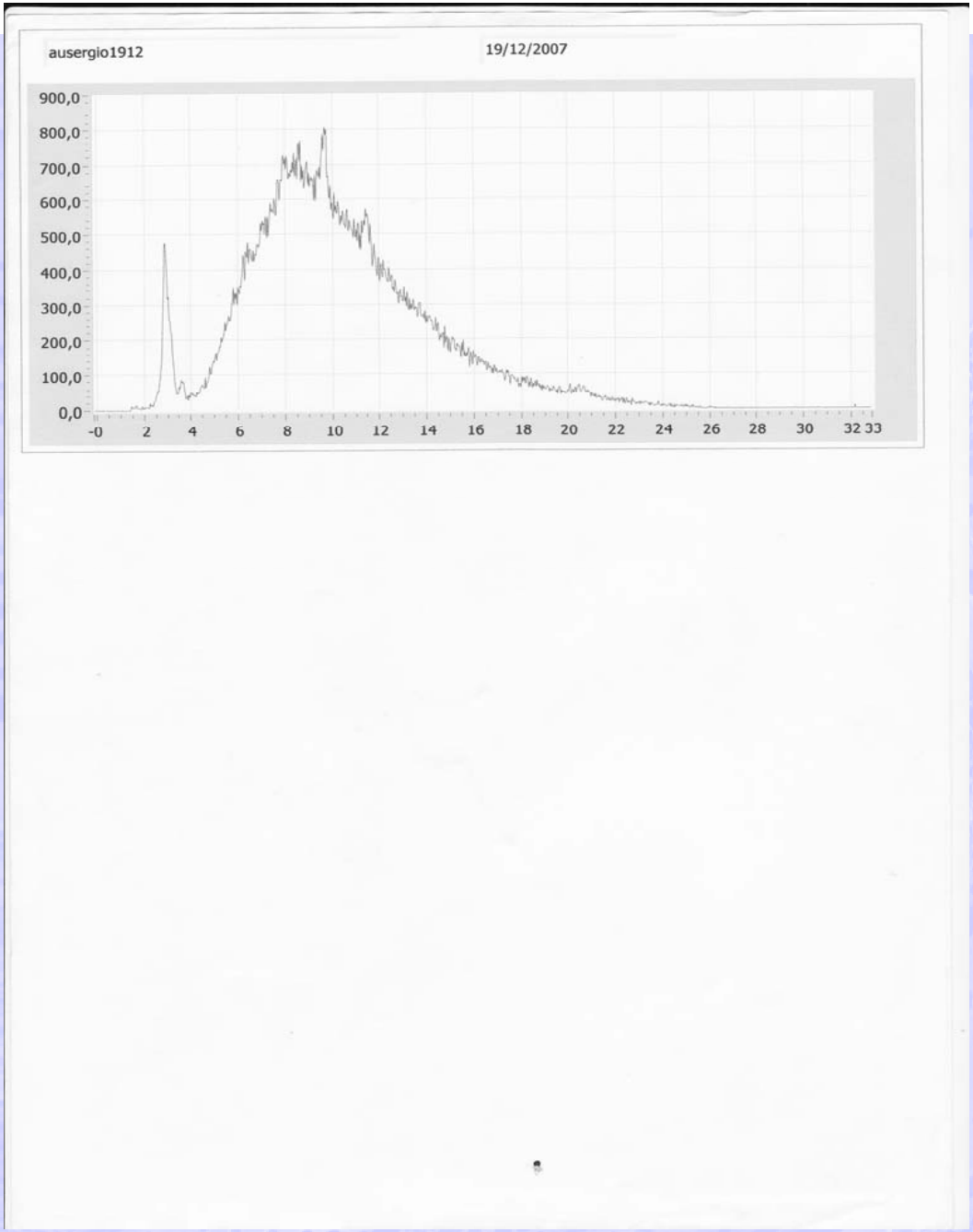
ausergio1912
19/12/2007
900,0
800,0
700,0
600,0
500,0
400,0
300,0
200,0
100,0
0,0
-0
2
4
6
8
10
12
14
16
18
20
22
24
26
28
30
32 33

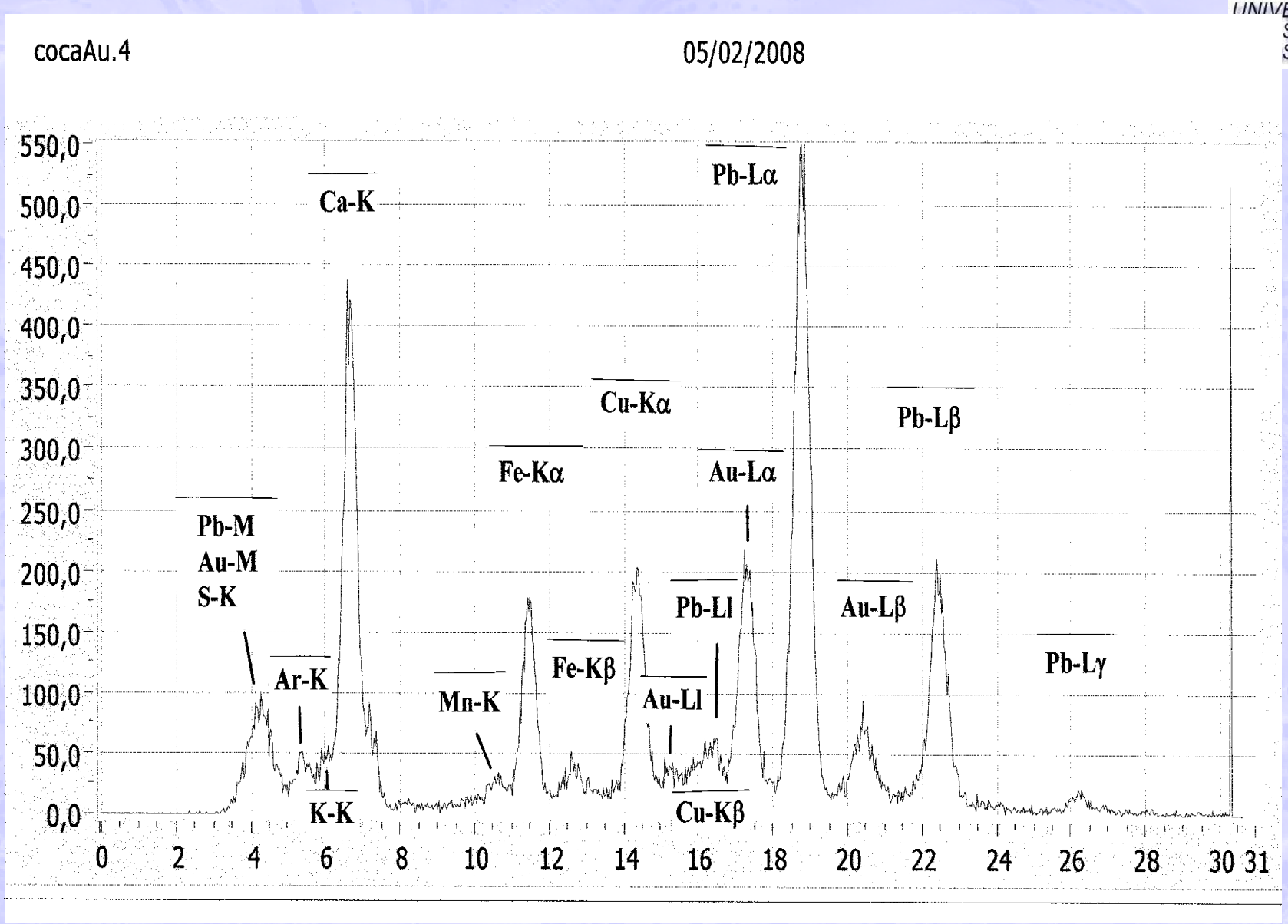
cocaAu.4
05/02/2008
550,0
500,0
450,0
400,0
350,0
300,0
250,0
200,0
150,0
100,0
50,0
0,0
0
2
4
6
8
10
12
14
16
18
20
22
24
26
28
30
31
Pb-M
Au-M
S-K
Ar-K
K-K
Ca-K
Mn-K
Fe-Kα
Fe-Kβ
Cu-Kα
Au-Ll
Pb-Ll
Cu-Kβ
Au-Lα
Pb-Lα
Au-Lβ
Pb-Lβ
Pb-Lγ

CHARACTERISTICS OF XRF

ELEMENTS WHICH CAN BE ANALYZED:

-FROM ATOMIC NUMBER 15 TO 92 ;

TYPICAL MINIMUM DETECTION LIMITS:

-STRONGLY DEPENDENT ON SOURCE, DETECTOR, GEOMETRY, MATRIX

(TYPICALLY ppm to percent

Nanograms to micrograms)

-MEASURING TIME : typically 100 s

XRF is not able to:

-detect low atomic number elements (up to 15 approximately)
-detect chemical bonds
-carry out volume analysis (in many cases)

X-RAY DETECTORS

LABORATORY XRF-SYSTEMS

-Si(Li)

-HpGe

Energy resolution about 130 eV at 5.9 keV

High geometrical efficiency

About 100% intrinsic efficiency

PORTABLE XRF-SYSTEMS

-thermoelectrically cooled

Si-PIN or Si-drift

Energy resolution about 140 eV at 5.9 keV

low geometrical efficiency

intrinsic efficiency depending on the energy

properly amplified and formed to give Gaussian pulses. These pulses are finally converte into numbers and classified with a pulse height analyzer that produces a "spectrum".

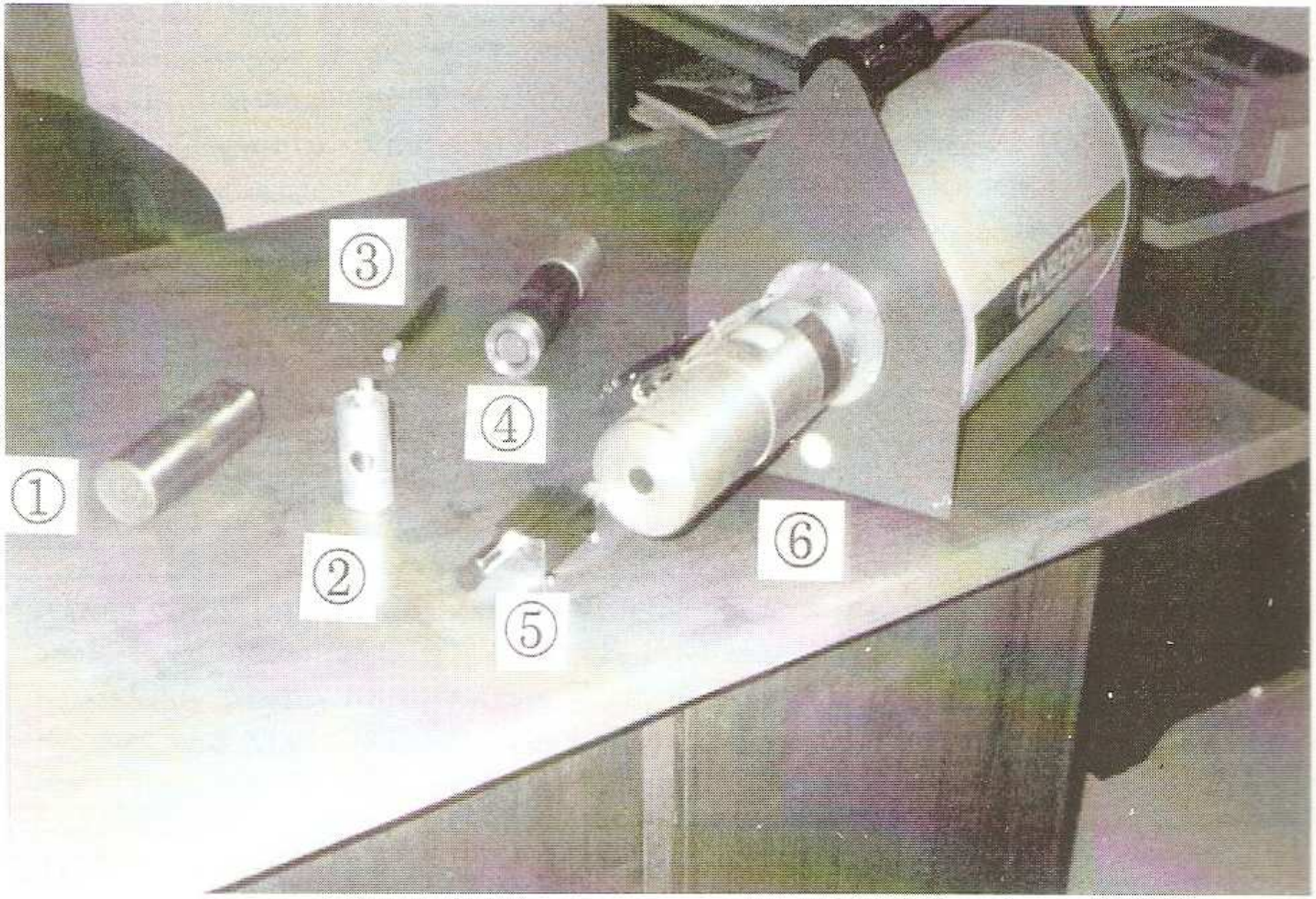

Fig. 5.1. – Photography of typical X-ray detectors. From left a Xe gas proportional counte (1), a Ne gas proportional counter (2), a small X-ray NaI(Tl) detector for tomography (3), a Al-window NaI(Tl) X-ray detector (4), an AMPTEK Si-PIN (5) and a HpGe (6).

Figure 16 – Typical X-ray detectors : from top left Si-PIN and CdZnTe by AMPTEK [31] , Si-drift by KETEK [37] and BRUKER [38] and Vortex Si-drift by SII Nano Technology [39], HgI_2 by Constellation Tech. [40], SPEAR CdZnTe by eV Products [41] and CdTe by AMPTEK [31] .

41

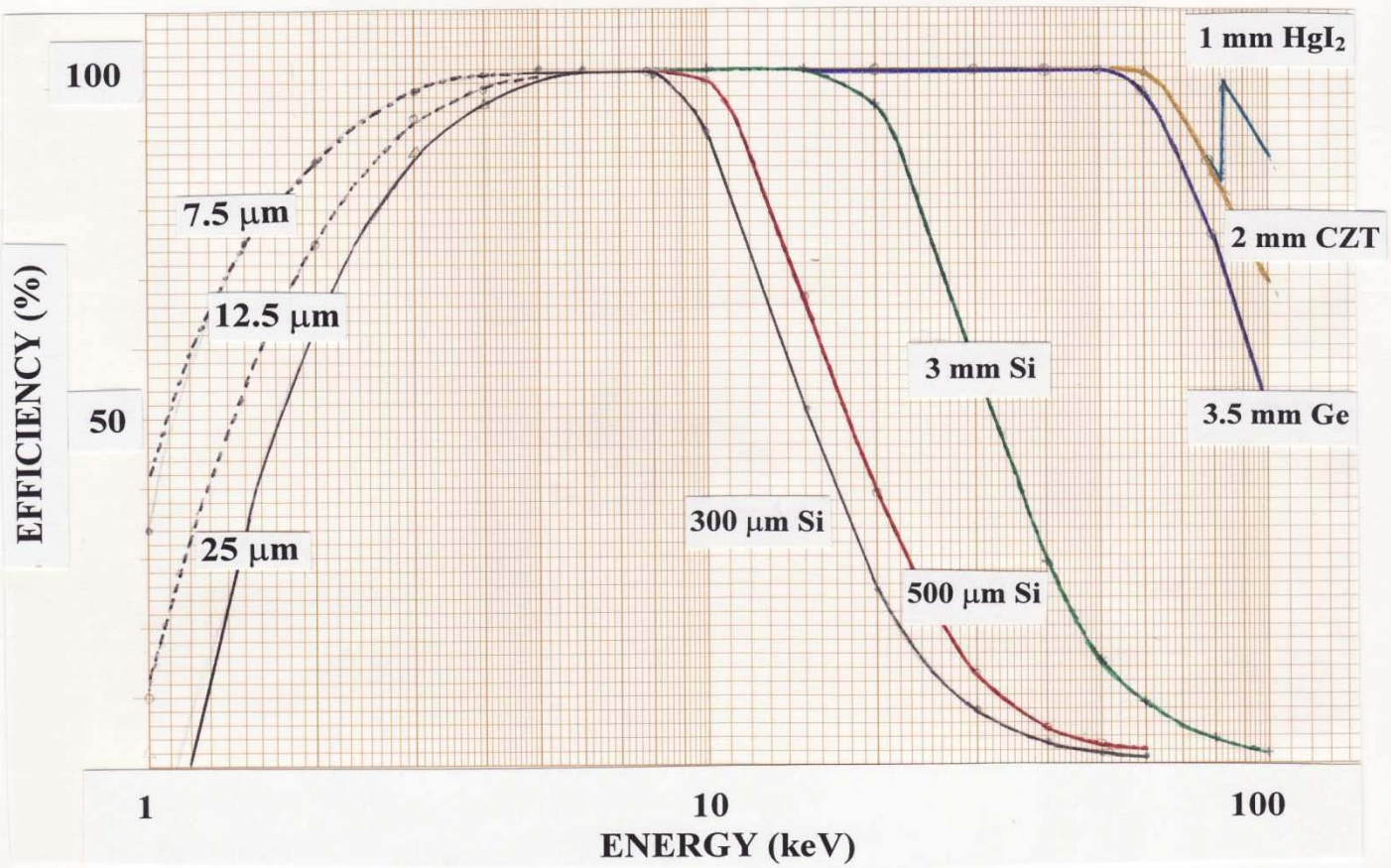
100
50
EFFICIENCY (%)
7.5 μm
12.5 μm
25 μm
300 μm Si
500 μm Si
3 mm Si
1 mm HgI2
2 mm CZT
3.5 mm Ge
1
10
100
ENERGY (keV)

With regard to the distances and geometry source-sample-detector, it is worthwhile to note that while the distance source-sample is not affecting too much the fluorescence spectrum, the distance source-sample is critical for the low-energy part of the spectrum, where the air attenuation plays an important role.

Air thickness attenuating 50% of the radiation, and attenuation by 2 cm air versus energy are shown in Table 10.

Concerning the angles, the X-ray detector is generally put orthogonally to the sample surface, while the X-ray tube is located at about 30-45° according to the sizes.

Table 10- X-rays attenuation by air

E_X (keV)	Air thickness for 50% attenuation	Attenuation of 2 cm air
1	1.2 mm	100%
1.5	4.1 mm	97%
2	9.6 mm	74%
2.5	1.9 cm	55%
3	3.2 cm	35%
5	14.4 cm	10%

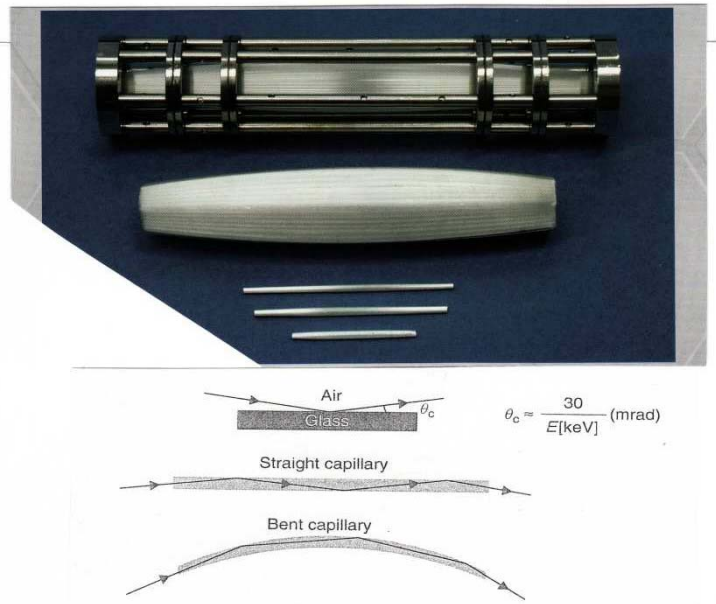

Figure 21 – Capillary collimators manufactured by IfG, Berlin, Germany, and principle of capillary optics, where ϑc is the critical angle for total reflection [45].

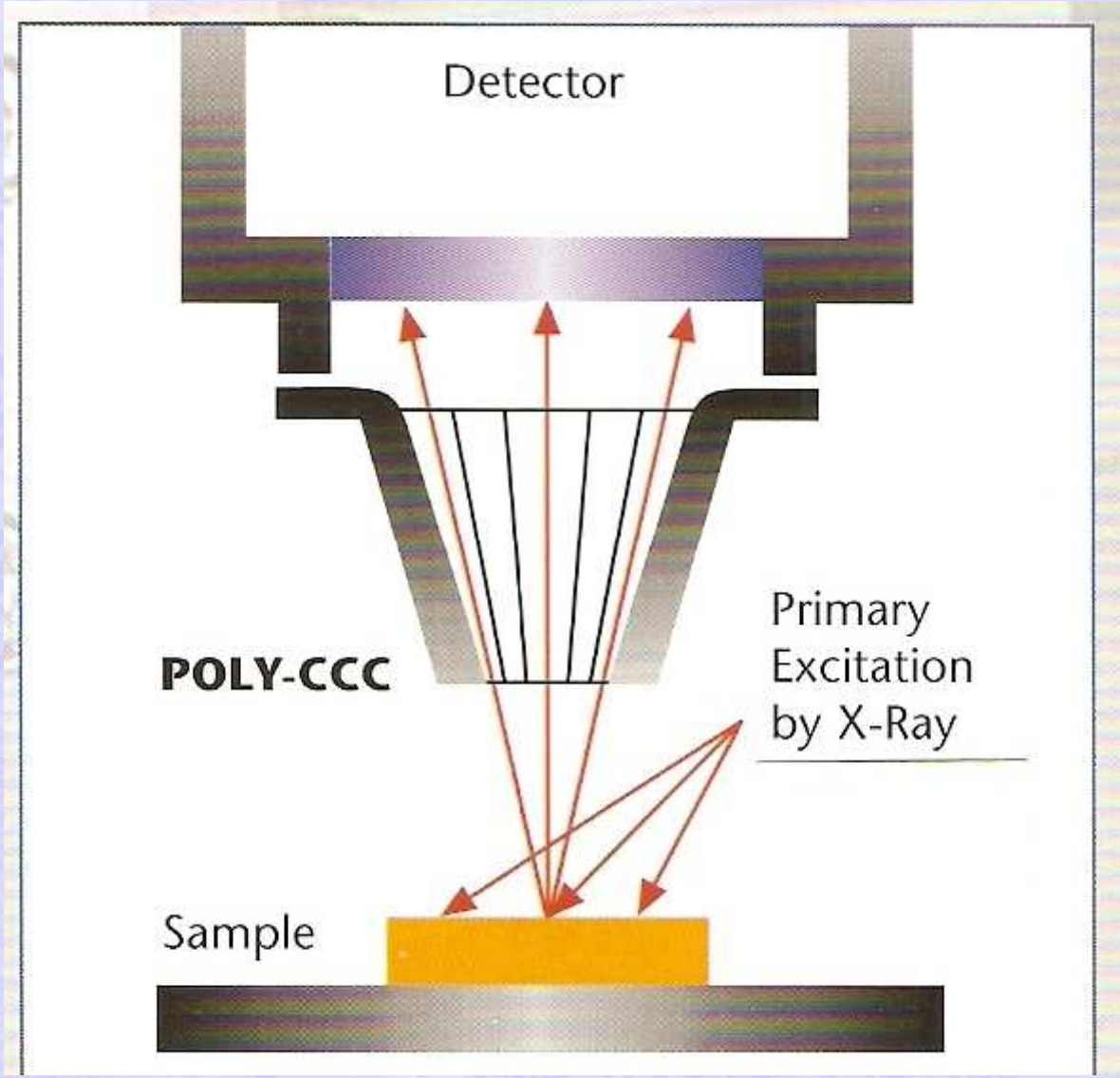
Detector
POLY-CCC
Primary
Excitation
by X-Ray
Sample

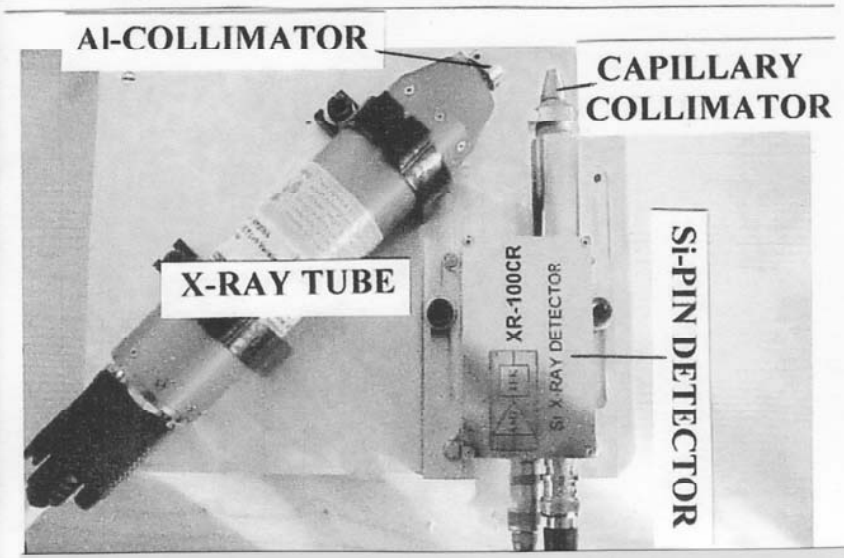
Al-COLLIMATOR
CAPILLARY COLLIMATOR
X-RAY TUBE
XR-100CR
Si X-RAY DETECTOR
Si-PIN DETECTOR

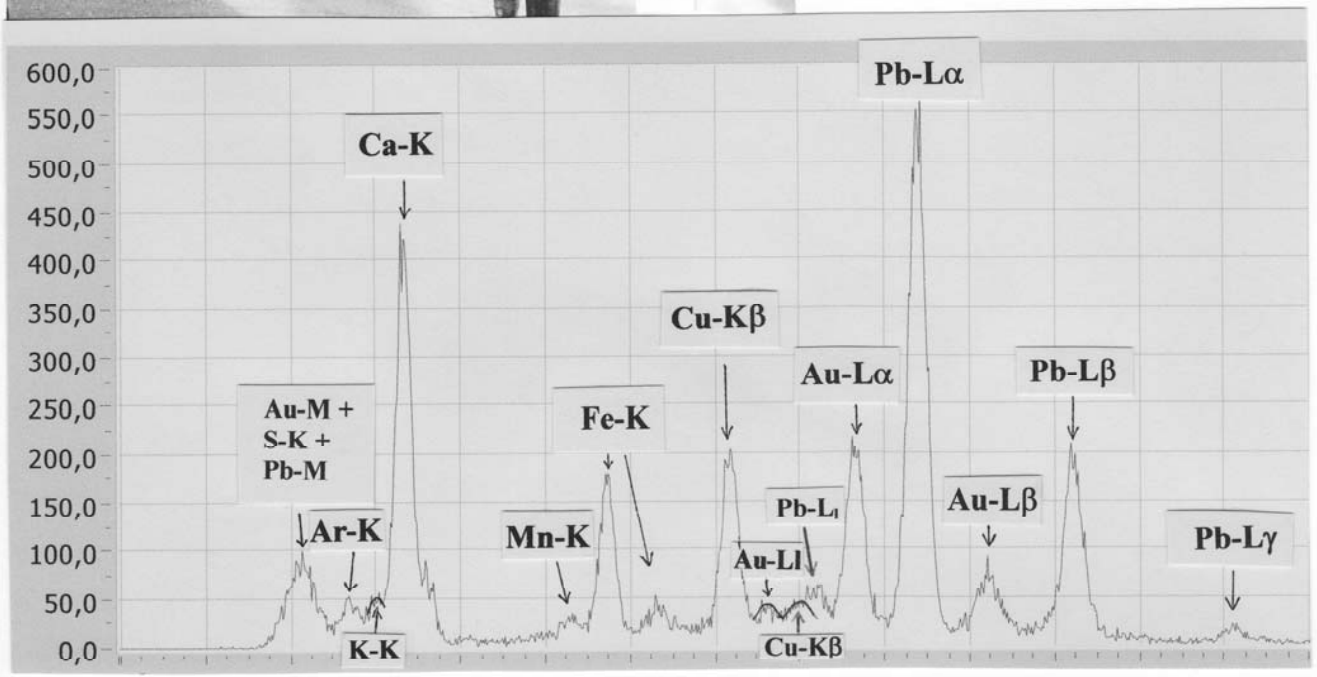
600,0
550,0
500,0
450,0
400,0
350,0
300,0
250,0
200,0
150,0
100,0
50,0
0,0
Ca-K
Pb-Lα
Cu-Kβ
Au-Lα
Pb-Lβ
Au-M +
S-K +
Pb-M
Fe-K
Ar-K
Mn-K
Pb-Lι
Au-Ll
Au-Lβ
Pb-Lγ
K-K
Cu-Kβ

UNIVERSITÀ degli STUDI di SASSARI

ENERGY–DISPERSIVE X-RAY FLUORESCENCE : ANALYSIS OF WORKS OF ART

FOLLOWING UNESCO INDICATIONS, ITALY HAS A CULTURAL HERITAGE BIGGER THAN ANY OTHER COUNTRY.

IT IS COMPOSED OF PAINTINGS FRESCOS, MARBLES, MONUMENTS, STATUES, ALLOYS....STARTING FROM ABOUT 1500 BC.

THIS CULTURAL HERITAGE NEEDS TO BE

-PRESERVED

-CONSERVED

-RESTORED (WHEN NECESSARY) AND FIRST OF ALL

-ANALYZED I

:

THE SCIENTIFIC AREA RELATED TO THE APPLICATION OF SCIENTIFIC METHODS AND TECHNIQUES TO STUDY WORKS OF ART IS CALLED ARCHAEOMETRY

A VARIETY 0F DIFFERENT WORKS OF ART MAY BE ANALYZED WITH EDXRF-ANALYSIS:

of matels may be studied by using a EDXRF-
ble equipment :

paintings and frescos,
illuminated manuscripts,
Alloys of all type,
ceramics,
papers,
stones,
enamels,
marbles,
Stamps
.

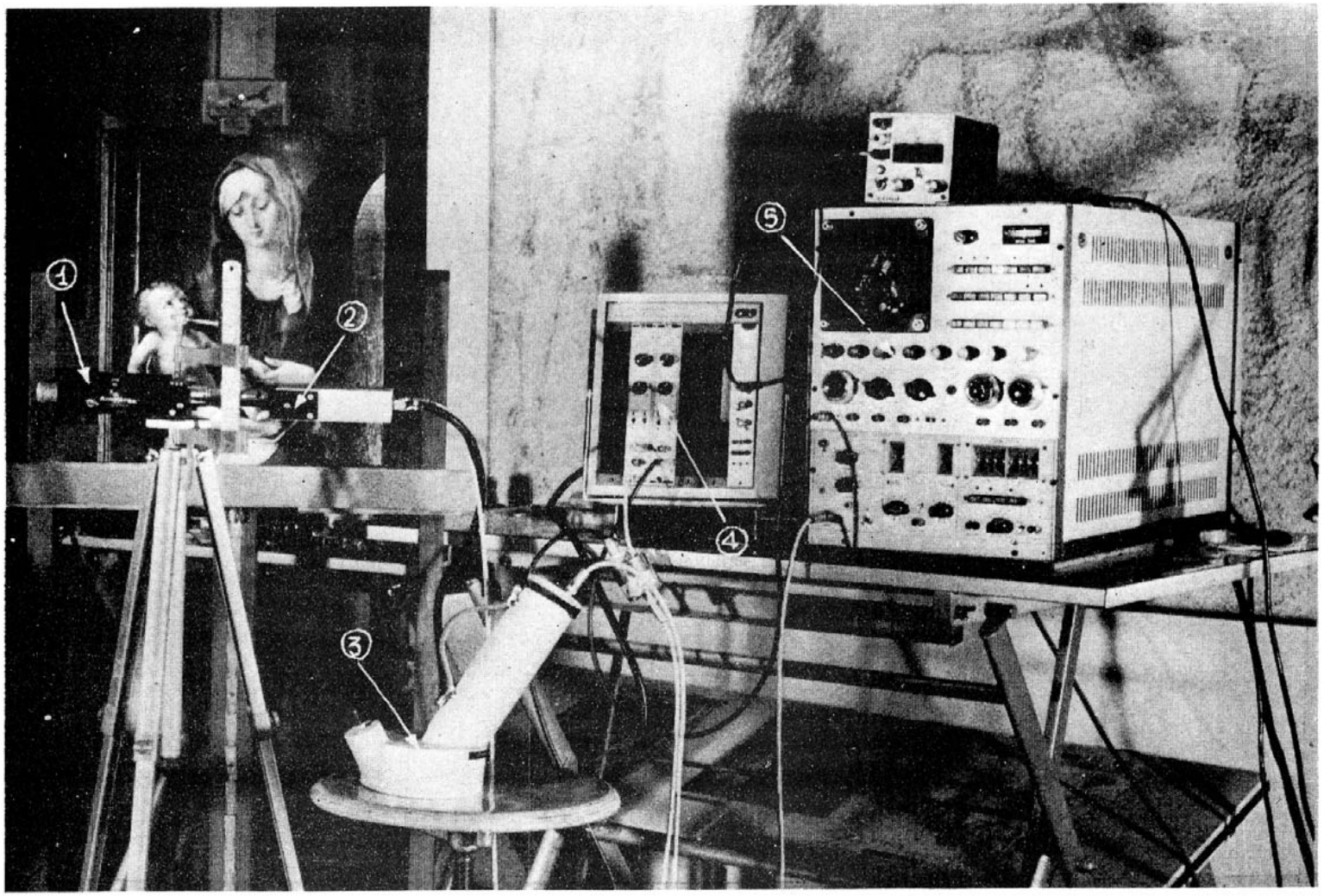

Plate 1 *Experimental layout.* (1) *measuring head* (*gas counter*), (2) *preamplifier*, (3) *measuring head* (*NaI*(*Tl*) *counter*), (4) *amplifier*, (5) *pulse height analyser.*

109. Raffaello, *Il trasporto di Cristo al Sepolcro* (*Deposizione Baglioni*), Roma, Galleria Borghese.

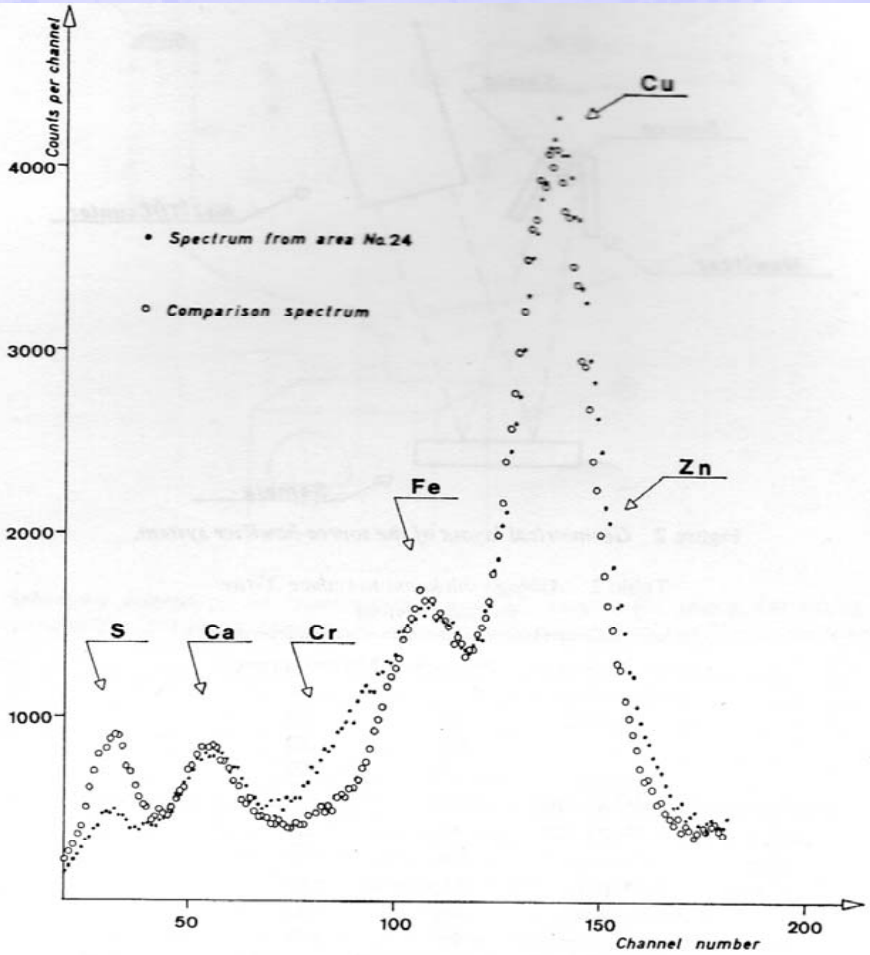

Figure 3 *Raffaello Sanzio, 'Deposizione.' XRF spectrum of area 24. A spectrum of pure elements (S, Ca, Fe, Cu) is superimposed. The presence of Cr and Zn in this area is evident.*

Archaeometry 14, 1 (1972), 65-78. Printed in Great Britain

NON-DESTRUCTIVE ANALYSIS OF CHEMICAL ELEMENTS IN PAINTINGS AND ENAMELS

R. CESAREO, F. V. FRAZZOLI, C. MANCINI, S. SCIUTI

Istituto di Fisica della Facoltà di Ingegneria, Rome, Italy

and M. MARABELLI, P. MORA, P. ROTONDI, G. URBANI

Istituto Centrale del Restauro, Rome, Italy

1. INTRODUCTION

Several non-destructive methods of analysis take advantage of the more sophisticated techniques which are commonly used to-day in atomic and nuclear spectroscopy. The fact that it is possible to carry out non-destructive analyses of chemical elements gives new possibilities for the study of works of art. This paper deals with various applications of X-ray fluorescence analysis (XRF) to paintings and enamels.

In the past an XRF system needed large complex equipment. To-day simplified versions are available which consist of a radioactive source instead of an X-ray tube and of a non-dispersive spectrometer, i.e. a proportional counter coupled with a pulse height multi-channel analyser. In our apparatus the proportional detector (gas counter or NaI(Tl) counter) and the exciting source form one unit. This 'measuring-head' weighs less than a kilogram and is the size of a tape-recorder microphone; the unit is connected by a flexible cable of variable length, to the multichannel analyser (figure 1). With a system of this kind one can conveniently delimit and analyse areas in the range 1–20 cm^2 (see section 2). To delimit extremely small areas (between 1 mm^2 and 1 μm^2), one has to employ more complex systems (see for instance Stolow *et al.* 1969).

When a mobile measuring head is not needed, one can use a semiconductor detector which has better resolution than a proportional counter and so considerably simplifies the interpretation of the X-ray spectrum (Bowman *et al.* 1966, Frankel 1969, 1970).

The XRF system is described in section 2 and the various analyses performed on paintings and enamels are presented and discussed in sections 3, 4 and 5.

2. EXPERIMENTAL DETAILS

Plate 1 illustrates the XRF unit complete with two measuring heads: one of these uses a proportional counter filled with Kr+10% CH_4; the other, a NaI(Tl) scintillator. The dimensions of the system, made up of standard laboratory equipment, can be drastically reduced by using more compact standard electronics; in this way a transportable system can easily be obtained.

The characteristics of the isotopic sources used are summarized in table 1. A ^3H source was used to excite X-ray fluorescence in light elements (from sulphur to zinc); ^{241}Am and ^{147}Pm sources were employed to excite medium and heavy elements and a ^{57}Co source was

F

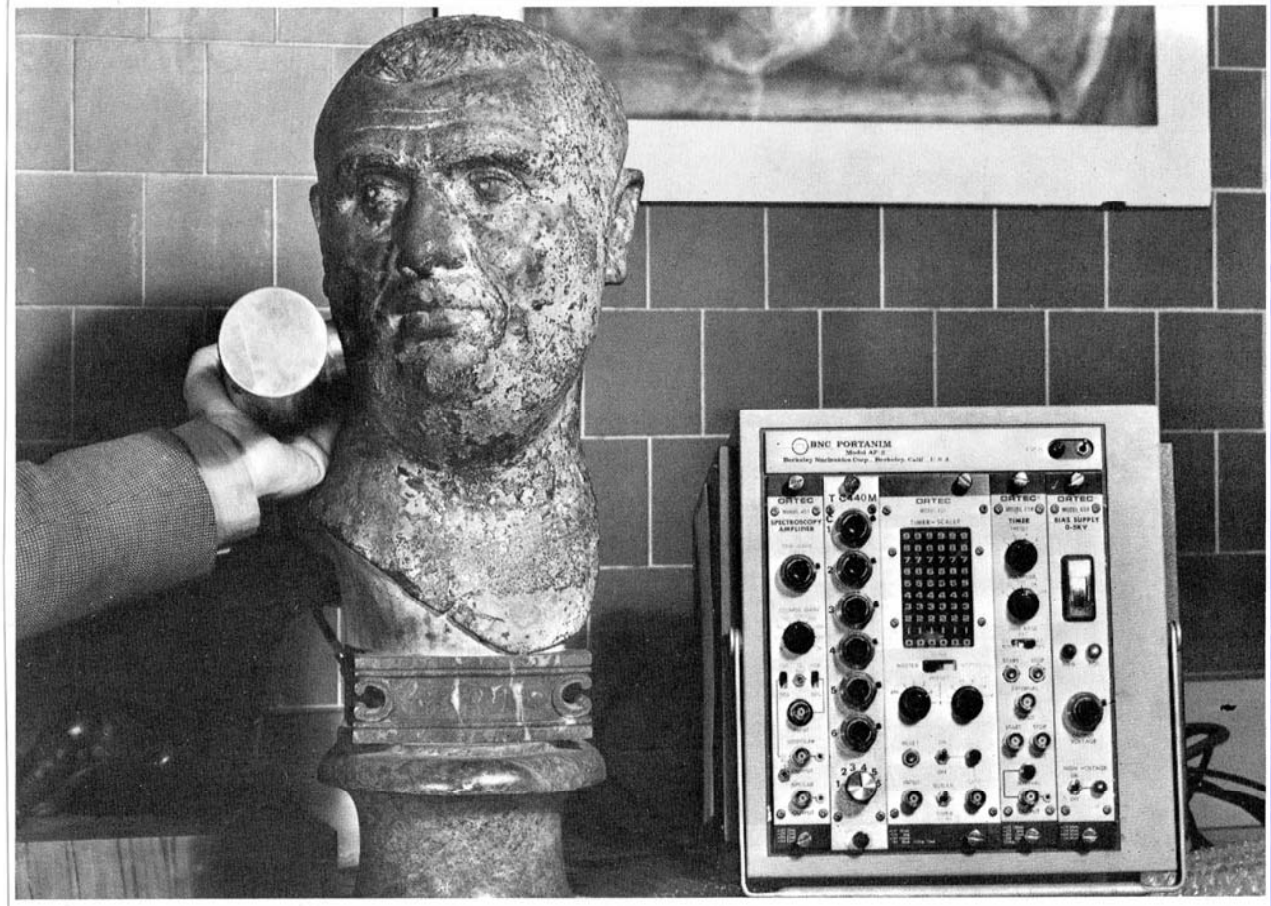

Testa bronzea di Balbino (epoca romana), presso la Biblioteca Vaticana, esaminata con il sistema XRF

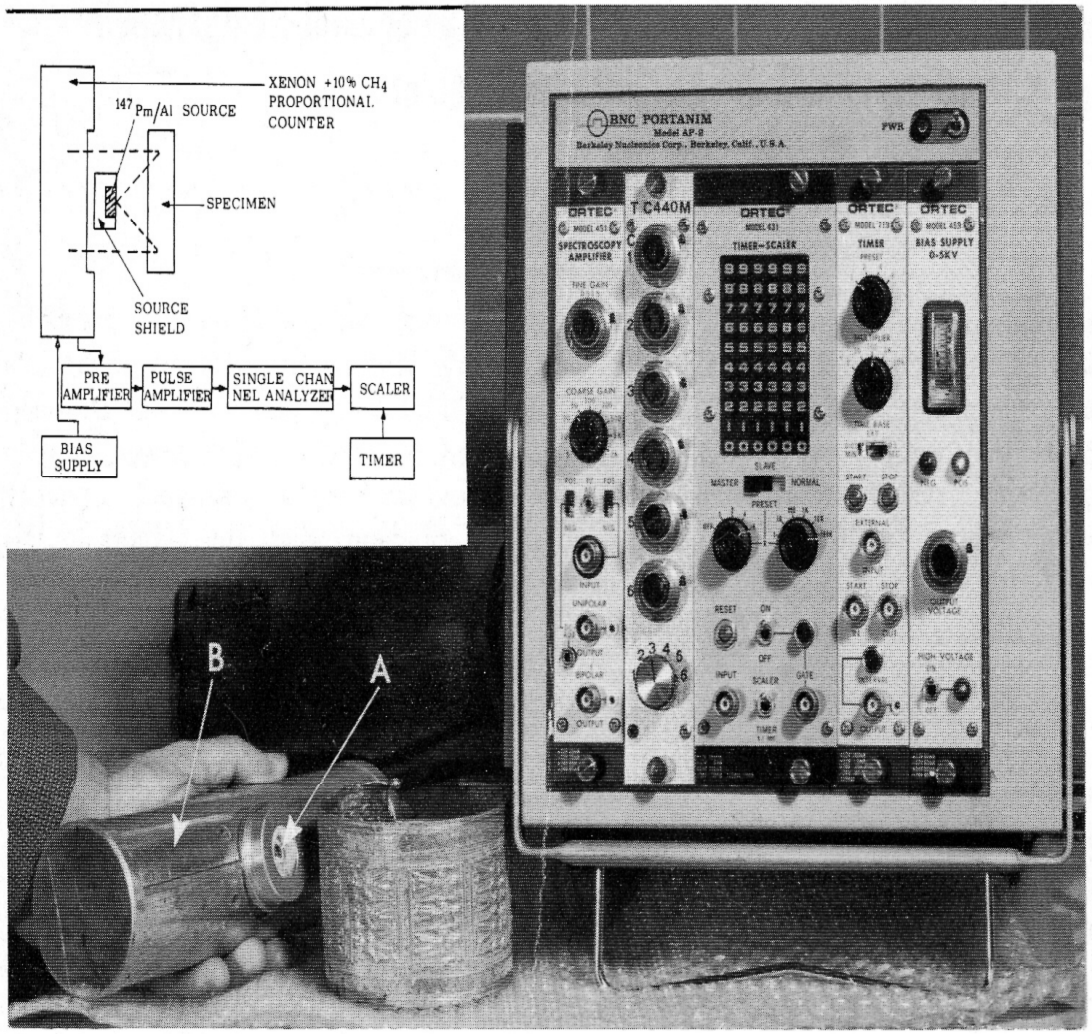

Fig. 1: Tragbares Radionuklid-Röntgen-fluoreszenzgerät. A: ^{147}PM/Al-Quelle; B: Proportionszähler. Oben links Block-diagramm

Fig. 1: Portable radionuclide X-ray fluor escence unit. A: ^{147}Pm/Al source; B: pro portional counter. Top left: Block dia-gram

VII Century B.C. etruscan golds

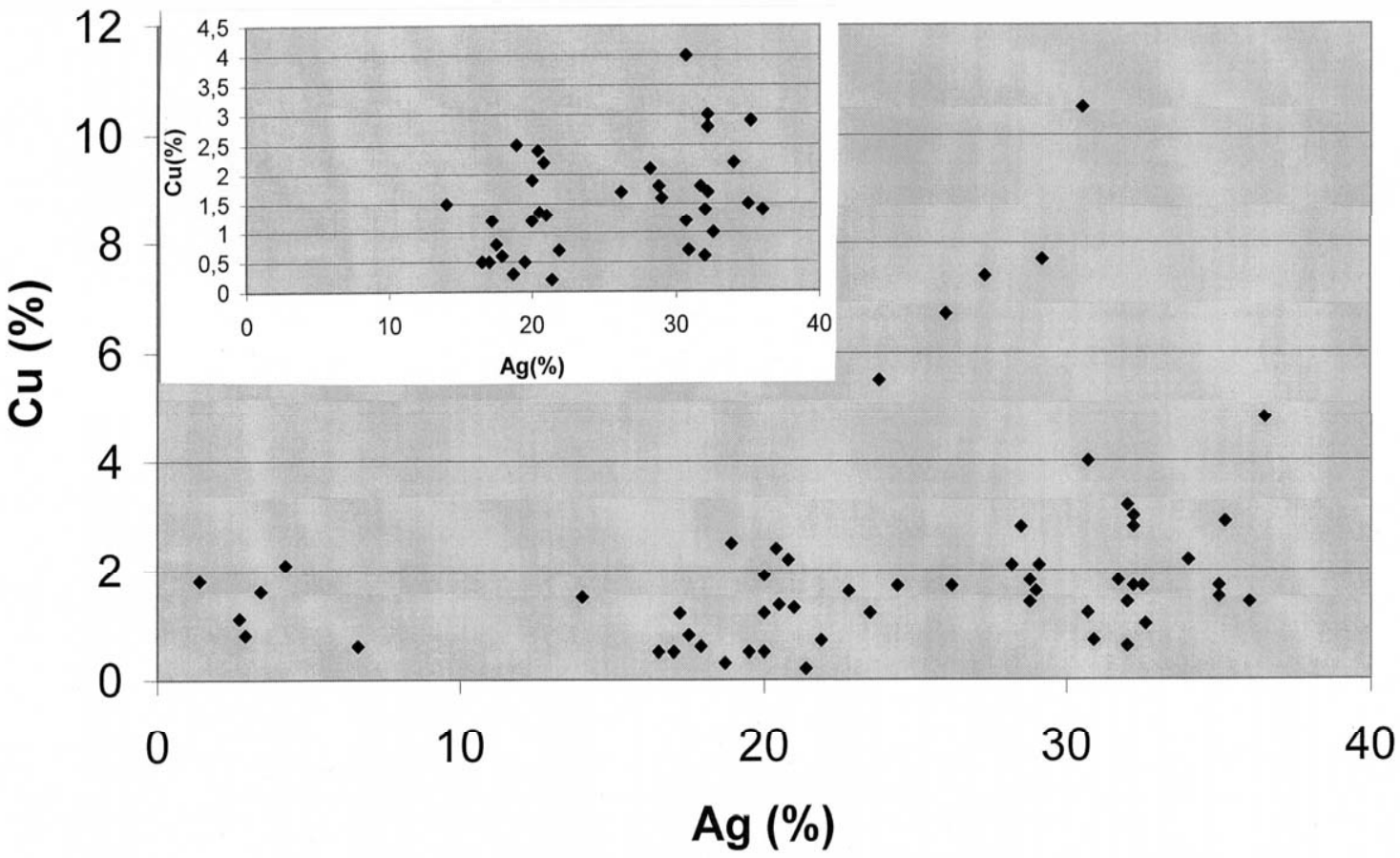

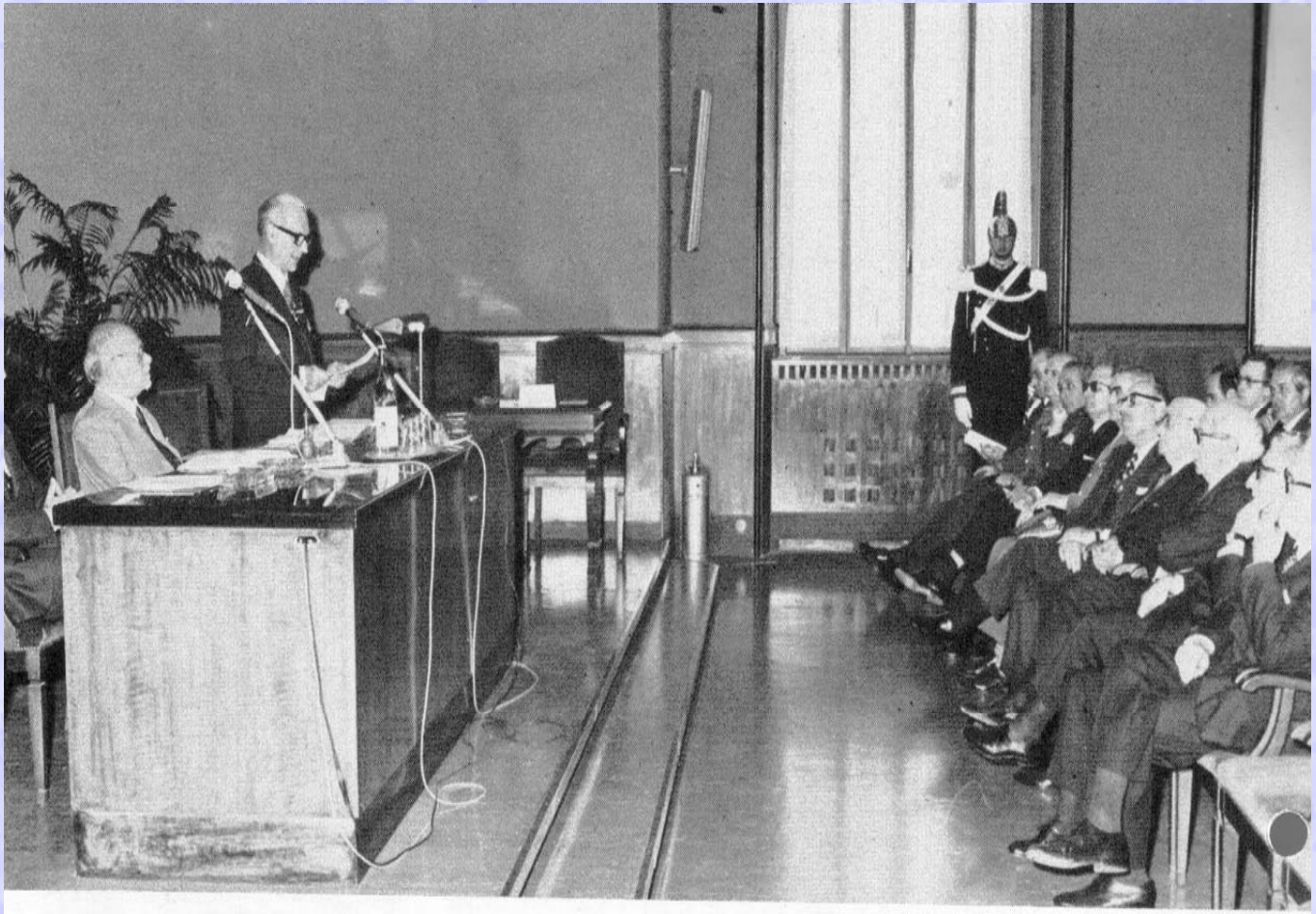

Roma, villa della Farnesina: il prof. Amaldi svolge la relazione introduttiva al Convegno

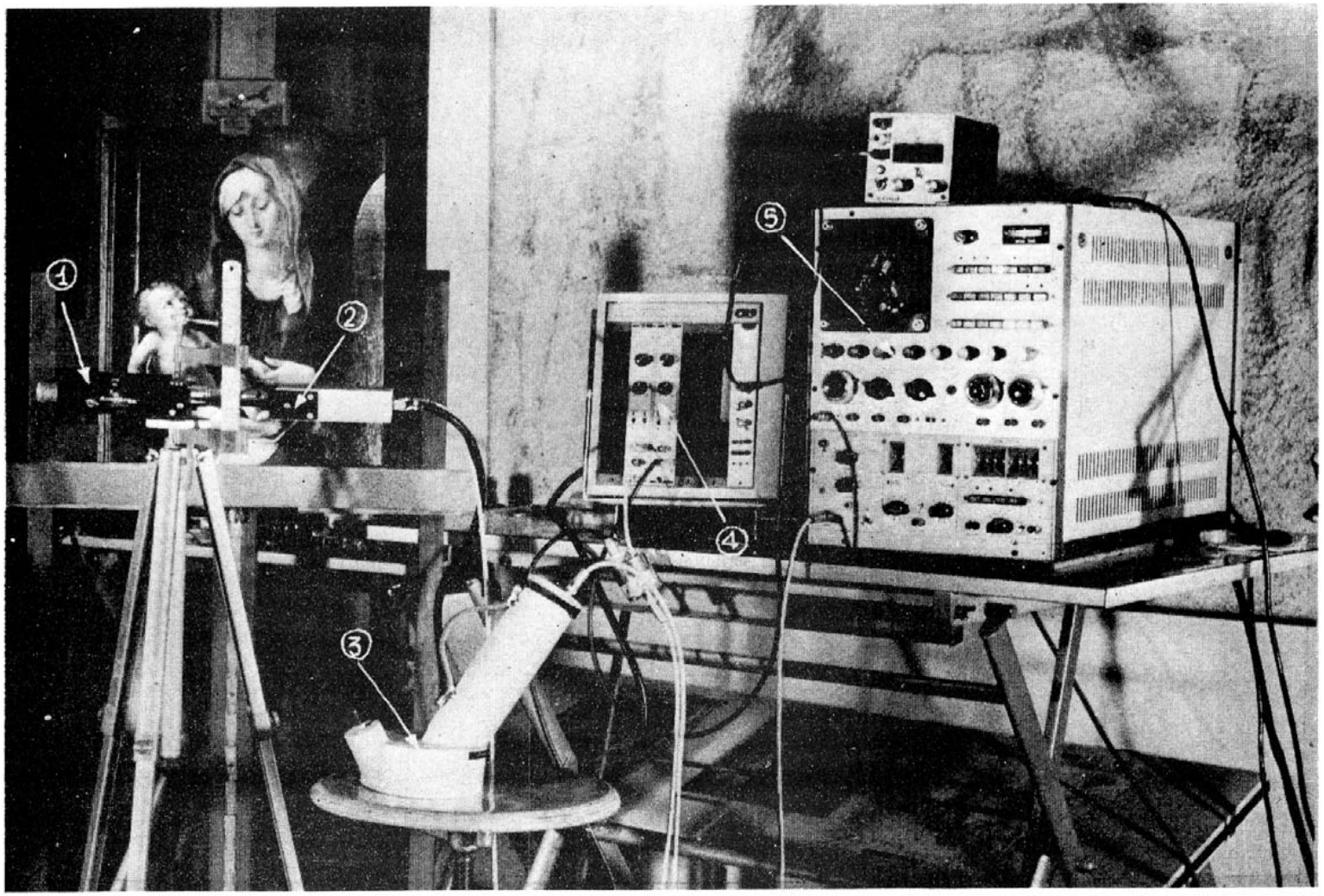

Plate 1 *Experimental layout.* (1) *measuring head* (*gas counter*), (2) *preamplifier*, (3) *measuring head* (*NaI*(*Tl*) *counter*), (4) *amplifier*, (5) *pulse height analyser.*

ANALYSIS OF PAINTINGS OF ALL TYPES

SEVERAL PIGMENTS CAN BE “DATED”

ZINC WHITE WAS STARTED TO BE USED AFTER 1840

TITANIUM WHITE AFTER 1918

CADMIUM RED AFTER 1920

CHROMIUM BASED PIGMENTS ARE RELATIVELY MODERN

EDXRF-ANALYSIS CAN BE THEREFORE USEFUL TO IDENTIFY:

- PREVIOUS RESTORATION AREAS
- TYPICAL PIGMENTS USED BY AN ARTIST IN A GIVEN PERIOD OF TIME
- FAKES
- POLLUTION EFFECTS ON THE SURFACE (PRESENCE OF S AND/OR Cl DUE TO BURNING OF WOOD, COAL, GASOLINE AND PRODUCING GYPSUM WHICH BLACKENS THE PAINTING

pigmenti: • egizi • greco-romani • indiani o messicani

Table 1. Survey of inorganic pigments and their chemical composition

White pigments		**Green pigments**	
o Calce	CaO	Basic copper sulfate	$Cu_x(SO_4)_y(OH)_z$
Antimony white	Sb_2O_3	Chromium oxide	Cr_2O_3
Lithopone	$ZnO + BaSO_4$	• Chrysocolla	$CuSiO_3 \cdot nH_2O$
Permanent white	$BaSO_4$	Cobalt green	$CoO \cdot 5ZnO$
Titanium white 1919	TiO_2	Emerald green	$Cu(CH_3COO)_2 \cdot 3Cu(AsO_2)_2$
o White lead (Kremserweiss)	$2PbCO_3 \cdot Pb(OH)_2$	Guignent green	$Cr_2O_3 \cdot nH_2O + H_3BO_3$
Zinc white >1840	ZnO	o • Malachite	$CuCO_3 \cdot Cu(OH)_2$
Zirconium oxide	ZrO_2	Verdigris	$Cu(CH_3COO)_2 \cdot nCu(OH)_2$
• Argilla	$Al_2O_3 \cdot SiO_2 \cdot nH_2O$	Paratachamite	$CuCl_2 \cdot Cu(OH)_2$
• Chalk	$CaCO_3$		
• • • Gypsum	$CaSO_4 \cdot 2H_2O$		
Yellow pigments		**Blue pigments**	
Terra d'ombra	$Fe_2O_3 \cdot 3H_2O + Mn^{2+}$	o • Azurite	$2CuCO_3 \cdot Cu(OH)_2$
• • Auripigmentum	As_2S_3	Cerulean blue	$CoO \cdot nSnO_2$
Cadmium yellow	CdS	Cobalt blue	$CoO \cdot Al_2O_3$
Chrome yellow	$2PbSO_4 \cdot PbCrO_4$	Cobalt violet	$Co_3(PO_4)_2$
Cobalt yellow	$K_3[Co(NO_2)_6] \cdot 1.5H_2O$	Egyptian blue	$CaO \cdot CuO \cdot 4SiO_2$
Lead–tin yellow	$Pb_2SnO_4/PbSn_2SiO_7$	Manganese blue	$BaSO_4 \cdot Ba_3(MnO_4)_2$
• Massicot	PbO	Prussian blue	$Fe_4[Fe(CN)_6]_3$
Naples yellow	$Pb(SbO_3)_2/Pb_3(SbO_4)_2$	Smalt	Co-glass ($K_2O + SiO_2 + CoO$)
Strontium yellow	$SrCrO_4$	• • Ultramarine (Lapislazzuli)	$Na_{8-10}Al_6Si_6O_{24}S_{2-4}$
Titanium yellow	$NiO \cdot Sb_2O_3 \cdot 20TiO_2$	Blu Maya	$(OH_2)_6 Mg_5 Si_8 O_{20} \cdot 4H_2O$
• • • • Yellow ochre	$Fe_2O_3 \cdot nH_2O$ (20–70%)		
Zinc yellow	$K_2O \cdot 4ZnO \cdot 4CrO_3 \cdot 3H_2O$		
Red pigments		**Black pigments**	
• • Minio	Pb_3O_4	Antimony black	Sb_2O_3
Cadmium red 1909	$CdS + CdSe$	Black iron oxide	$FeO \cdot Fe_2O_3$
Cadmium vermilion	$CdS + HgS$	• Carbon or charcoal black	C (95%)
Chrome red	$PbO \cdot PbCrO_4$	Cobalt black	CoO
Molybdate red	$7PbCrO_4 \cdot 2PbSO_4 \cdot PbMoO_4$	Ivory black	$C + Ca_3(PO_4)_2$
• • Realgar	As_2S_3	Manganese oxide	$Mno + Mn_2O_3$
Red lead	Pb_3O_4	Pirolusite	MnO_2
o • Red ochre	Fe_2O_3 (up to 90%)		
o • • Vermilion (Cinabro)	HgS >600 B.C.		

• Ocra Purpurea Fe_2O_3

Porpora 6-6' dibromoindaco

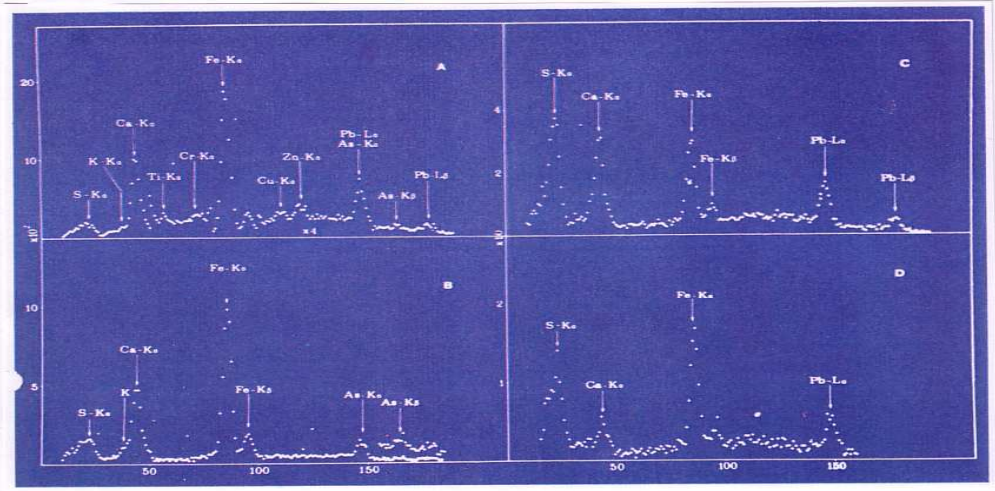

Figure 48 – The painting on wood "pala di Santa Lucia" of Lorenzo Lotto, painted in 1532, at the Pinacoteca Civica of Jesi, and X-ray spectra of the orange mantle of the monk at the right after successive cleaning procedures.

c. Identification of fakes

In some cases the classification of the pigments employed by an artist in a well defined period of time may help in the identification of fakes. An example of this point is related to the analysis of De Chirico paintings of his last period, and of paintings attributed to De Chirico (of the same period) and subject to judicial skill.

15 paintings of De Chirico have been analyzed, showing common Characteristics, such as:

-preparation based on the use of lead white and zinc white;

-a systematic use of lead;

-red colours based on the use of cinnabar (HgS);

-moderate use of organic pigments.

On the north coast of present-day Perù evolved between 50 A.D. and 700 A.D. approximately the MOCHE civilization. It was an advanced culture and the Moche were very sophisticated metalsmiths. They are considered the finest producers of jewels of the central Andes, both in terms of their technological sophistication and their beauty.

The Moche culture was influenced by the Chavin and Vicus civilizations (1000-200 B.C.) and strongly influenced the Sican (750-1375 A.D.) and Chimù (1000-1460 A.D.).

The Moche metalworking ability was impressively Demonstrated by the excavations of the "Tumbas Reales de Sipan", discovered by Walter Alva and coworkers in 1987. The spectacular gold, silver and copper funerary ornaments are now in the namesake Museum, in Lambayeque.


ECUADOR
COLOMBIA
BRAZIL
BOLIVIA
CHILE
Amazon River
Marañon River
Ucayali River
Moche River
Santa River
Rimac River
Lake Titicaca
Cerro Vicús
Loma Negra
Frias
Batán Grande
Túcume
Sipán
Kuntur Wasi
Morro Eten
CHICLAYO
San José de Moro
Cajamarca
Cupisnique
Chan Chán
TRUJILLO
Huaca del Sol y
Huaca de la Luna
Cerro Sechín
Chavín de Huántar
Caral
Chancay
LIMA
Pachacámac
Mina Perdida
Wari
Machu Picchu
Ollantaytambo
CUZCO
AYACUCHO
Waywaka
Paracas
Nazca
Cahuachi
PUNO
MAP OF MAIN PERUVIAN ARCHAEOLOGICAL SITES
Main archaeological sites
Principal cities
Lakes
Main Rivers
International Boundaries
N
W
E
S

NORTH COAST AND NORTH ANDES CIVILIZATIONS

600 BC	CHAVÍN (1000-200 BC)
400 BC	
200 BC	
0	VICÚS (200 BC-400AD)
200 AD	FRIAS (200-400 AD)
400 AD	MOCHE (0-700 AD)
600 AD	
800 AD	
1000 AD	SICÁN (750-1375 AD)
1200 AD	CHIMÚ (1000-1460 AD)
1400 AD	INCA (1450-1533 AD)
1600 AD	

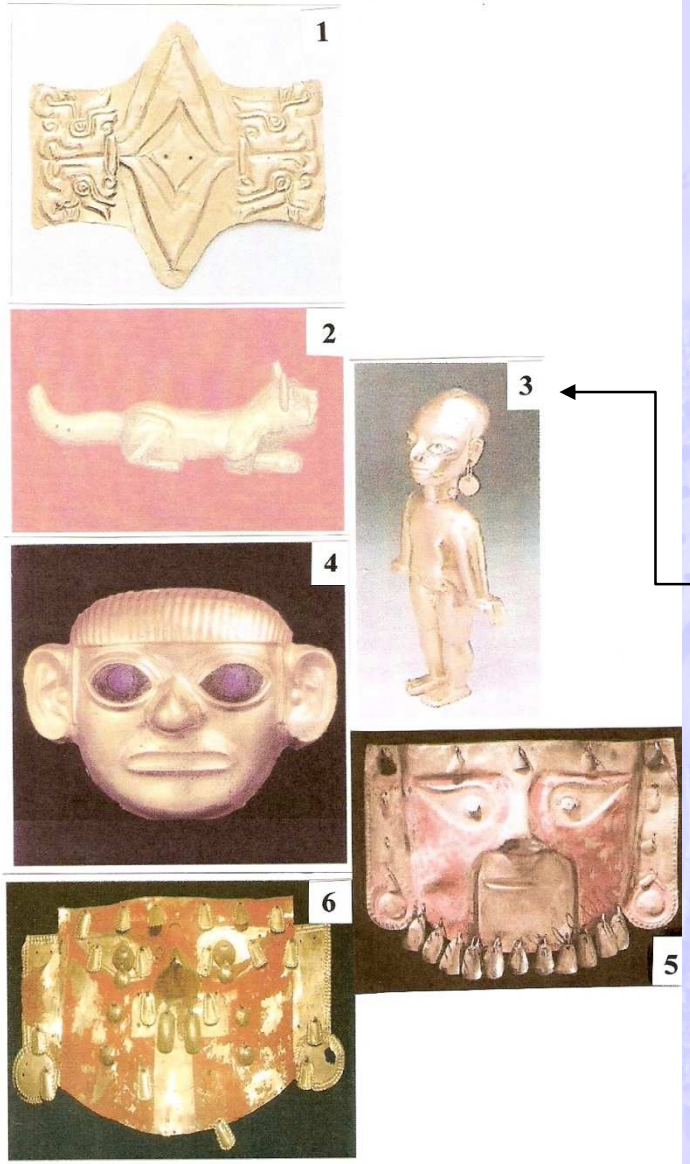

FRIAS

CHIMU

A. Bustamante, J. Fabian
Universidad Nacional Mayor de S. Marcos
Lima, Peru (oro de Sipan, Sican, Vicus)
C. Calza, M. dos Anjos, R. Lopes
COPPE, Universidade Federal do Rio de Janeiro (oro de Sipan e Sican)
M.Rizzutto, USP Sao Paulo
(oro Vicus 2009)

THREE POSSIBLE GOLD COMBINATIONS HAVE BEEN DETECTED :

GOLD (Au, Ag and Cu alloy)

GILDED COPPER (a Au-leaf of less than 1 micron overimposed to almost pure Cu)

TUMBAGA (a poor Au-alloy enriched by depletion gilding);
Tumbagas of Cu (Cu+Au) and of Ag (Ag+Au) are known
Gold leafs of 2-5 microns

GOLD MASK

FRONT SIDE
Au=74.5%
Ag= 23%
Cu=2.5%

BACK SIDE
Au=64.5%
Ag=20%
Cu=15.5%

LEFT EYE
Ag=91%
Cu=5%
Au=1.5%
Br=2%

RIGHT EYE
Copper

SOLDERING
MAINLY ON Cu
In some areas Cu+Ag

The soldering is clearly shown (arrow)

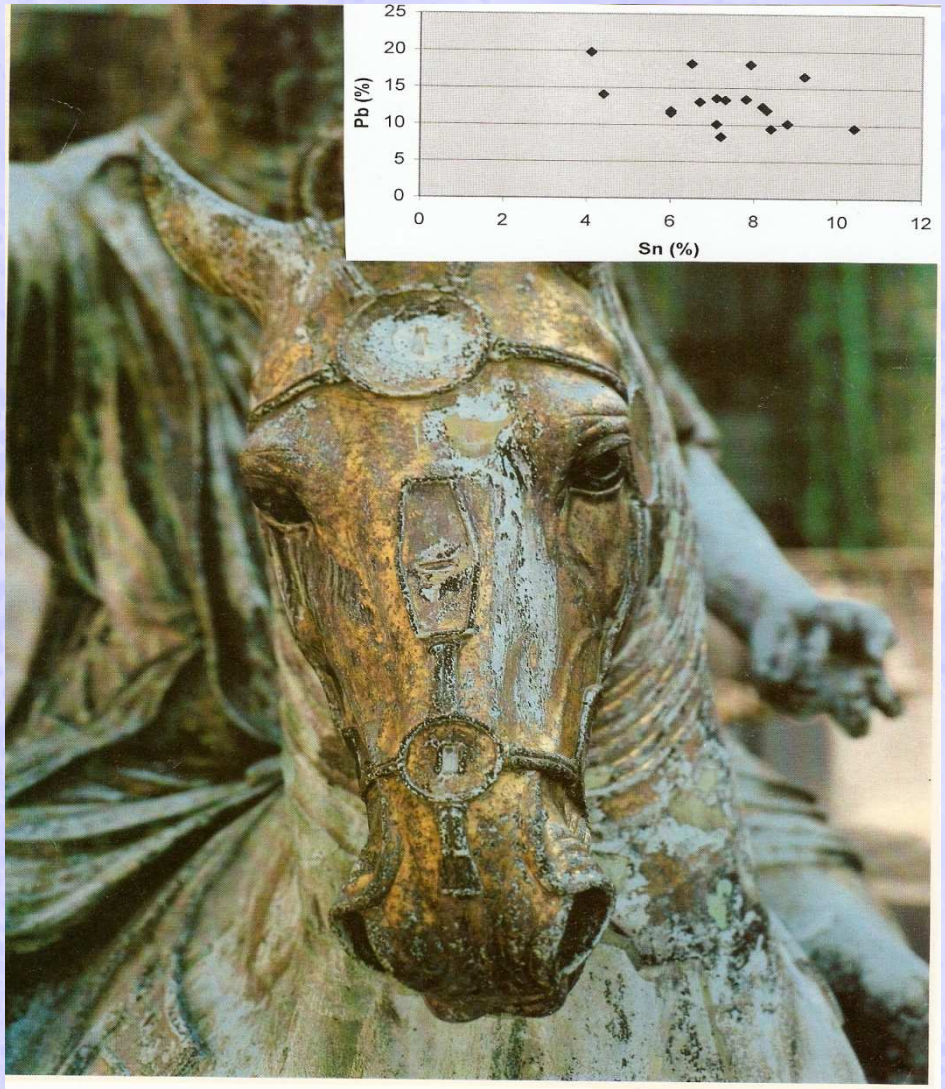

Figure 29 – The huge equestrian bronze statue of Marco Aurelio, previously in the piazza del Campidoglio, Rome, currently, after restoration, in the Museum inside the Palazzo. A summary of the results is also shown, where results on the horse, knight and original weldings are grouped.

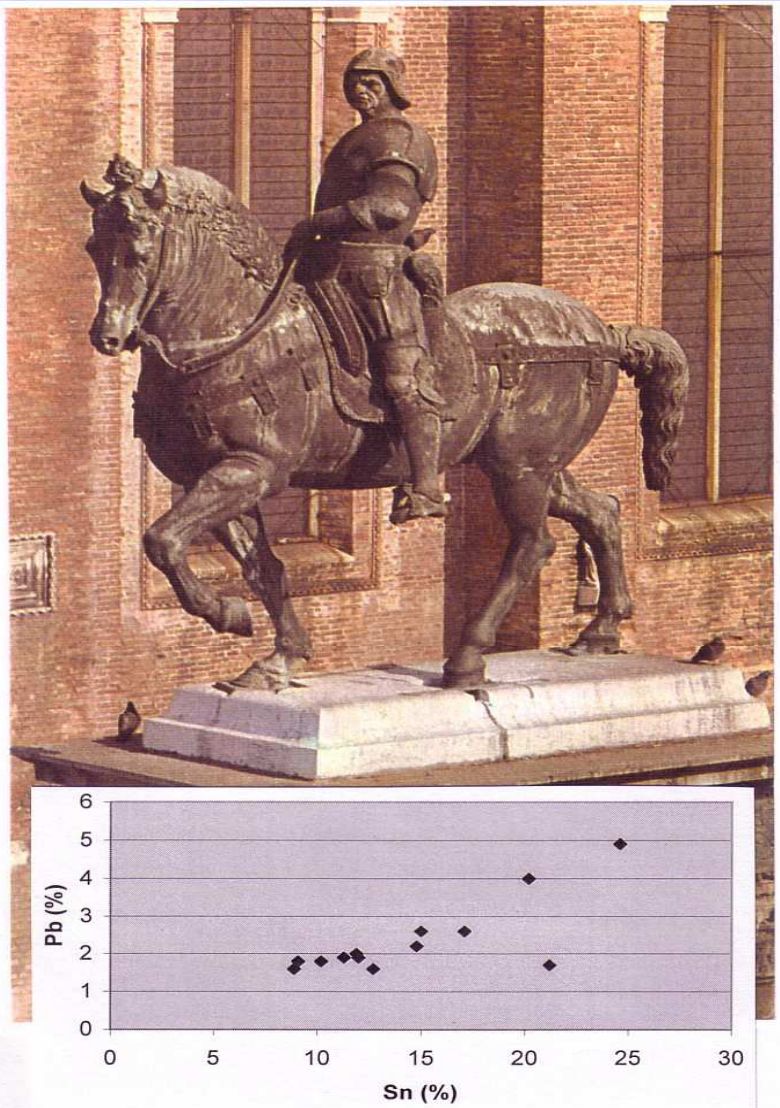

Figure 31 – The huge equestrian statue of Bartolomeo Colleoni by Andrea del Verrocchio (about 1480) , located in Campo SS. Giovanni e Paolo in Venice, and currently under restoration.
A summary of the Sn-Pb correlation obtained in cleaned areas is also shown.

A FLUORESCENCIA DE RAIOS X E UMA TECNICA ANALITICA FACIL

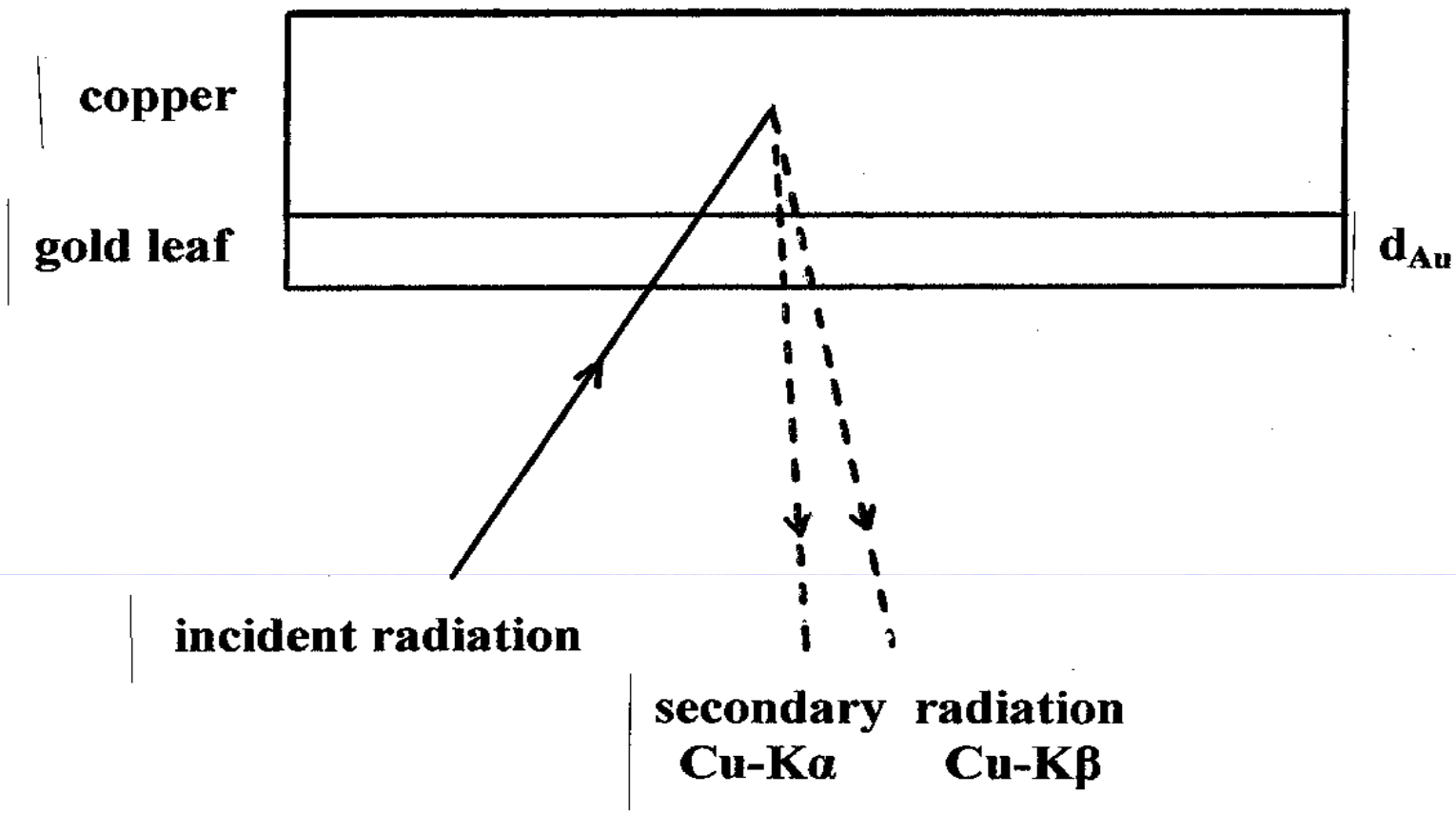
copper
gold leaf
d_{Au}
incident radiation
secondary radiation
Cu-Kα
Cu-Kβ

Figure 2

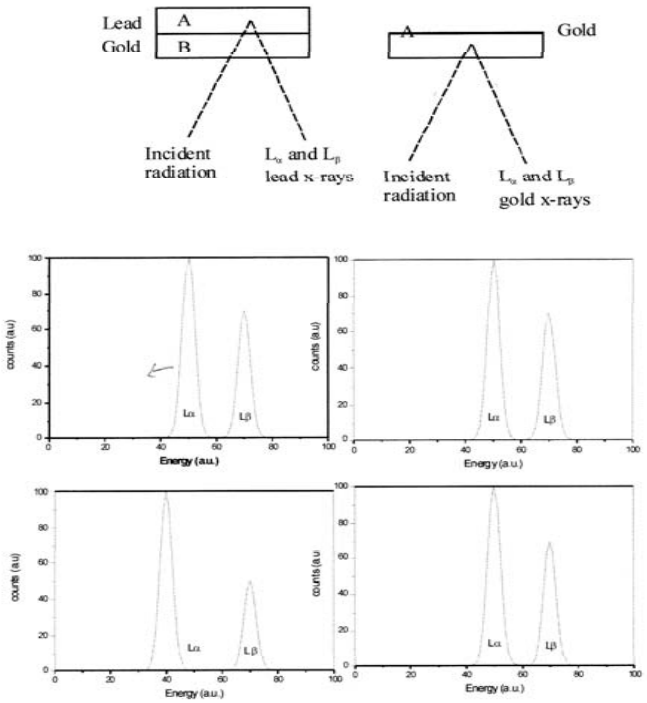
Lead
Gold
A
B
Incident radiation
L_α and L_β lead x-rays
A
Gold
Incident radiation
L_α and L_β gold x-rays
counts (a.u)
Energy (a.u.)
Lα
Lβ

MASK ON GILDED COPPER

GILDING COMPOSITION :

Au=97.5%

Ag=2.5%

(Cu difficult to determine, because present as support)

GILDING THICKNESS :

~0.6 µm

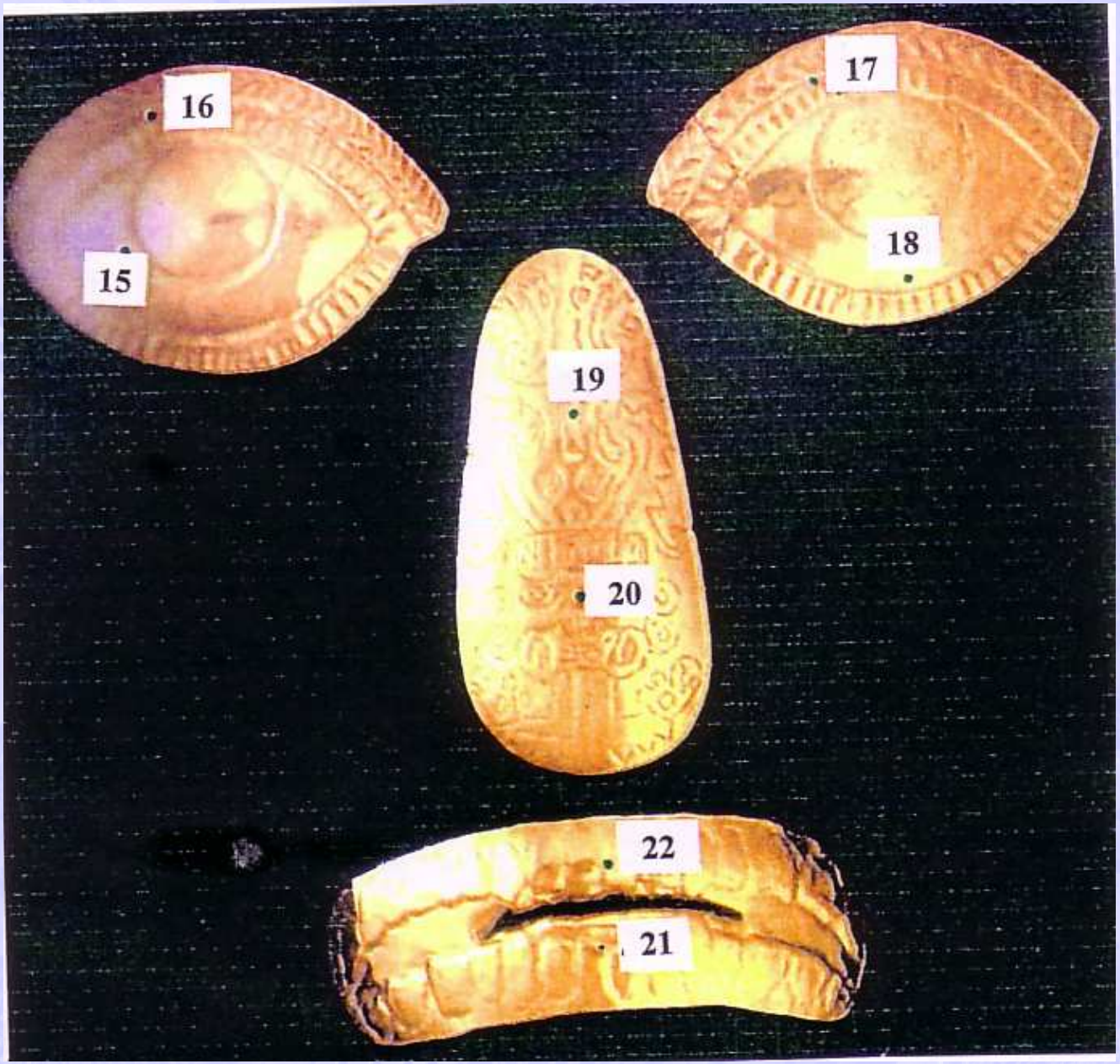
16
15
17
18
19
20
22
21

FACE COVERING, ON TUMBAGA

LEFT EYE:	RIGHT EYE	THICKNESS
Au=47.5%	Au=47.5%	2 µm
Cu=45.5%	Cu=45.5%	
Ag=8%	Ag=8%	

NOSE

Au=52.5%
Cu=34.5%
Ag=13%

THICKNESS : 2.7 µm

MOUTH

Au=49%
Cu=34%
Ag=17%

THICKNESS : 2.7 µm

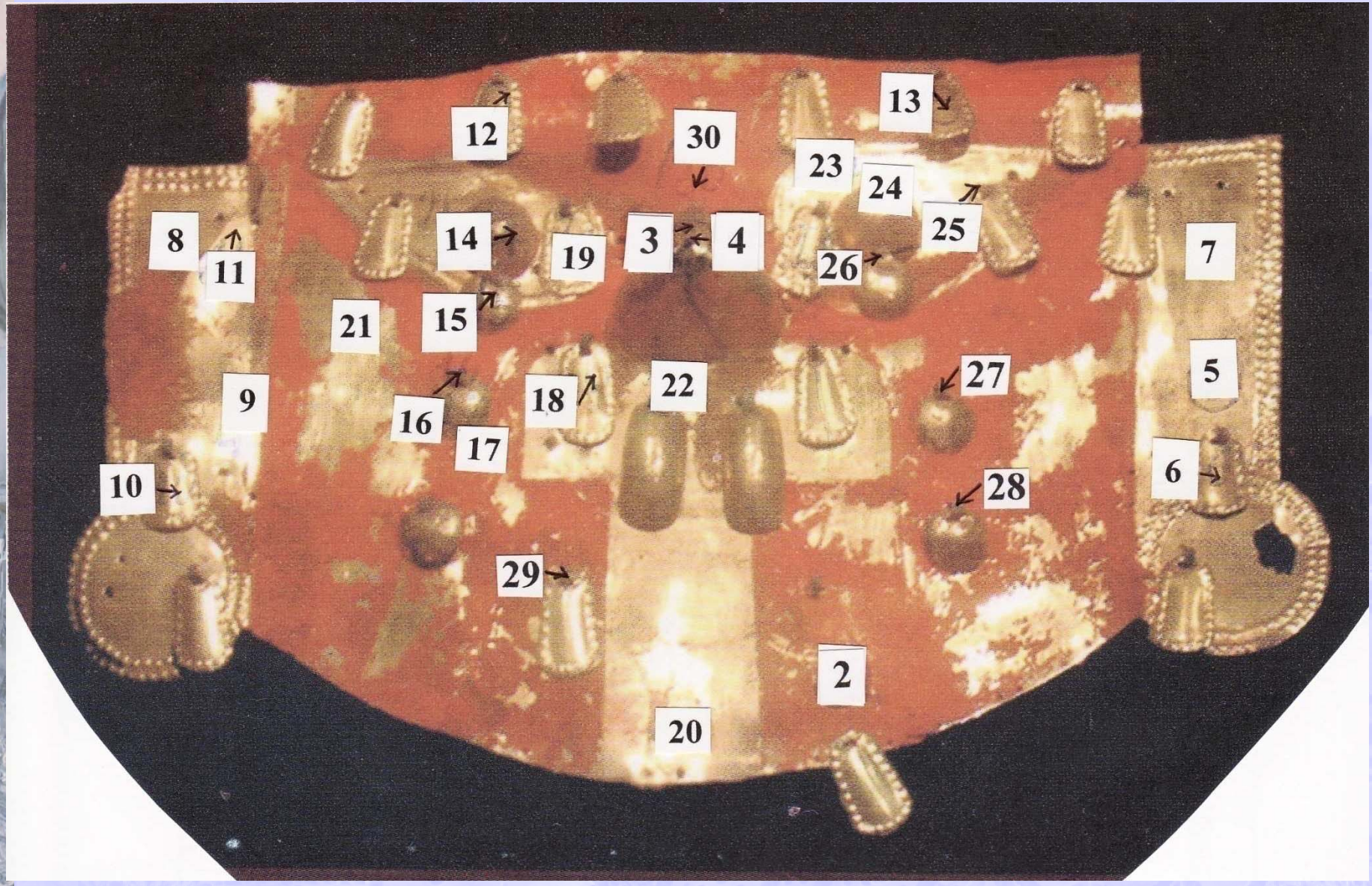
12
30
13
23
24
25
8
11
14
19
3
4
26
7
21
15
27
5
9
16
18
22
17
10
28
6
29
2
20

FUNERARY MASK ON TUMBAGA (MUSEUM OF SICÁN)

NOSE : **THICKNESS:**

Au=51%

Cu=37.5% **8 µm**

Ag=9.5%

MAIN SHEET AND PENDANTS

Au=34%

Cu=57%

Ag=7% **THICKNESS: 5 µm**

RED PIGMENT : CINNABAR

CLAMPS : ON TUMBAGA OR SILVERED COPPER

RESULTS OF THE ANALYSIS OF SIPAN ALLOYS:

GOLD

	Au(%)	Ag(%)	Cu(%)
Tomb n. 1 :	72.5	18.5	10
Tomb n.2 :	70	23	7
Tomb n.6 :	74	16	10
Mean value	70±7	20±7	10±4

SILVER

	Ag(%)	Cu(%)	Au(%)
Mean value	92.5±3	4.5±2	3±1.5

TURQUOISE

	Cu(%)	Fe(%)	Zn(%)
Mean value	81.5±6	10±4	8.5±3.5

COPPER

Mean value Cu ≥ 99.5%

SOLDERING

Copper or silver/copper alloy

COMPARISON BETWEEN SIPAN (400 A.C.) AND SICAN (>750 A.C.)

SIPAN	Au(%)	Ag(%)	Cu(%)	Pb(%)	Br(%)	As(%)	Fe(%)
GOLD:	70	20	10	-	-	-	-
SILVER:	3	92	5	-	-	-	-
COPPER :	-	-	> 99.5	-	-	-	-
GILDING :	9	2.5	-	-	-	-	-
TUMBAGA :	50	13	37	-	-	-	-
SICAN							
GOLD	62	32	6	-	-	-	-
SILVER	0.5	94	3.7	0.8	1	-	-
COPPER	-	-	97.9	-	-	0.9	2.4
GILDING	66	35	?	-	-	-	-
TUMBAGA	34	7	57	-	-	-	-

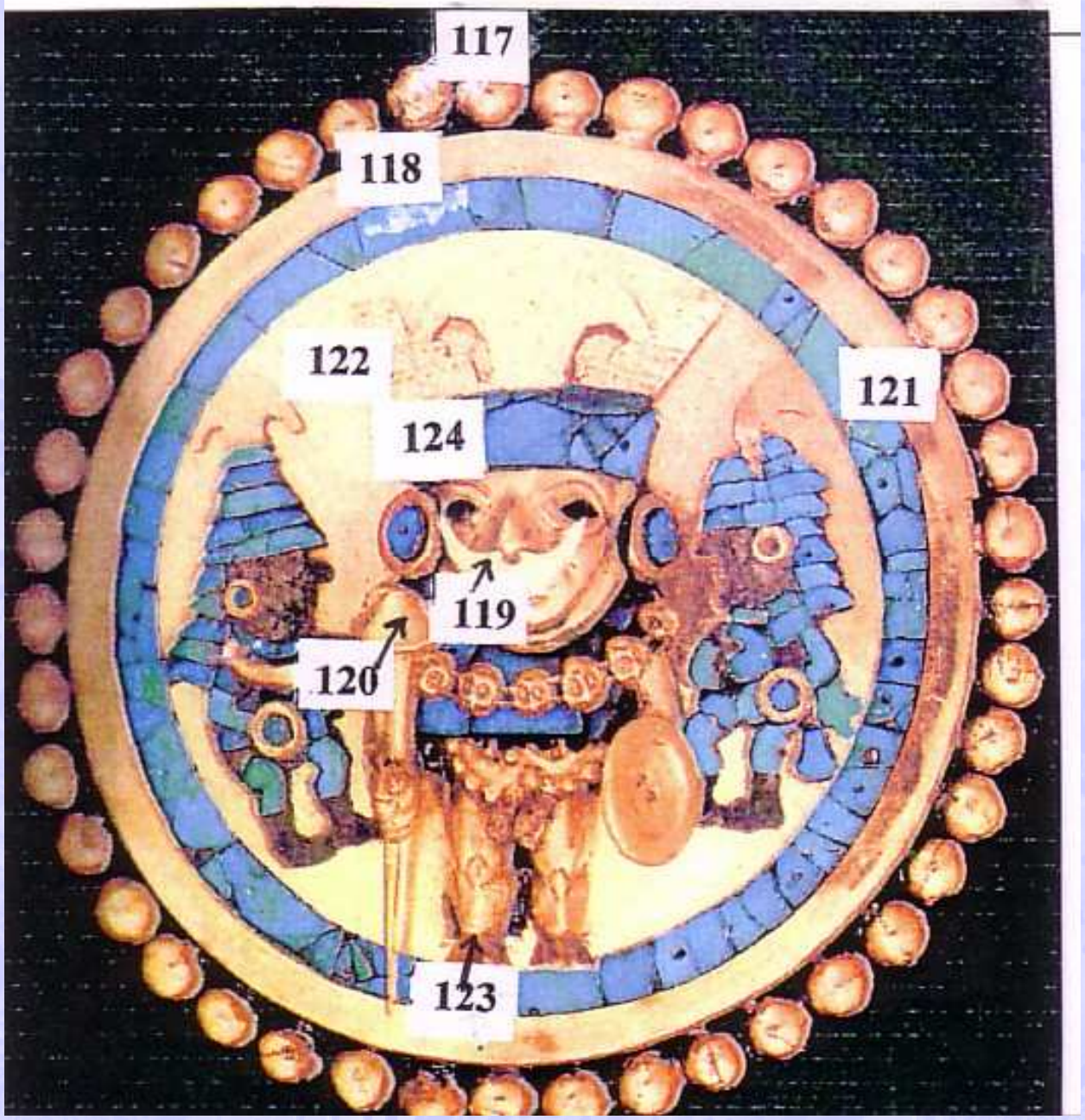

earring

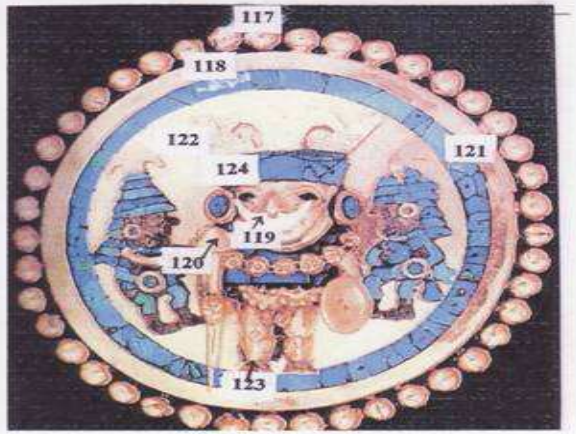
117
118
122
124
121
119
120
123

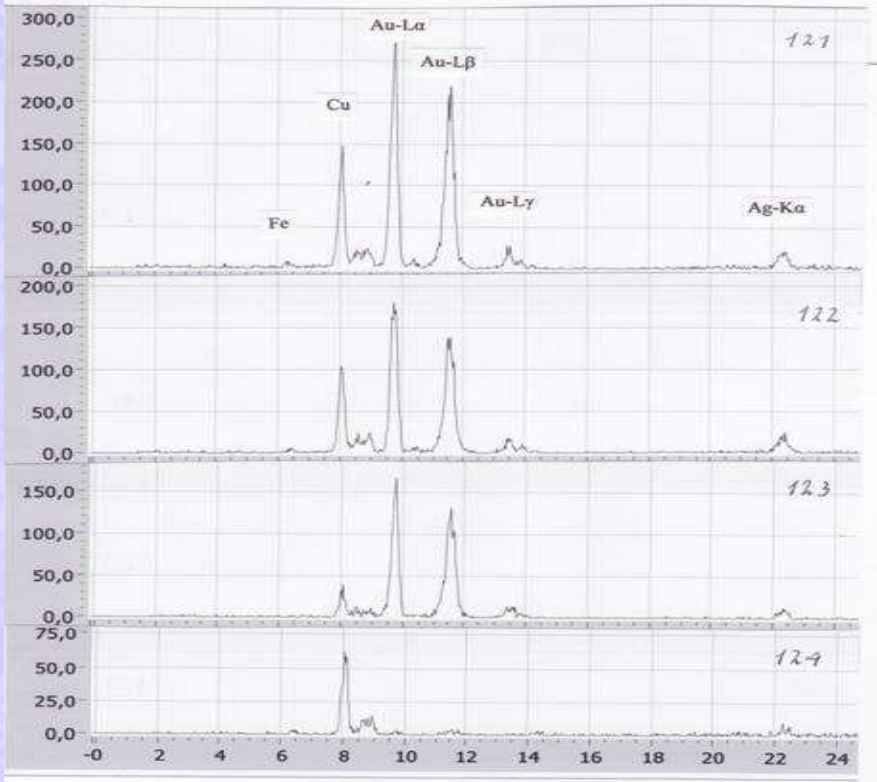
Au-Lα
Au-Lβ
Cu
Fe
Au-Lγ
Ag-Kα
121
122
123
124
300,0
250,0
200,0
150,0
100,0
50,0
0,0
75,0
25,0
-0
2
4
6
8
10
12
14
16
18
20
22
24

earring

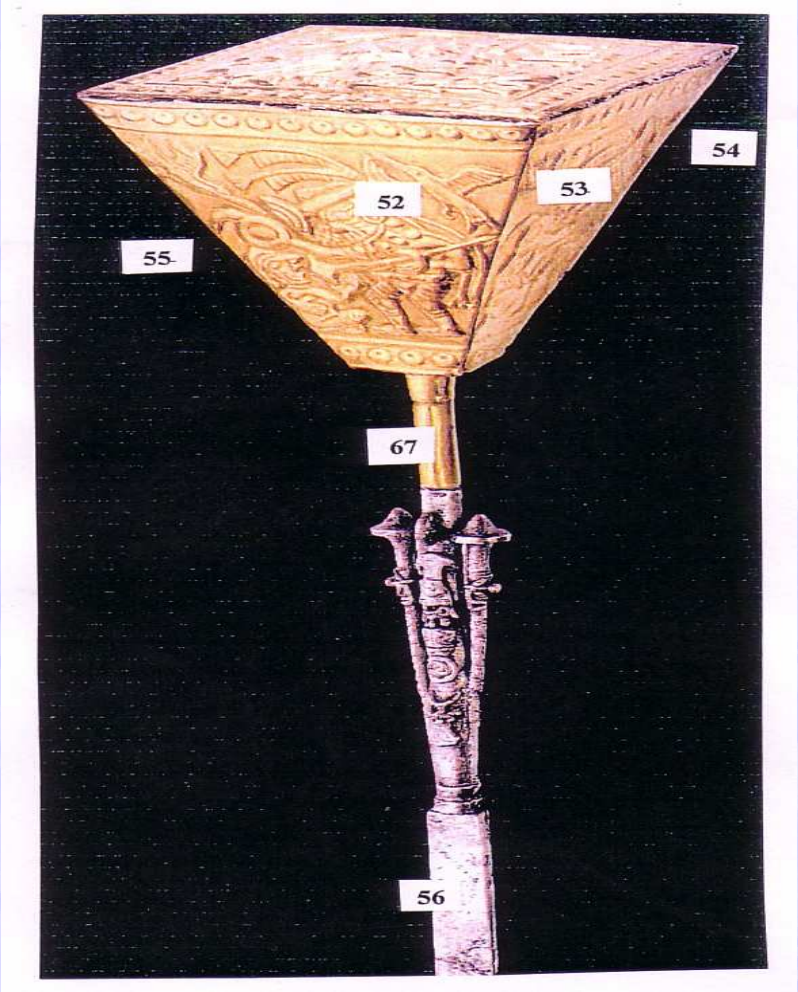

Command stick of the “Señor de Sipan” on gold, with a support on silver

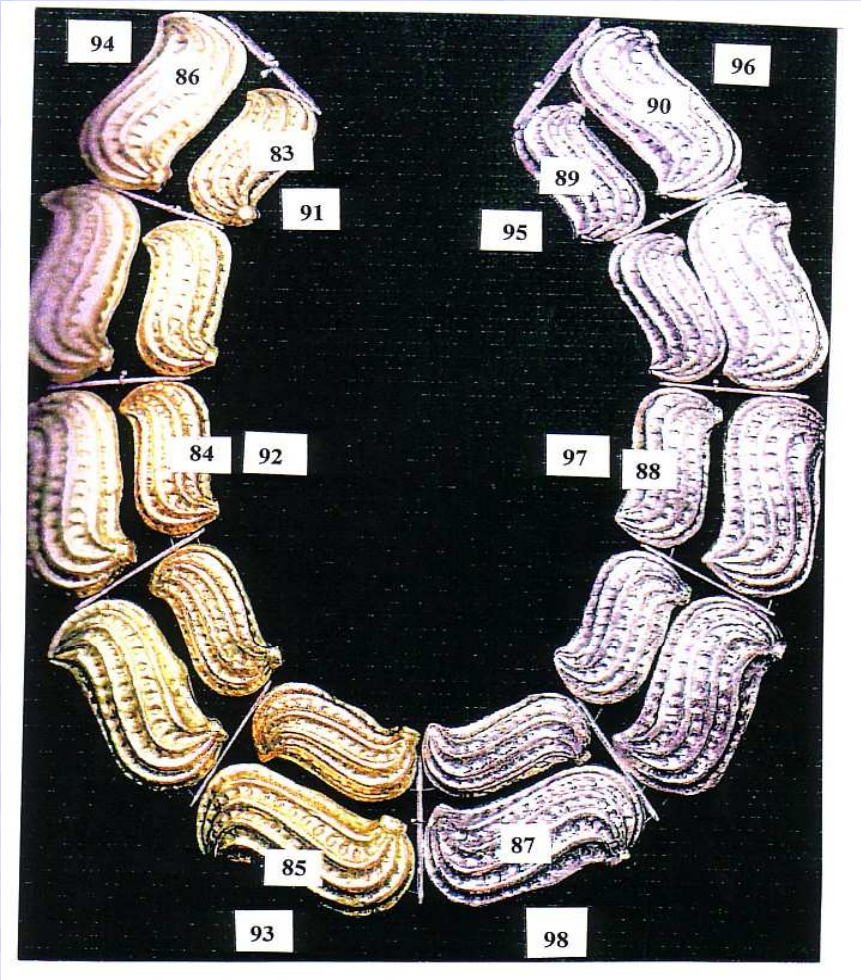

Necklace with peanuts on gold and silver

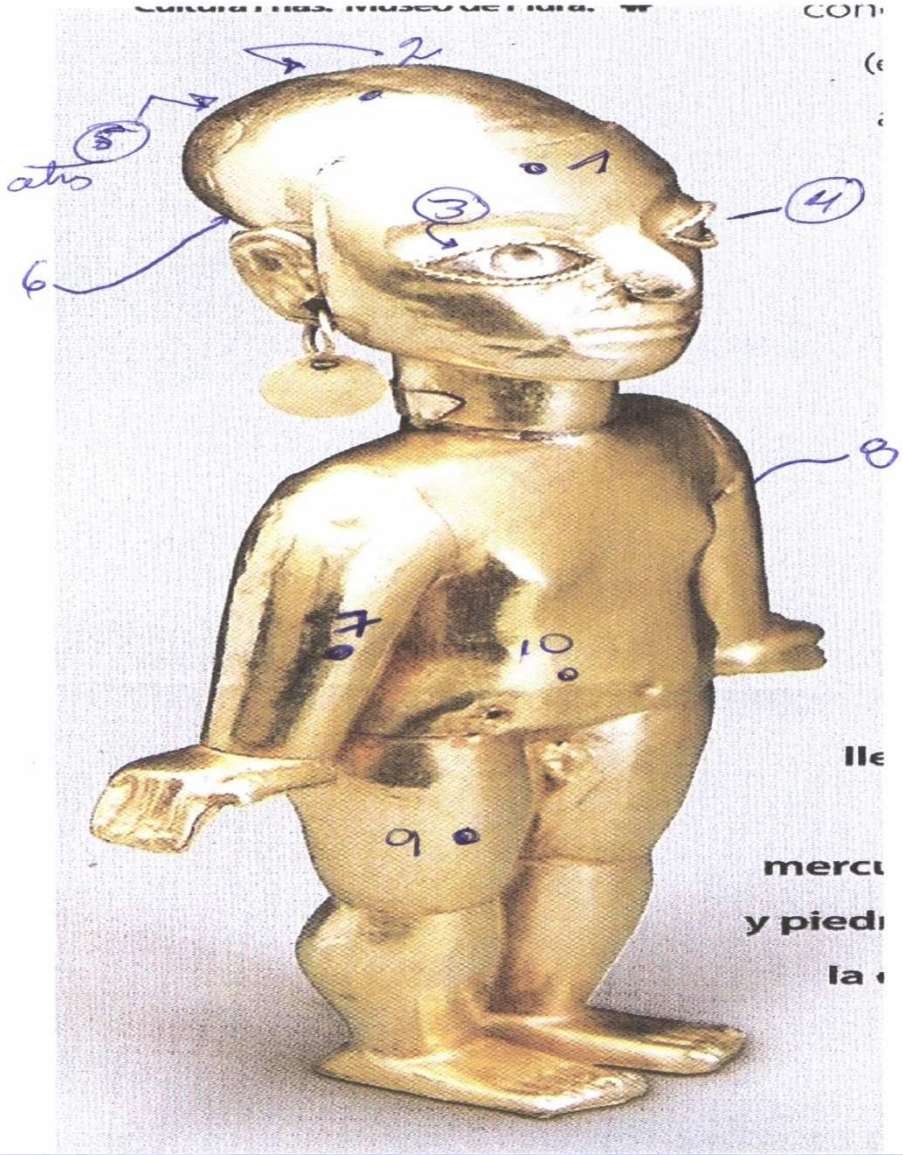
1
2
3
4
5
6
7
8
9
10


1
2
3
4
5
6
7
8
2

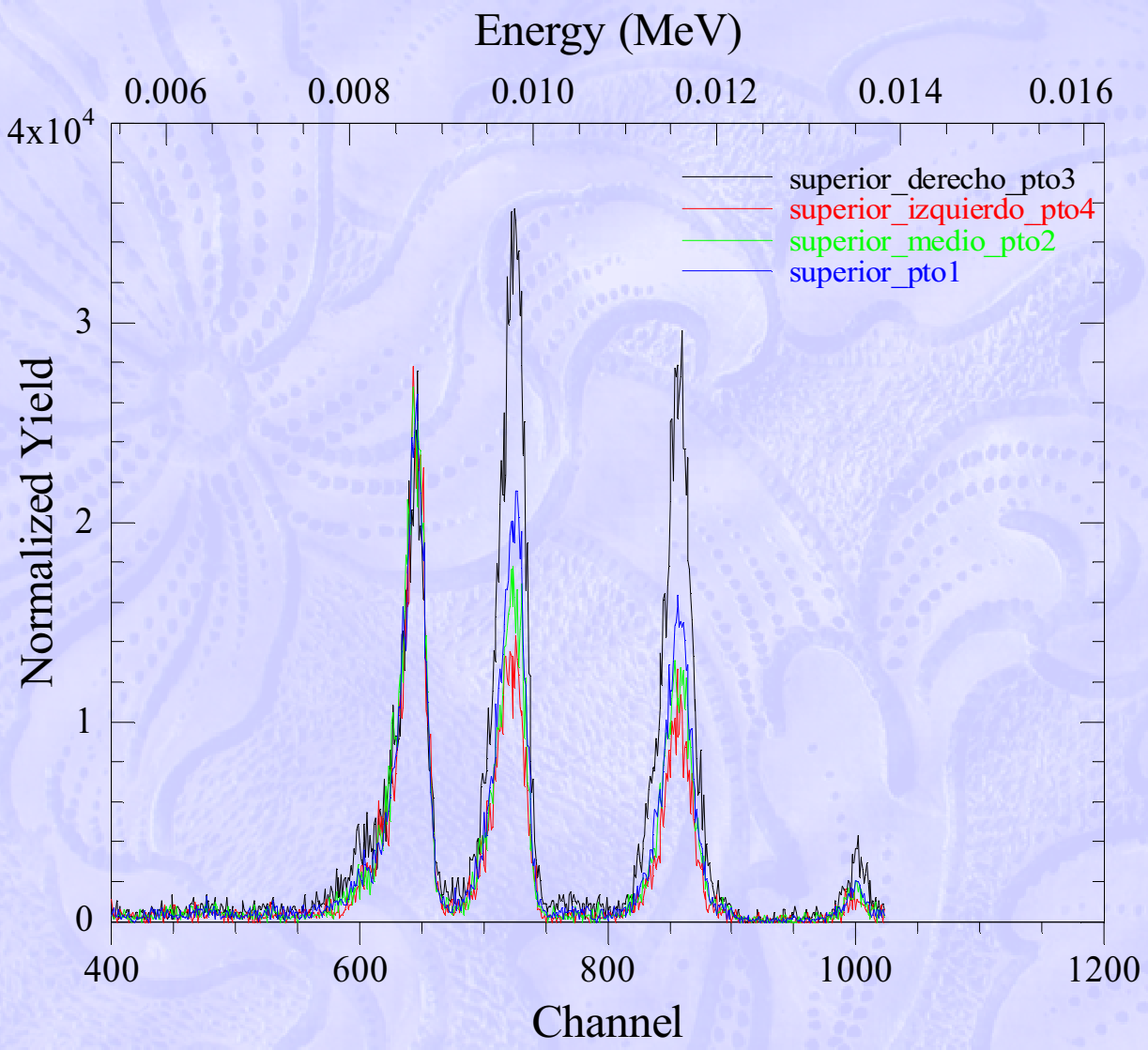
Energy (MeV)
0.006
0.008
0.010
0.012
0.014
0.016
4x10^4
3
2
1
0
Normalized Yield
superior_derecho_pto3
superior_izquierdo_pto4
superior_medio_pto2
superior_pto1
400
600
800
1000
1200
Channel


4
2
1
6
3

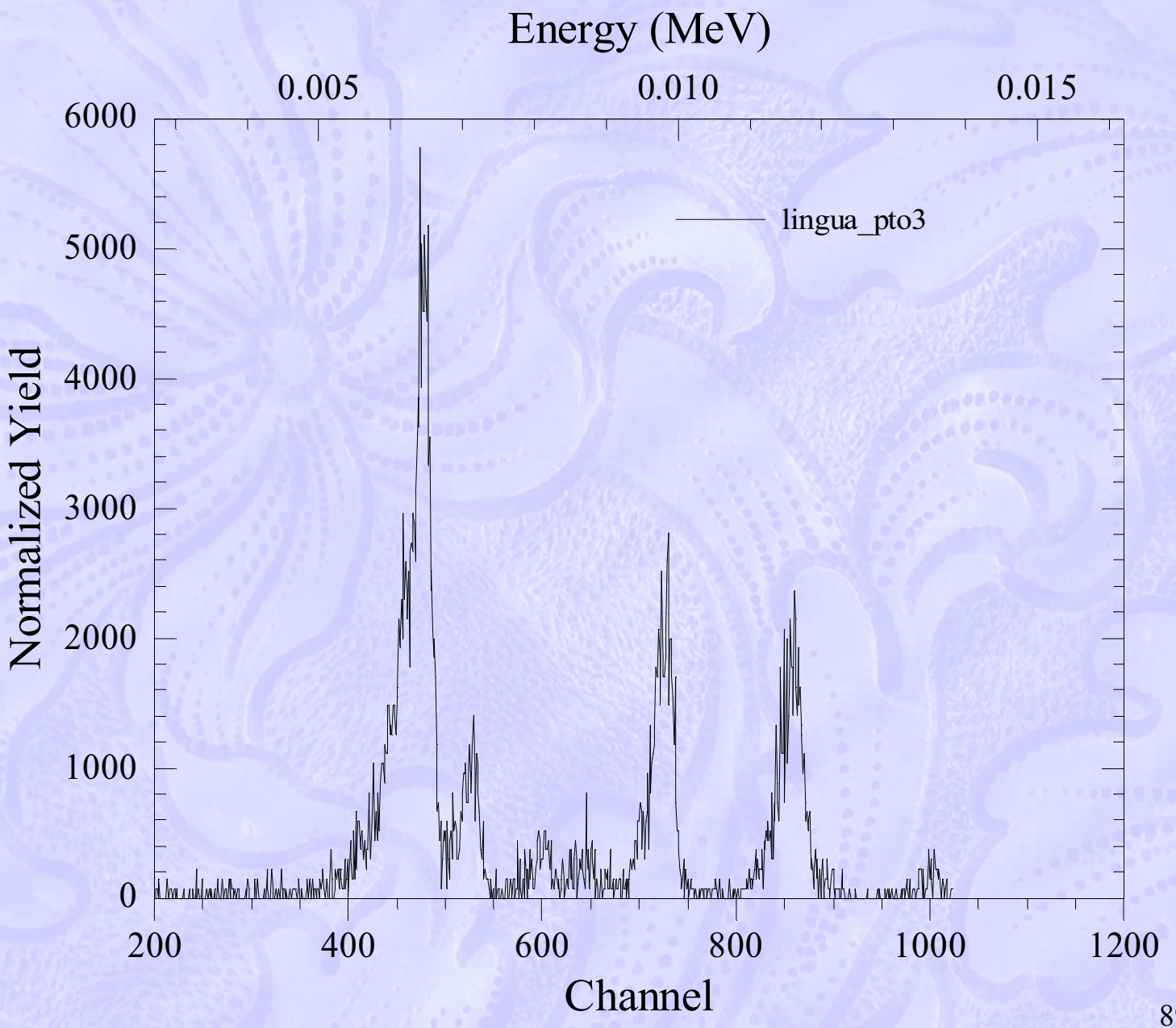
Energy (MeV)
0.005
0.010
0.015
6000
5000
4000
3000
2000
1000
0
Normalized Yield
lingua_pto3
200
400
600
800
1000
1200
Channel

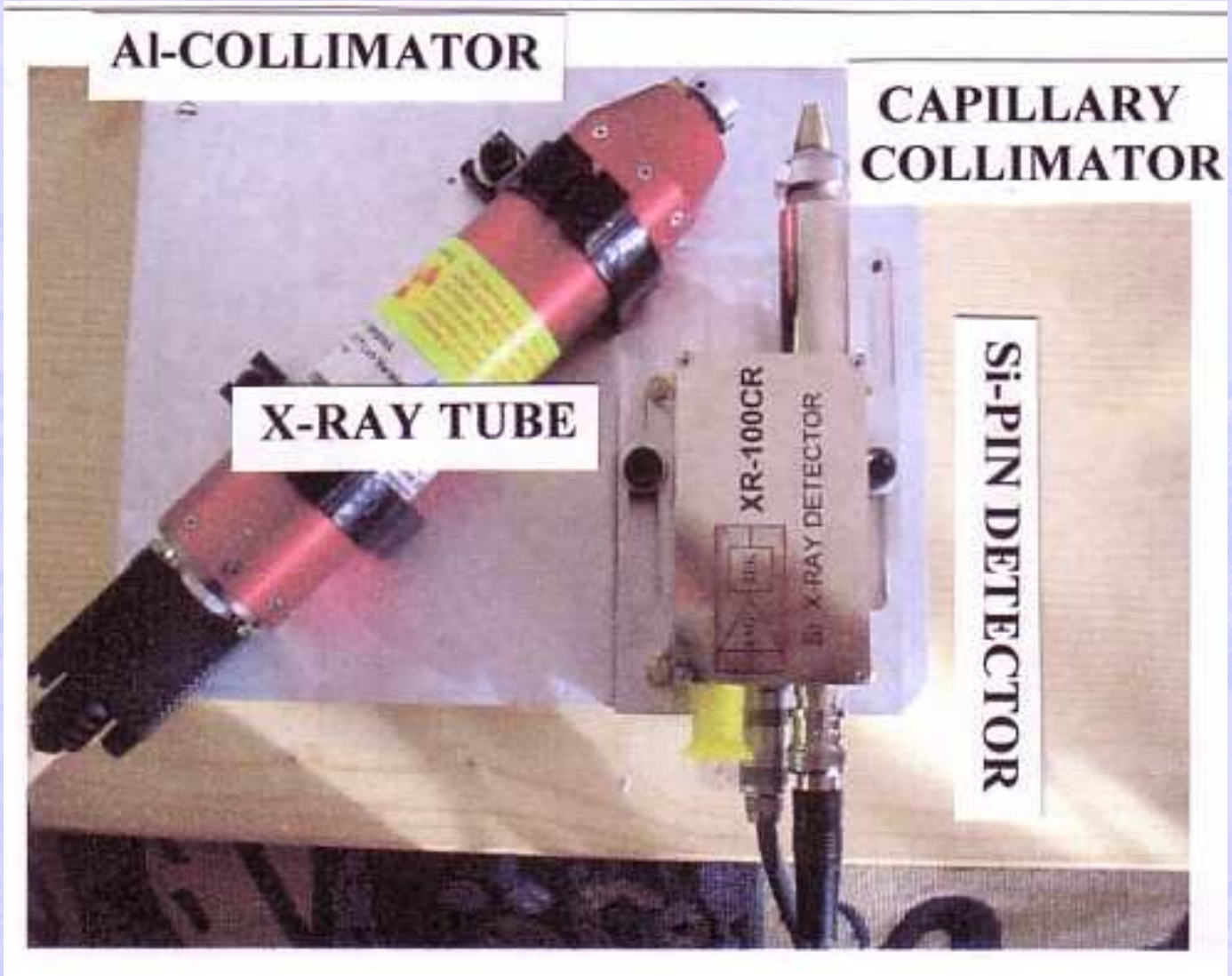

EDXRF-equipment with a conic capillary collimator on the detector window

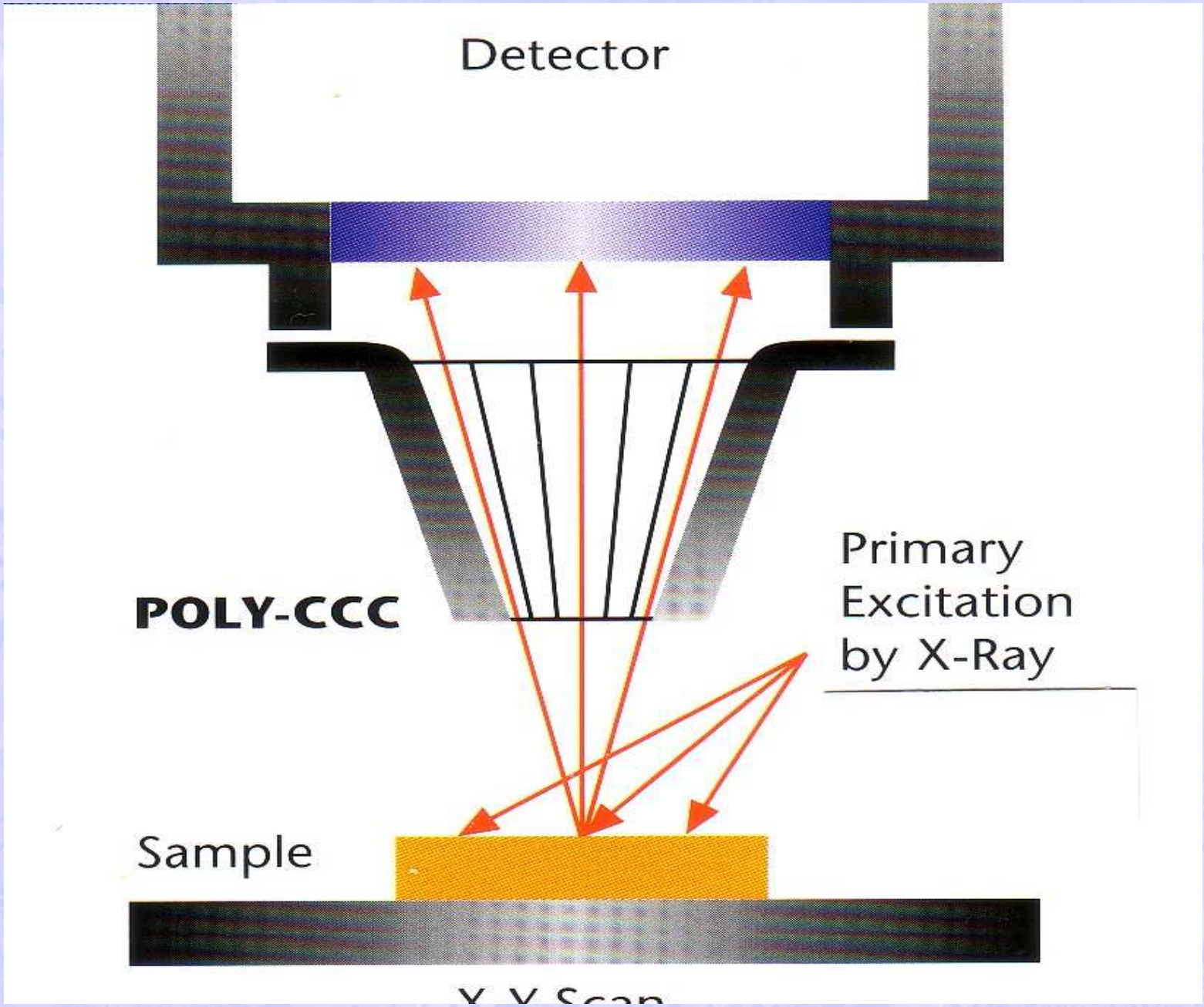
Detector
POLY-CCC
Primary
Excitation
by X-Ray
Sample

In the case of Sipan alloys (gold, silver, copper alloys) , Different situation have been observed:

-gold, composed as usually of gold, silver and copper;

-gilded copper ;

-tumbaga gold (poor Au-alloys enriched at the surface) ;

-silver, composed as usually of silver and copper (but also gold is generally present);

-tumbaga silver ;

-copper , generally almost pure.

How gold, gilded copper and tumbaga can be differentiated ?

How can be determined the gilding thickness ?

-by accurately measuring the Kα/Kβ-ratio emitted by the deeper element (for example Cu or Ag for gilded copper or gilded silver respectively);

-by plotting the ratio between (Cu/Au) or (Ag/Au) counts

-by carrying out EDXRF-measurements at various angles source-sample-detector, to help in the thickness determination.

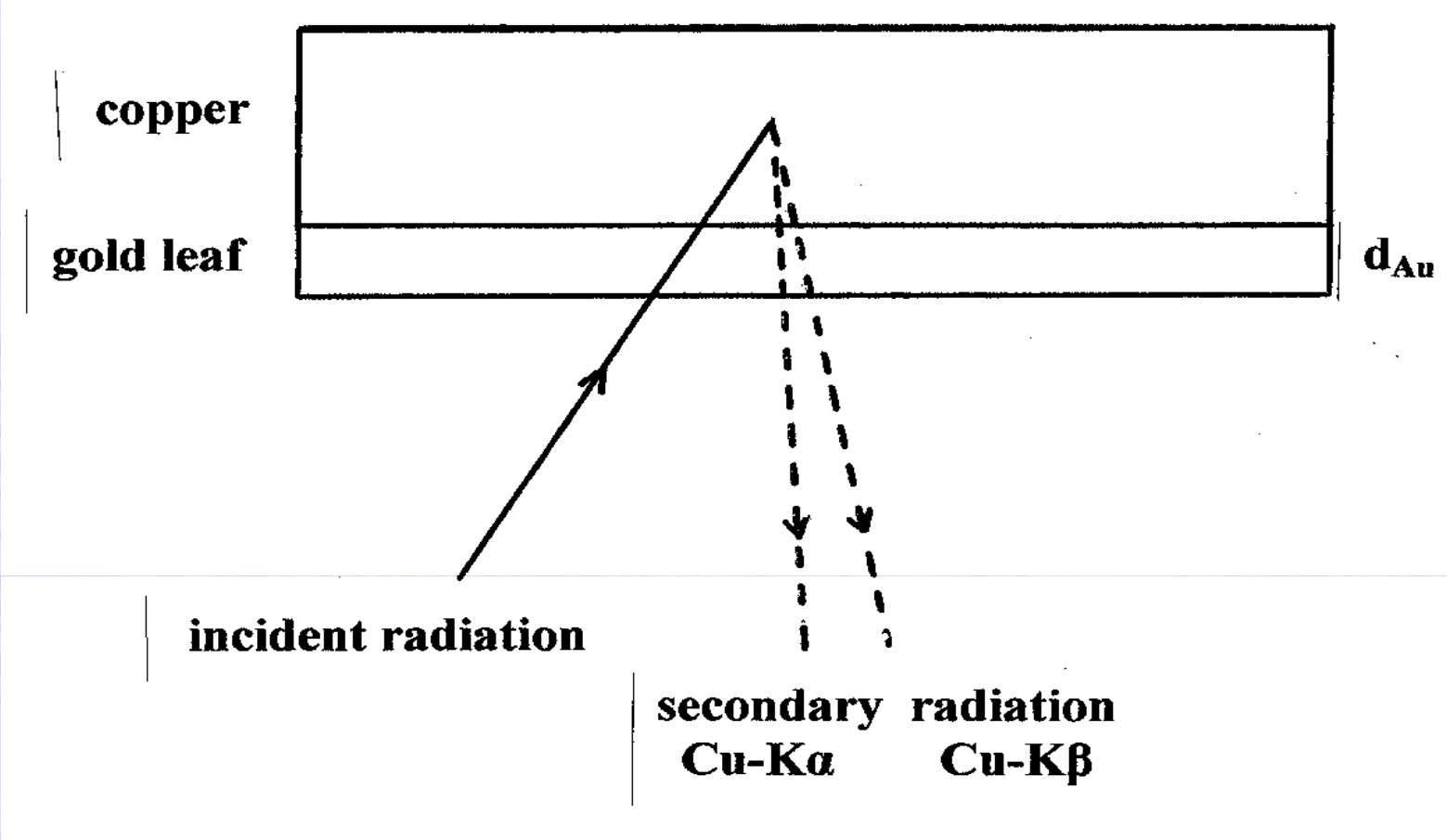

Gilding thickness determined by an altered Cu(Kα/Kβ)-ratio, when Cu-lines cross the Au-leaf, or by (Cu-K/Au-L)-ratio,

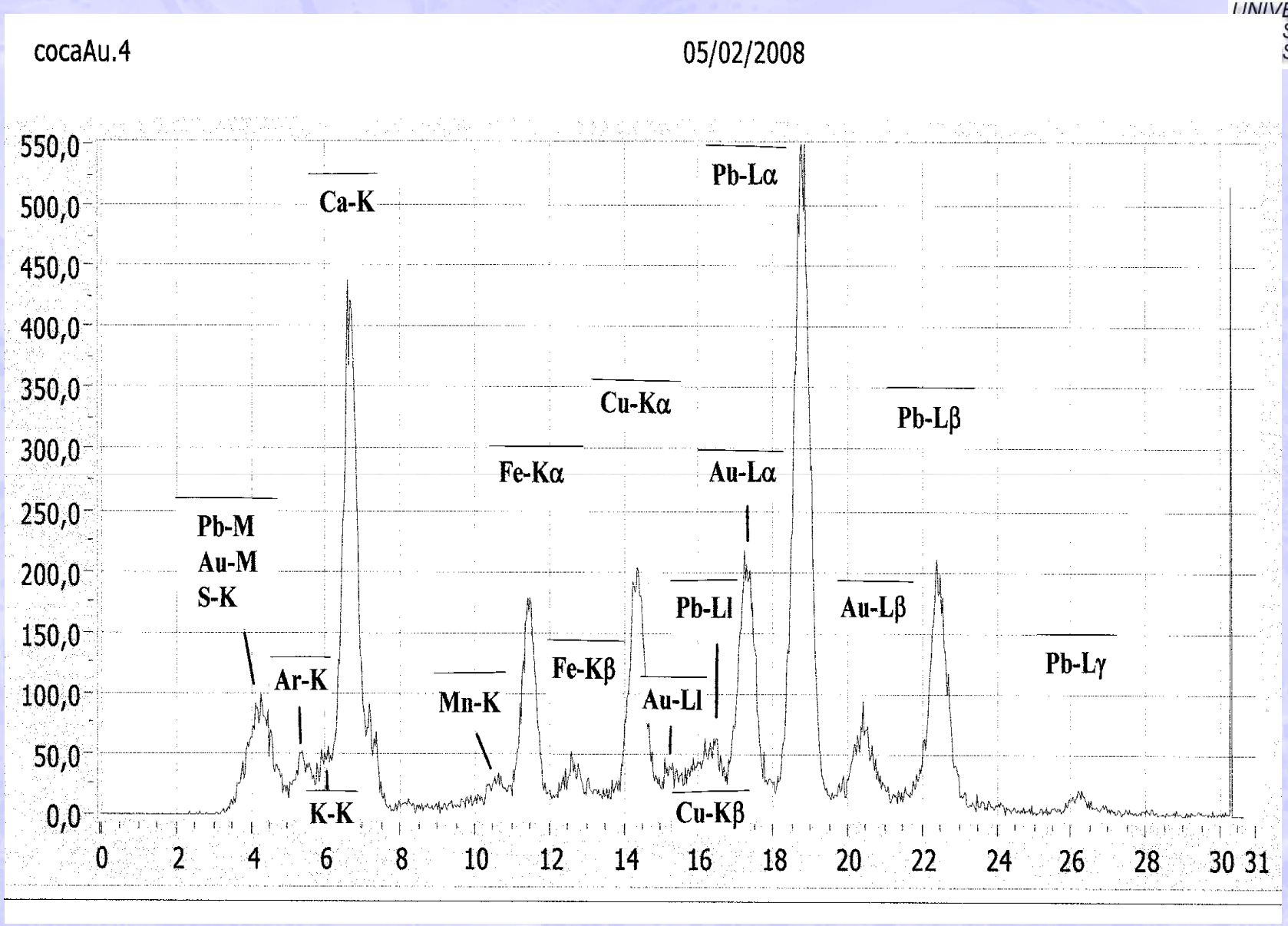
cocaAu.4
05/02/2008
550,0
500,0
450,0
400,0
350,0
300,0
250,0
200,0
150,0
100,0
50,0
0,0
Ca-K
Pb-Lα
Cu-Kα
Pb-Lβ
Fe-Kα
Au-Lα
Pb-M
Au-M
S-K
Pb-Ll
Au-Lβ
Ar-K
Fe-Kβ
Pb-Lγ
Mn-K
Au-Ll
K-K
Cu-Kβ
0
2
4
6
8
10
12
14
16
18
20
22
24
26
28
30
31

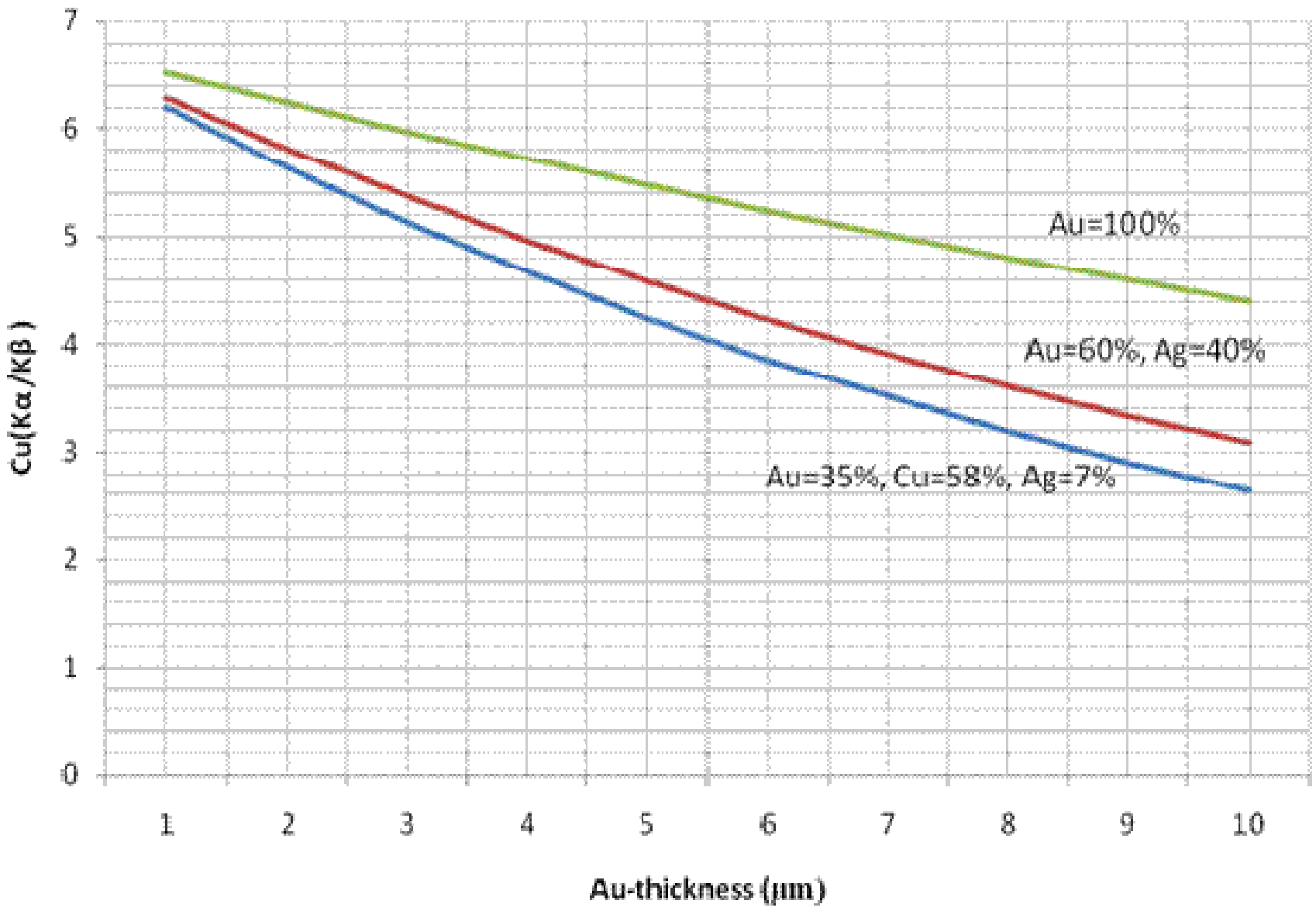
Cu(Kα/Kβ)
7
6
5
4
3
2
1
0
1
2
3
4
5
6
7
8
9
10
Au-thickness (μm)
Au=100%
Au=60%, Ag=40%
Au=35%, Cu=58%, Ag=7%

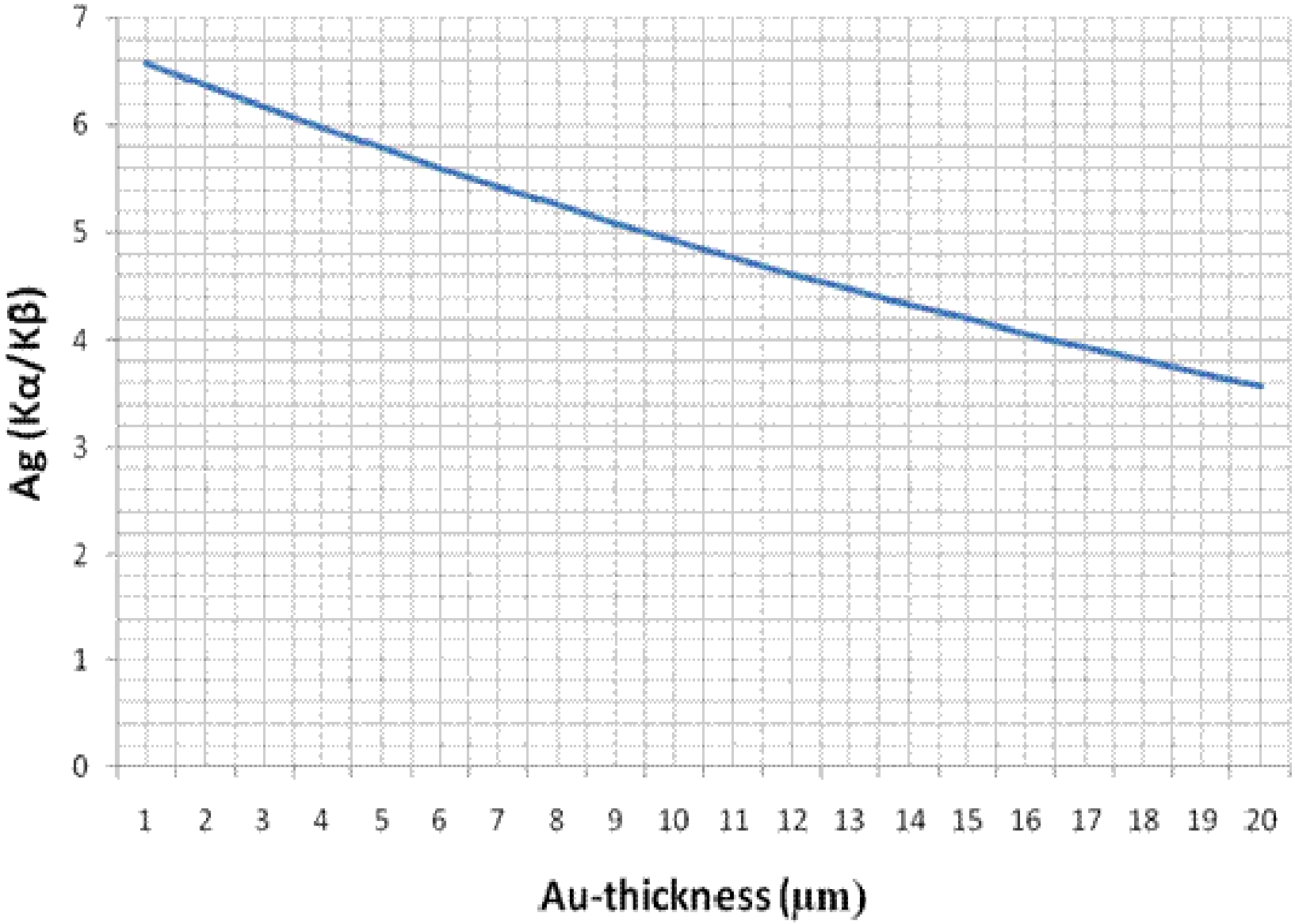
Ag (Kα/Kβ)
7
6
5
4
3
2
1
0
1 2 3 4 5 6 7 8 9 10 11 12 13 14 15 16 17 18 19 20
Au-thickness (µm)

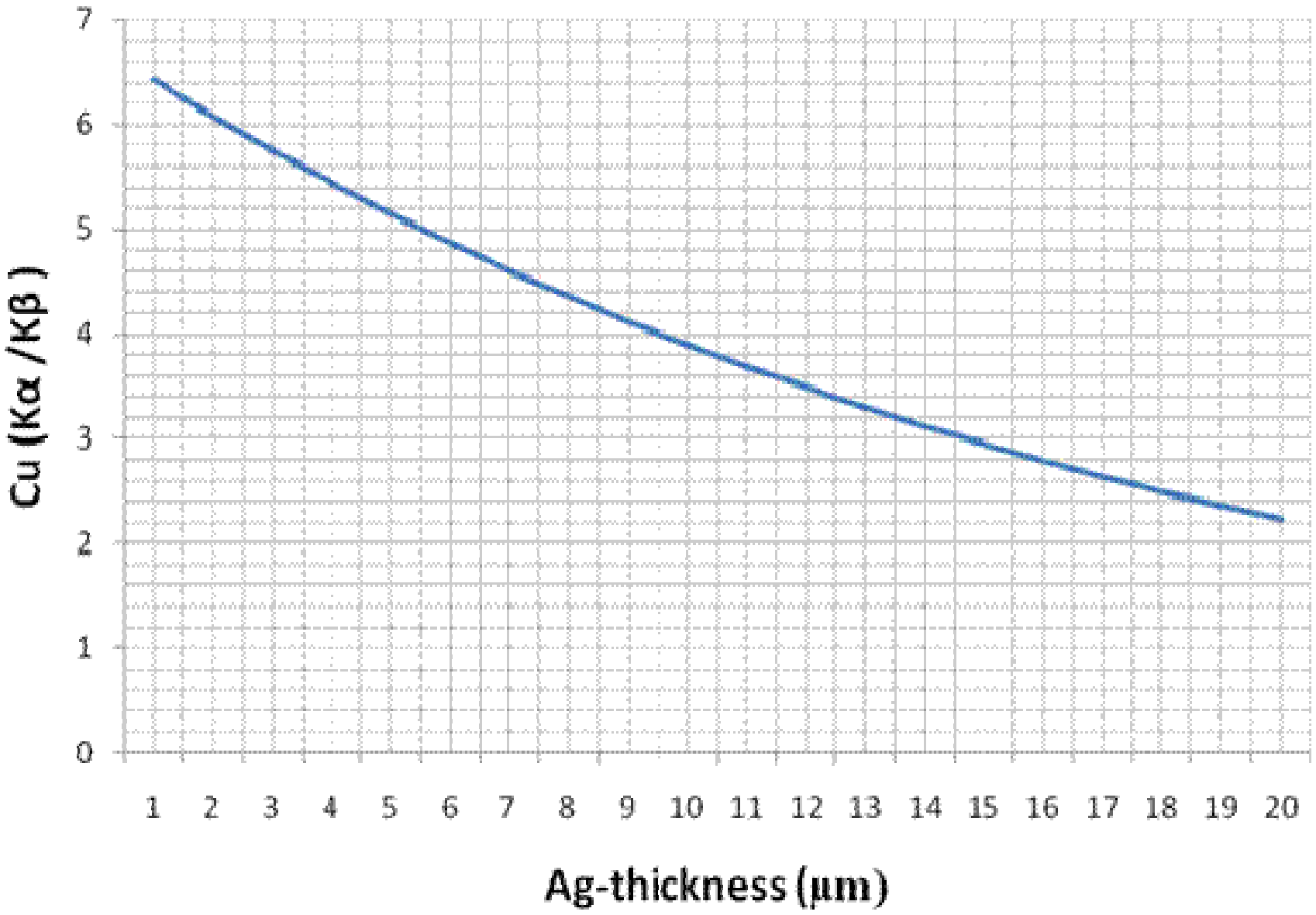
Cu (Kα /Kβ)
0
1
2
3
4
5
6
7
1 2 3 4 5 6 7 8 9 10 11 12 13 14 15 16 17 18 19 20
Ag-thickness (µm)

RESULTS OF THE ANALYSIS OF SIPAN ALLOYS:

GOLD

	Au(%)	Ag(%)	Cu(%)
Tomb n. 1 :	72.5	18.5	10
Tomb n.2 :	70	23	7
Tomb n.6 :	74	16	10
Mean value	70±7	20±7	10±4

SILVER

	Ag(%)	Cu(%)	Au(%)
Mean value	92.5±3	4.5±2	3±1.5

TURQUOISE

	Cu(%)	Fe(%)	Zn(%)
Mean value	81.5±6	10±4	8.5±3.5

COPPER

Mean value Cu ≥ 99.5%

SOLDERING

Copper or silver/copper alloy

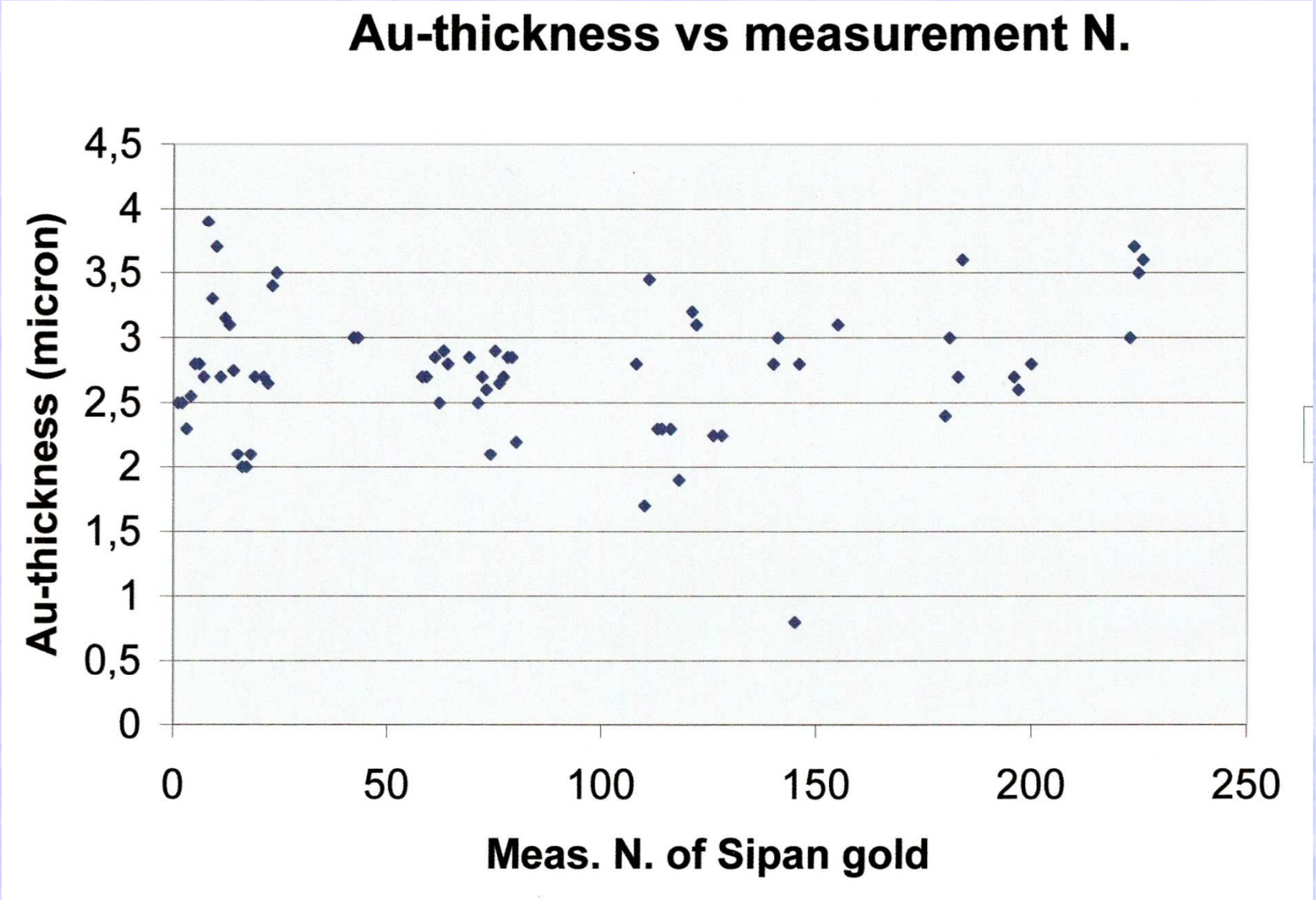
Au-thickness vs measurement N.
Au-thickness (micron)
4,5
4
3,5
3
2,5
2
1,5
1
0,5
0
0
50
100
150
200
250
Meas. N. of Sipan gold

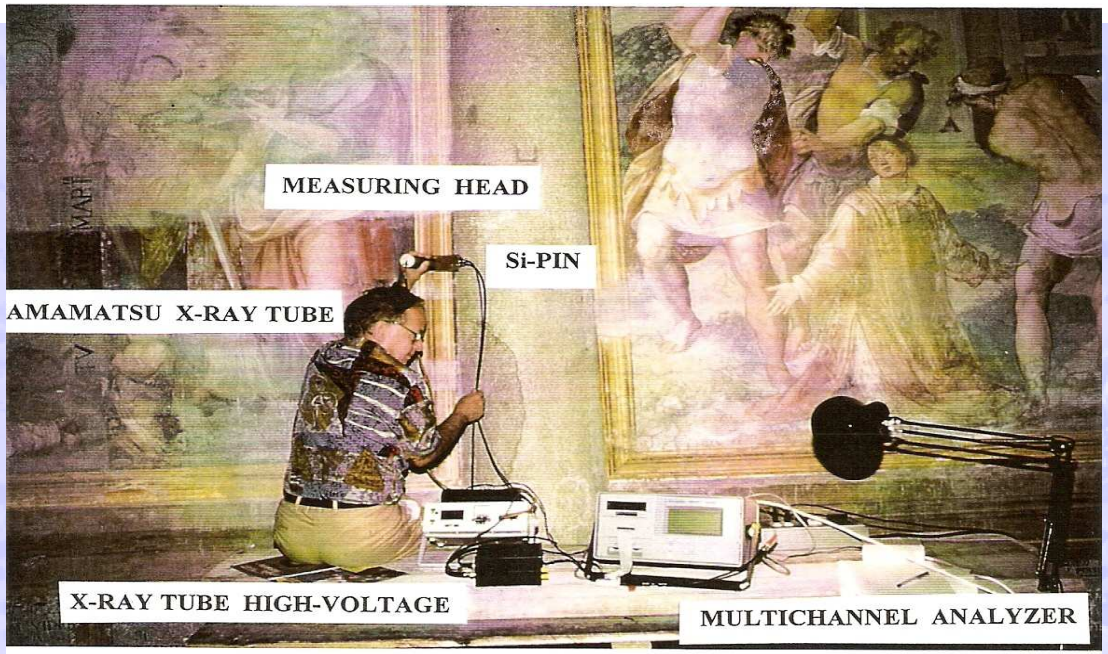
MEASURING HEAD
Si-PIN
AMAMATSU X-RAY TUBE
X-RAY TUBE HIGH-VOLTAGE
MULTICHANNEL ANALYZER

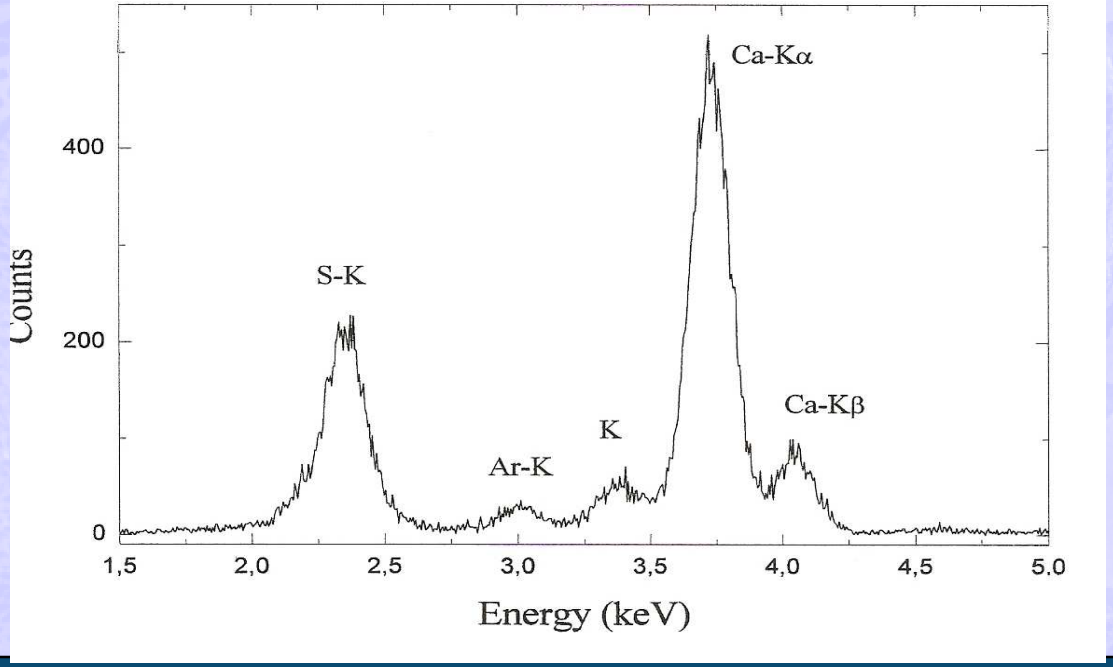
Counts
400
200
0
S-K
Ar-K
K
Ca-Kα
Ca-Kβ
1,5
2,0
2,5
3,0
3,5
4,0
4,5
5,0
Energy (keV)

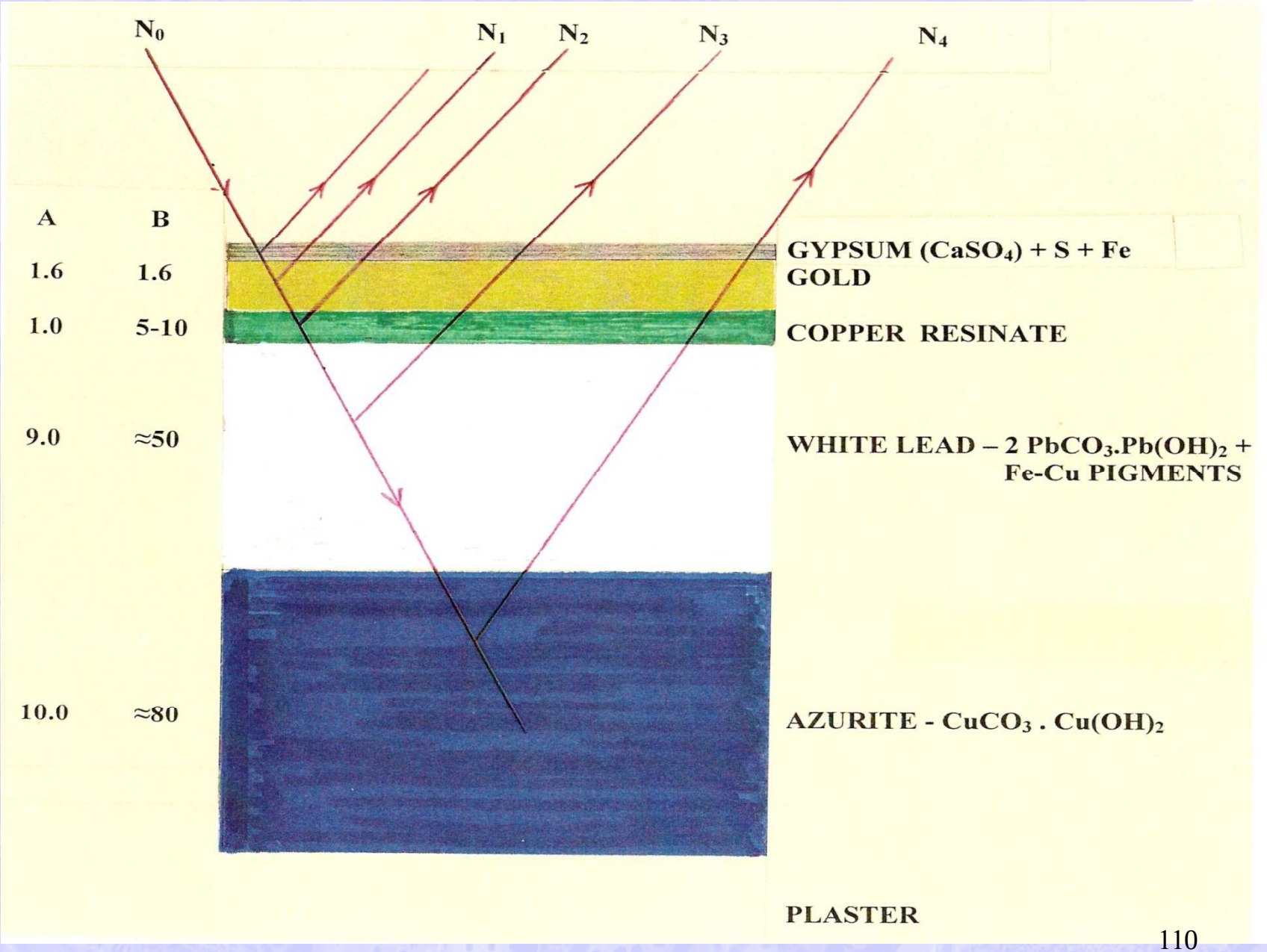
N_0
N_1
N_2
N_3
N_4
A
B
1.6
1.6
1.0
5-10
9.0
≈50
10.0
≈80
GYPSUM ($CaSO_4$) + S + Fe
GOLD
COPPER RESINATE
WHITE LEAD – 2 $PbCO_3.Pb(OH)_2$ +
Fe-Cu PIGMENTS
AZURITE - $CuCO_3$. $Cu(OH)_2$
PLASTER

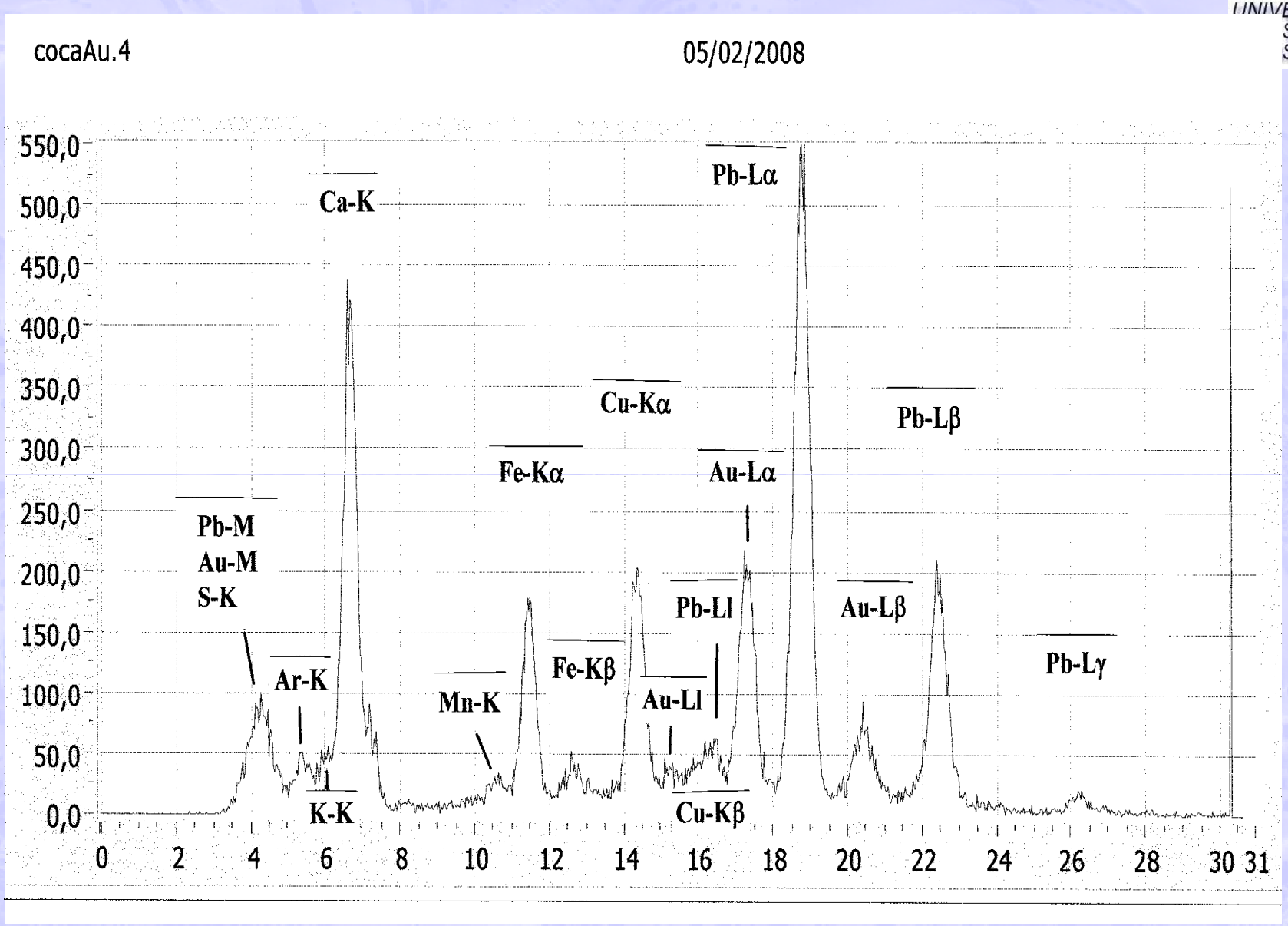
cocaAu.4
05/02/2008
550,0
500,0
450,0
400,0
350,0
300,0
250,0
200,0
150,0
100,0
50,0
0,0
0
2
4
6
8
10
12
14
16
18
20
22
24
26
28
30
31
Ca-K
Pb-Lα
Cu-Kα
Pb-Lβ
Fe-Kα
Au-Lα
Pb-M
Au-M
S-K
Pb-Ll
Au-Lβ
Ar-K
Fe-Kβ
Pb-Lγ
Mn-K
Au-Ll
K-K
Cu-Kβ

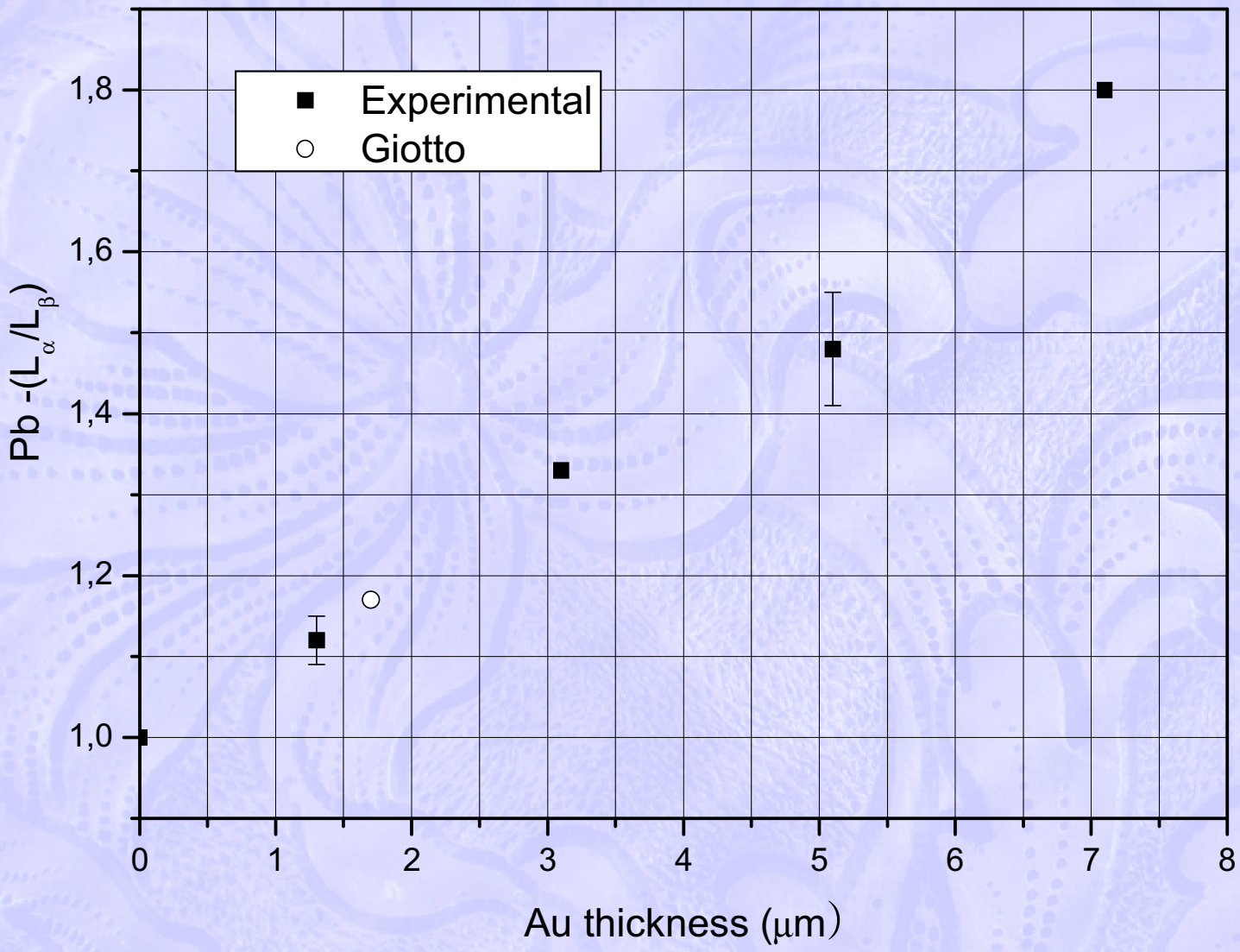
Experimental
Giotto
1,8
1,6
1,4
1,2
1,0
Pb -(L$_\alpha$/L$_\beta$)
0
1
2
3
4
5
6
7
8
Au thickness (μm)

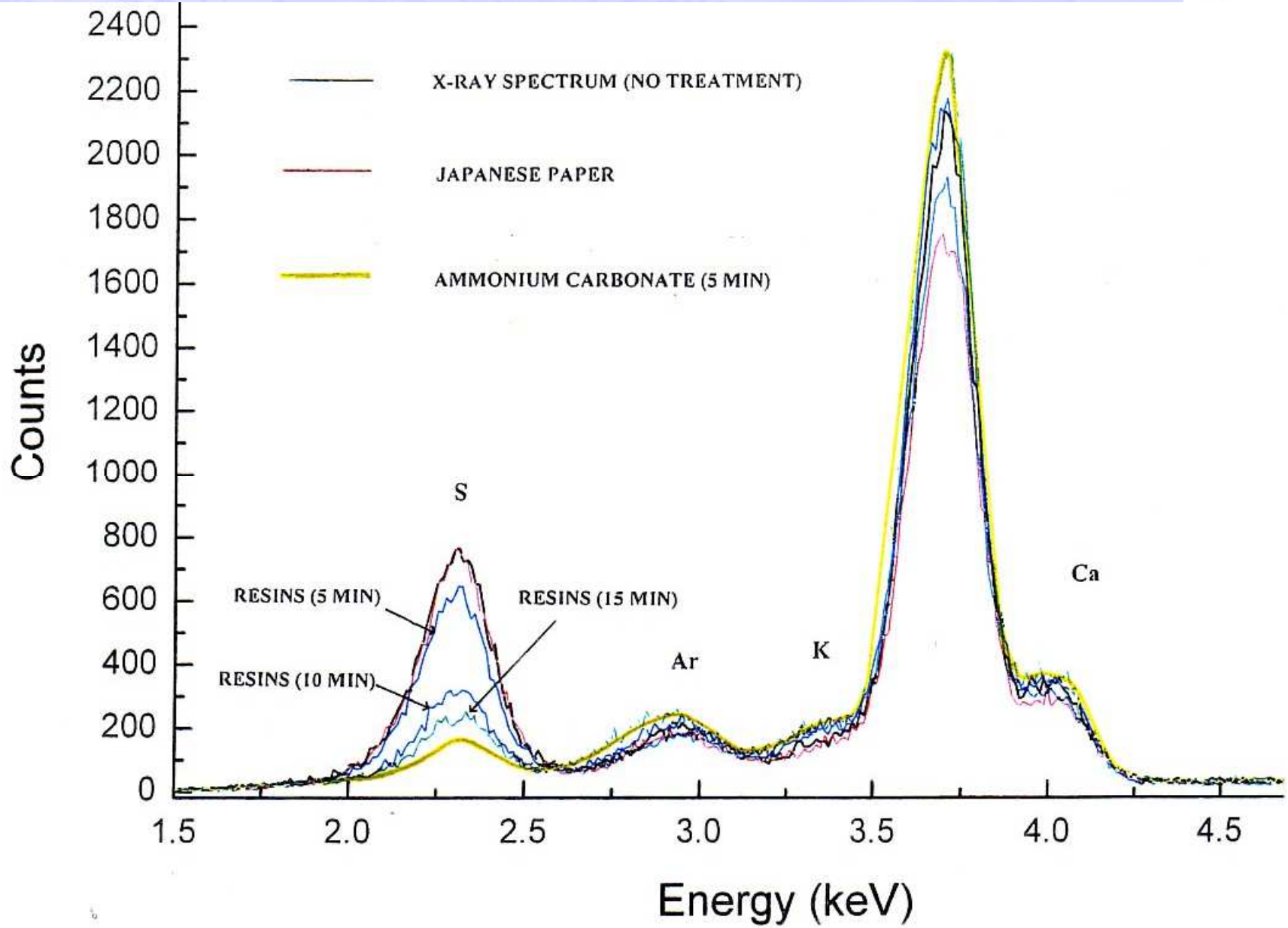
X-RAY SPECTRUM (NO TREATMENT)
JAPANESE PAPER
AMMONIUM CARBONATE (5 MIN)
Counts
2400
2200
2000
1800
1600
1400
1200
1000
800
600
400
200
0
S
RESINS (5 MIN)
RESINS (15 MIN)
RESINS (10 MIN)
Ar
K
Ca
1.5
2.0
2.5
3.0
3.5
4.0
4.5
Energy (keV)

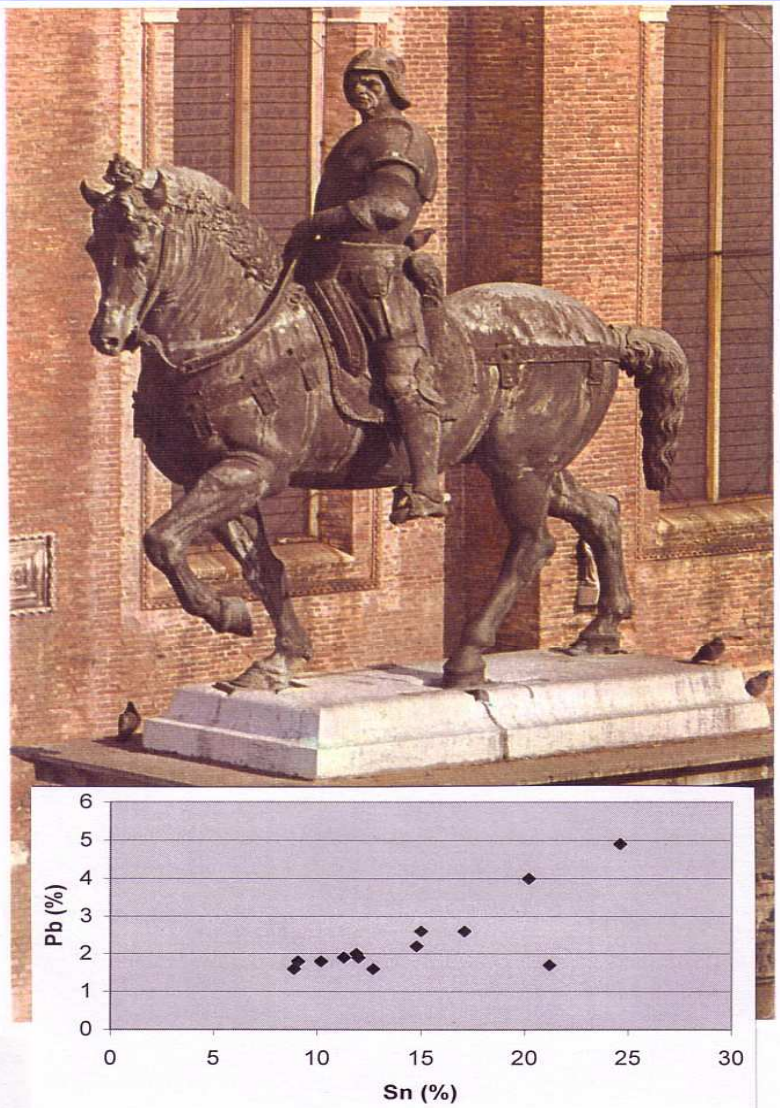

Figure 31 – The huge equestrian statue of Bartolomeo Colleoni by Andrea del Verrocchio (about 1480) , located in Campo SS. Giovanni e Paolo in Venice, and currently under restoration.
A summary of the Sn-Pb correlation obtained in cleaned areas is also shown.

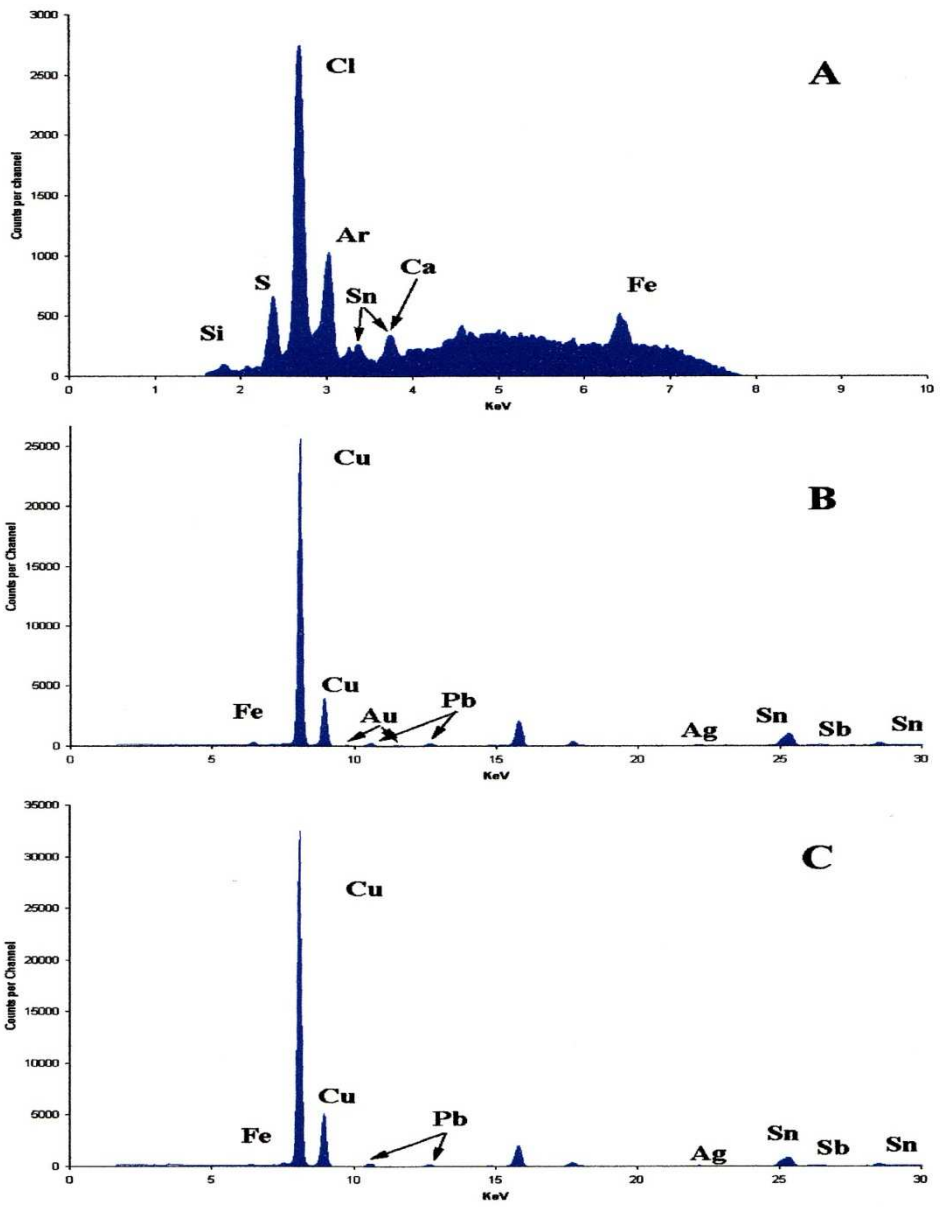
A
Cl
Ar
Ca
S
Sn
Fe
Si
Counts per channel
KeV
B
Cu
Cu
Fe
Au
Pb
Ag
Sn
Sb
Sn
Counts per Channel
KeV
C
Cu
Cu
Fe
Pb
Ag
Sn
Sb
Sn
Counts per Channel
KeV

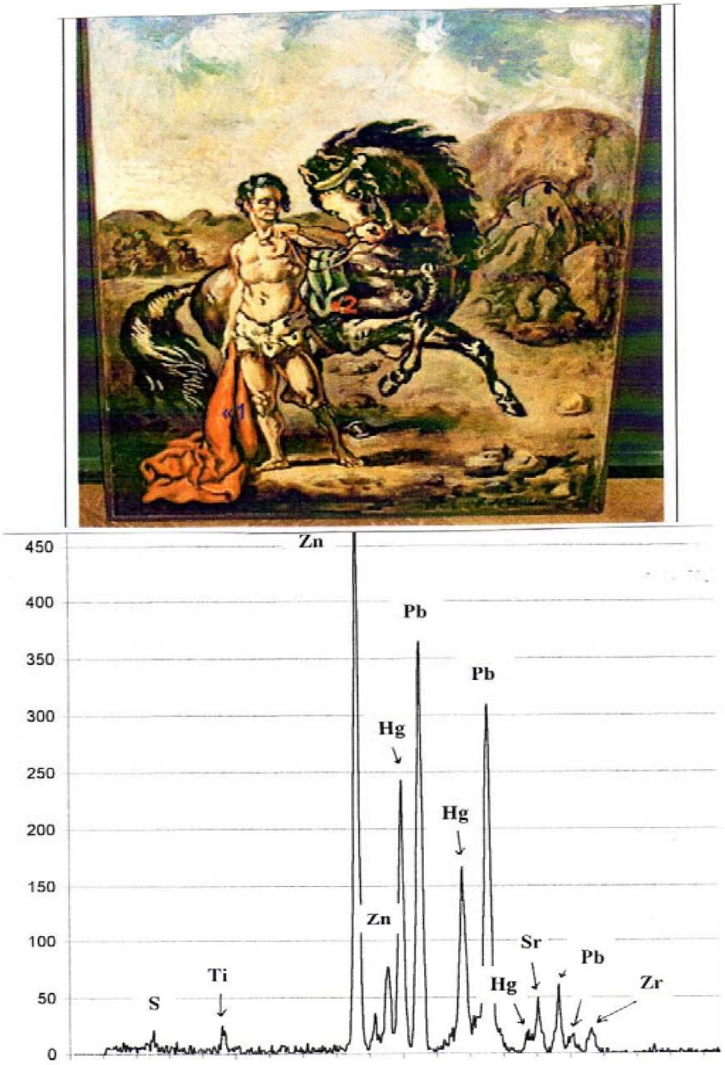

Figure 45 – Young man with horse (Inv. N. 292) by De Chirico, Fondazione De Chirico, piazza di Spagna, Rome, and X-ray fluorescence spectrum of a red area.

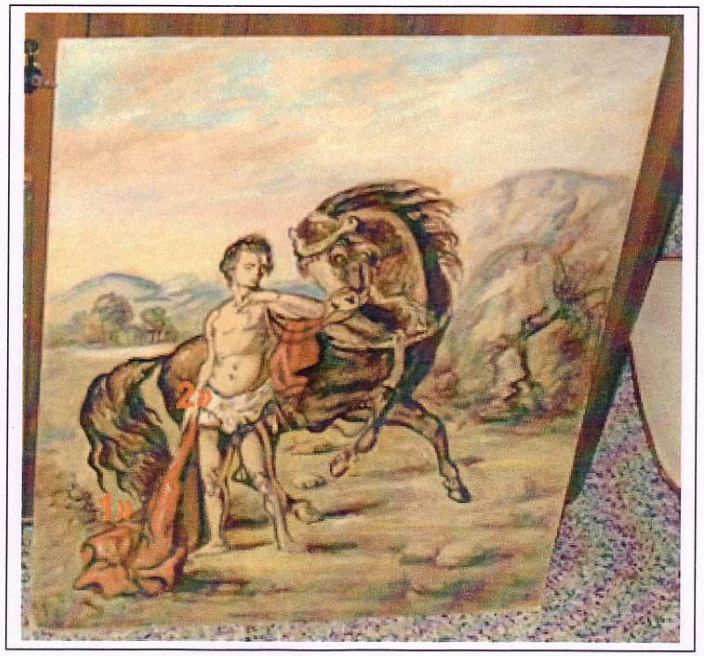
2b
1b

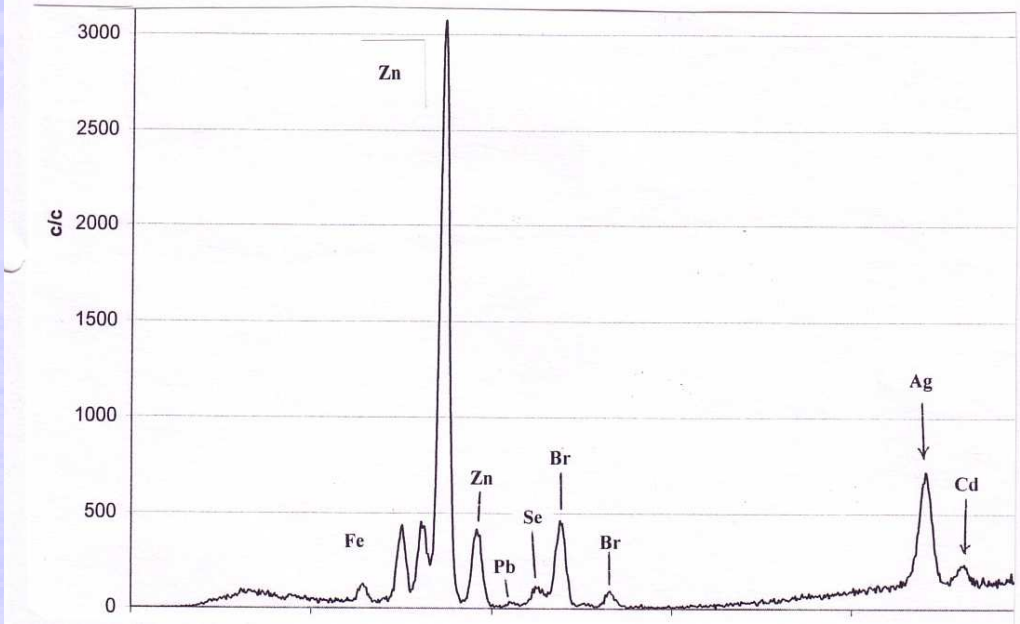
3000
2500
2000
1500
1000
500
0
c/c
Zn
Fe
Zn
Pb
Se
Br
Br
Ag
Cd

ADDITIONAL APPLICATIONS OF X-RAY FLUORESCENCE

TO IDENTIFY:
-NANOPARTICLES IN BIOLOGICAL MATERIALS
-NANOPARTICLES IN FOOD, PHARMACEUTICALS AND ENVIRONMENTAL SAMPLES
-INDUSTRIAL PRODUCTS

THE TECHNIQUE IS:
-NON DESTRUCTIVE
-SIMPLE
-THE RELATED EQUIPMENT IS PORTABLE
-SPECIFIC

X-RAY FLUORESCENCE TO STUDY TRACE ELEMENTS IN SOIL AND CONTAMINATED SOIL

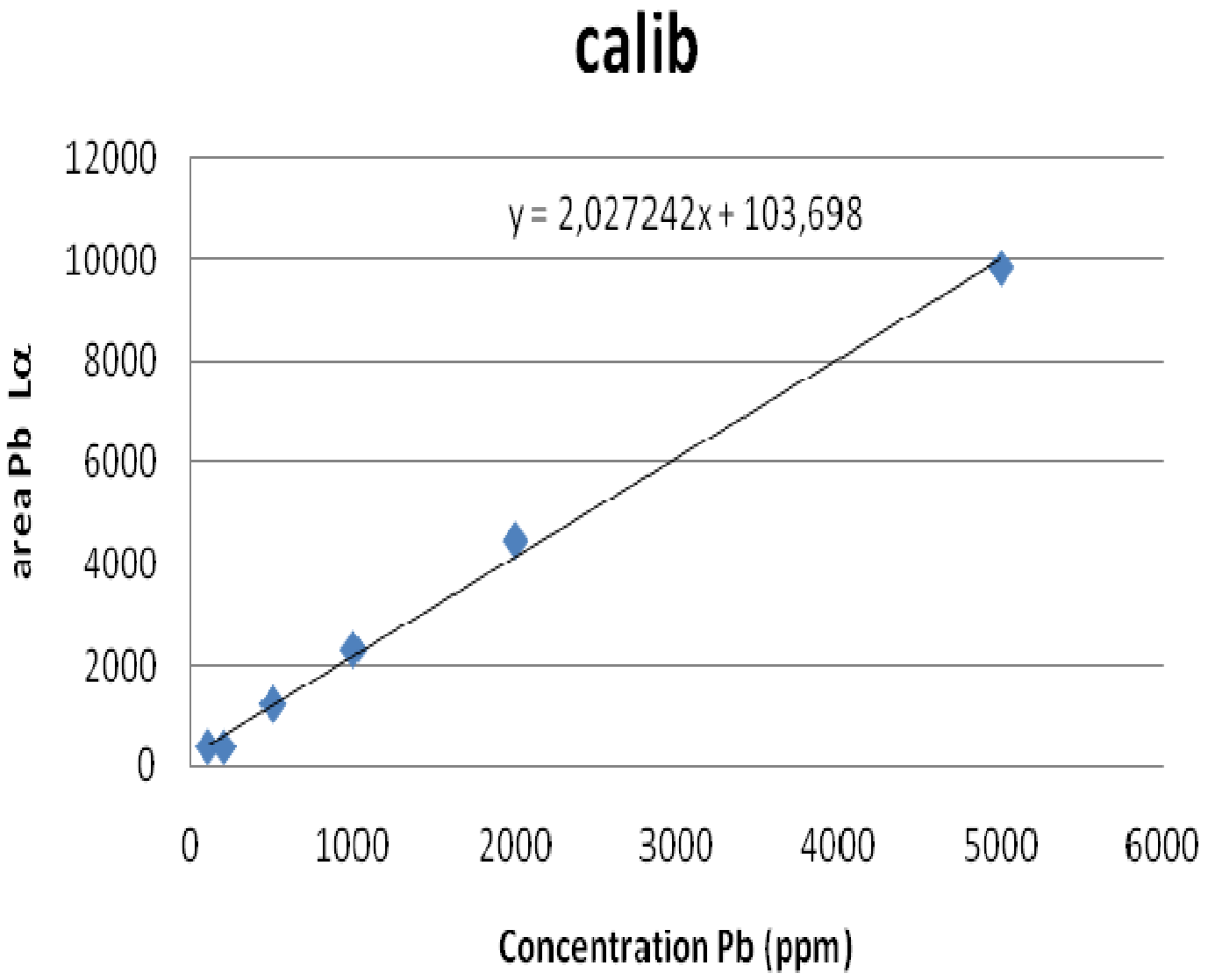
calib
y = 2,027242x + 103,698
area Pb Lα
12000
10000
8000
6000
4000
2000
0
0
1000
2000
3000
4000
5000
6000
Concentration Pb (ppm)

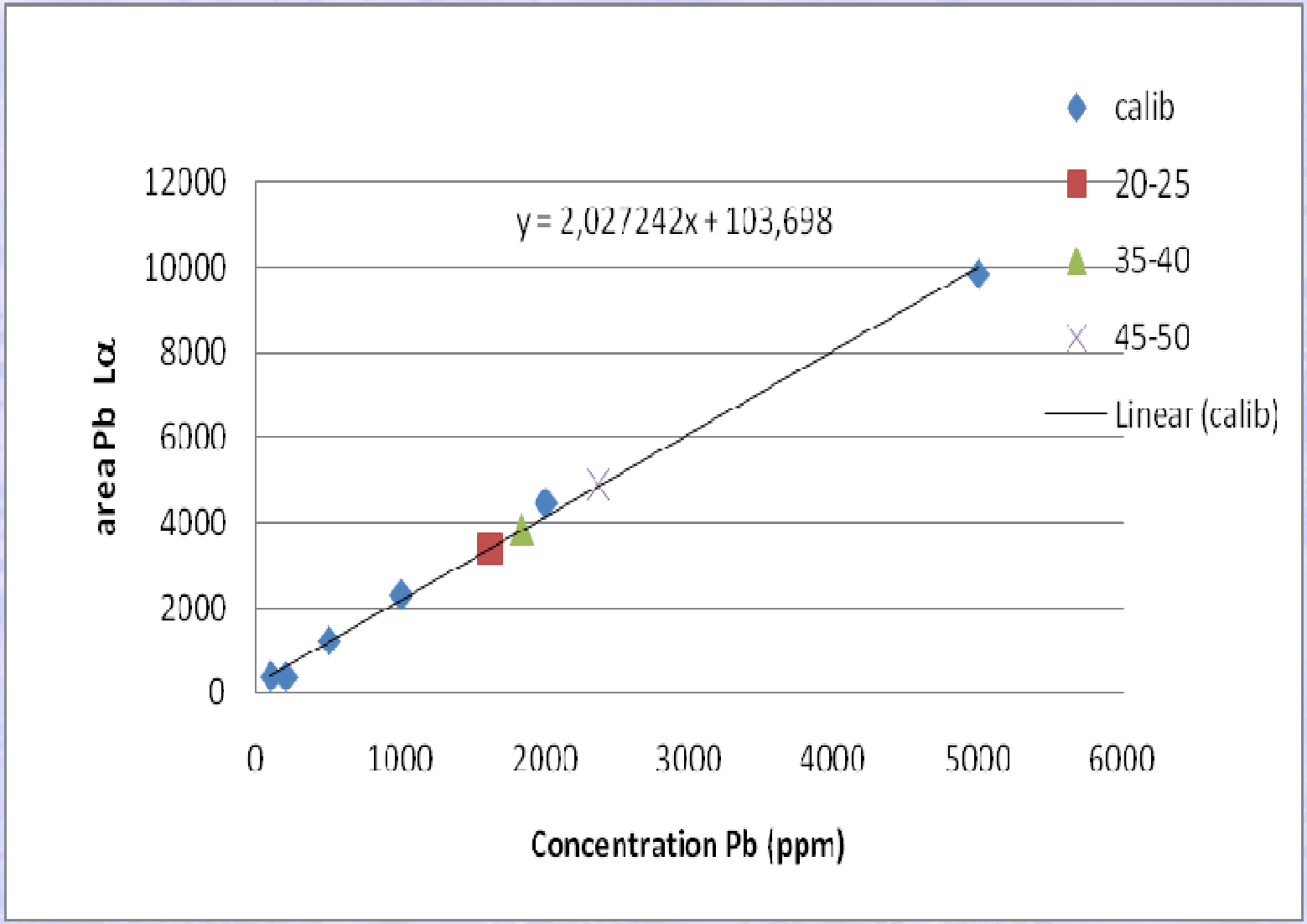
calib
20-25
35-40
45-50
Linear (calib)
y = 2,027242x + 103,698
12000
10000
8000
6000
4000
2000
0
area Pb Lα
0
1000
2000
3000
4000
5000
6000
Concentration Pb (ppm)

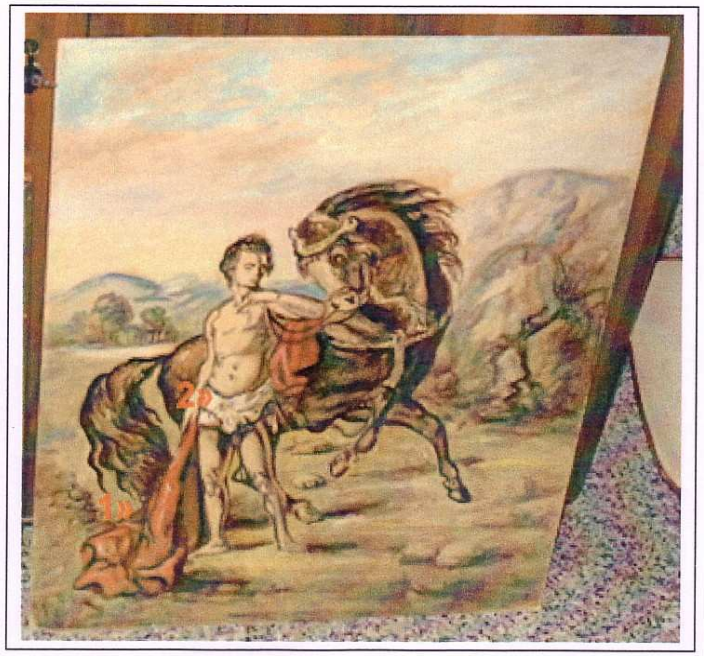
2a
1a

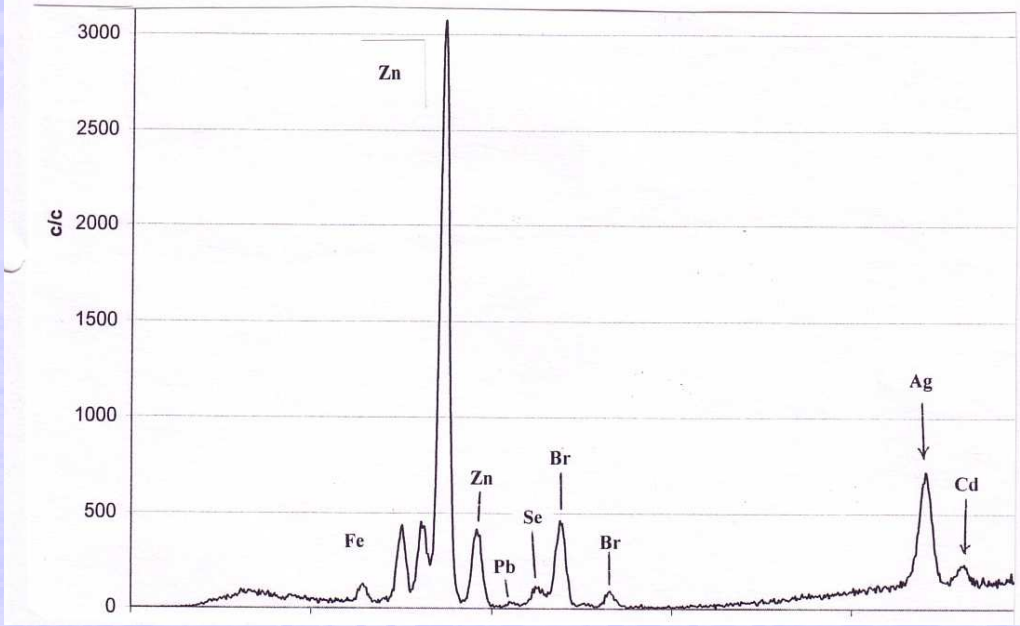
3000
2500
2000
1500
1000
500
0
c/c
Zn
Fe
Zn
Pb
Se
Br
Br
Ag
Cd

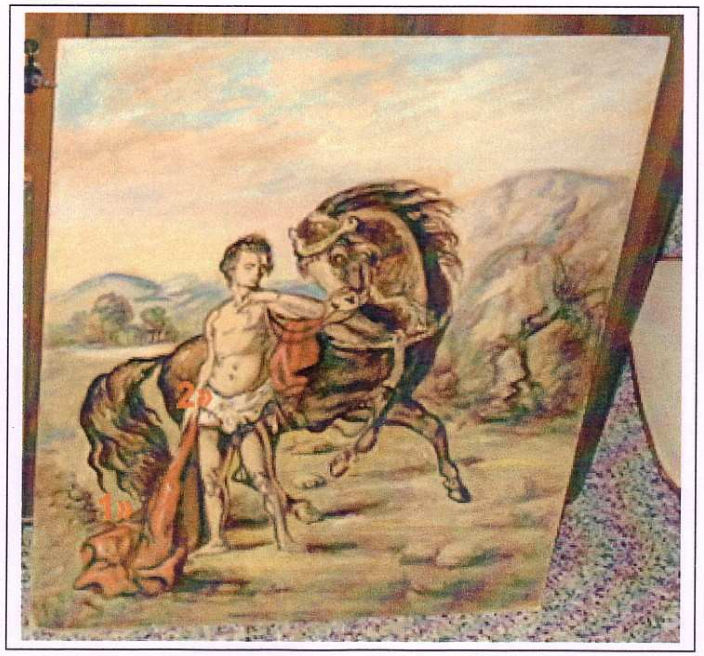
2b
1b

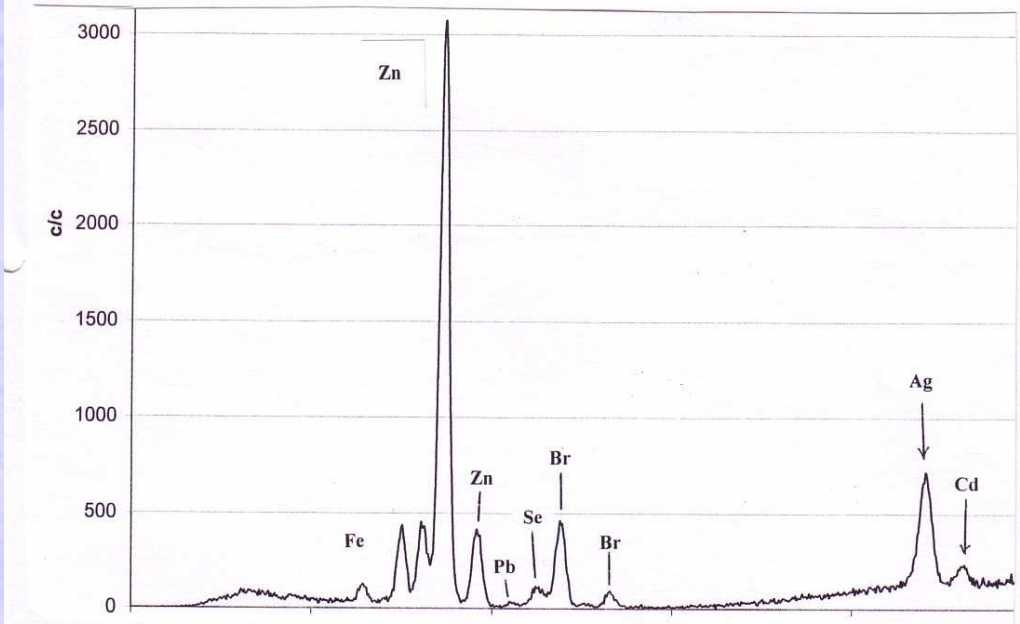
3000
2500
2000
1500
1000
500
0
c/c
Zn
Fe
Zn
Pb
Se
Br
Br
Ag
Cd

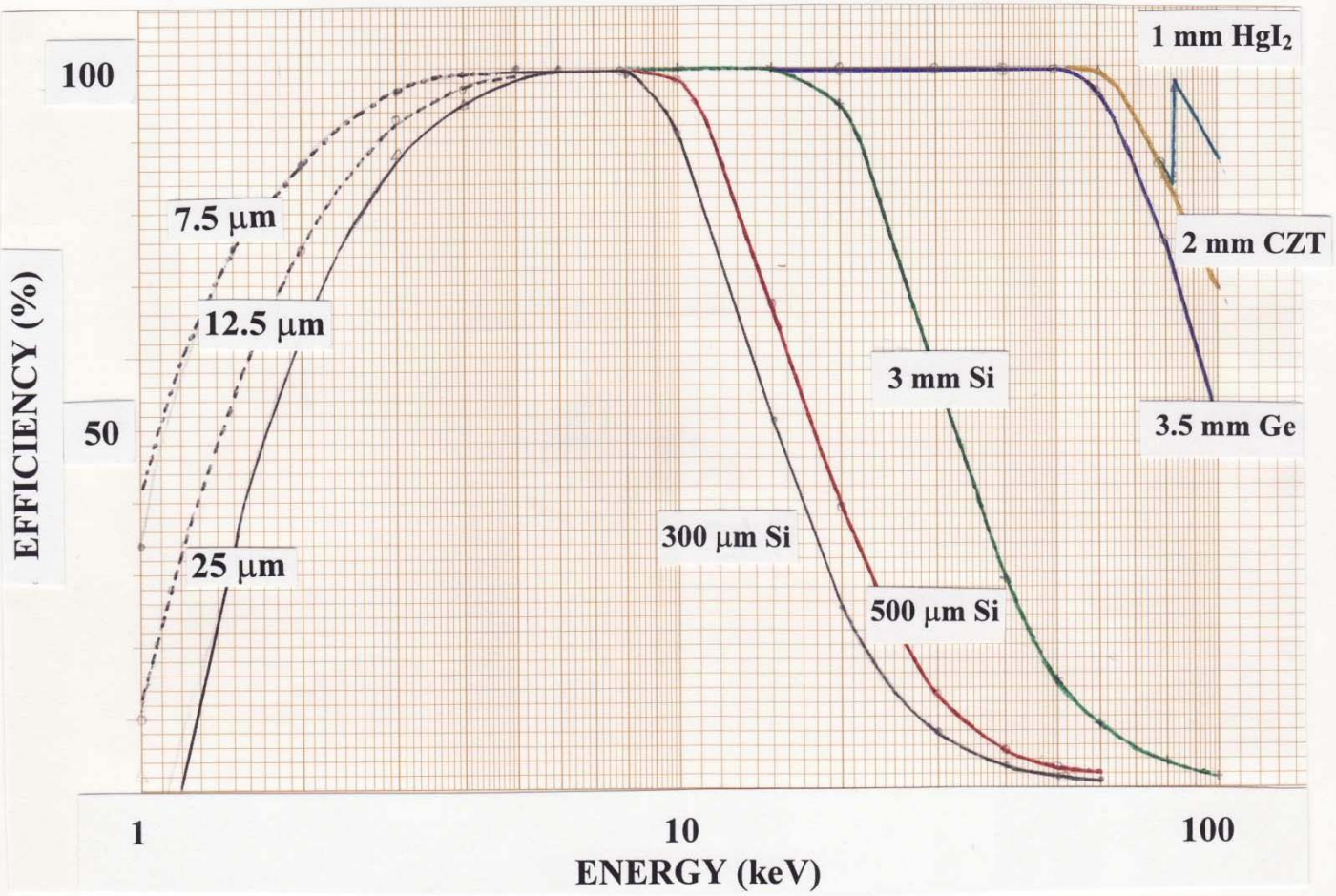

PRINCIPALI RAGGI X

ELEMENTO	Kα	Kβ	Lα	Lβ	Lγ
SODIO	1.04				
MAGNESIO	1.25				
ALLUMINIO	1.49				
SILICIO	1.74				
FOSFORO	2.01				
ZOLFO	2.31				
CLORO	2.62	2.81			
ARGON	2.96	3.2			
POTASSIO	3.31	3.6			
CALCIO	3.69	4.0			
TITANIO	4.51	4.93			
CROMO	5.41	5.95			
MANGANESE	5.90	6.5			
FERRO	6.40	7.06			
COBALTO	6.93	7.65			
NICHEL	7.48	8.26			
RAME	8.05	8.9			
ZINCO	8.64	9.6			
ARSENICO	10.54	11.7			
SELENIO	11.22	12.5			
BROMO	11.92	13.3			
RUBIDIO	13.39	15.0	1.7		
STRONZIO	14.16	15.8	1.8		
ITTRIO	14.96	16.7	1.92		
ZIRCONIO	15.77	17.7	2.04		
NIOBIO	16.61	18.6	2.16		
MOLIBDENO	17.5	19.6	2.3	2.5	
ARGENTO	22.2	24.9	2.98	3.2	
CADMIO	23.2	26.1	3.13	3.45	
STAGNO	25.3	28.5	3.4	3.8	
ANTIMONIO	26.4	29.7	3.6	4.0	
BARIO	32.2	36.4	4.45	5.0	
TUNGSTENO	59.3	67.2	8.4	9.9	
ORO	68.8	78.0	9.7	11.5	
MERCURIO	70.8	80.3	9.95	11.9	
PIOMBO	75	84.9	10.5	12.6	
URANIO	98.4	111.3	13.5	17.5	

VARIAN medical systems | X-RAY PRODUCTS

VF-50J
Industrial X-Ray Tube

APPLICATION

The VF-50 series x-ray tube is a beryllium window x-ray tube designed for use as a radiation source for x-ray fluorescence systems.

CONSTRUCTION

The beryllium x-ray window is located at the end of the tube and the beam is projected along the longitudinal axis of the tube. The cathode operates at ground potential and the envelope is ceramic with the high voltage section potted to increase the high voltage stand off.

Specification

Envelope	Ceramic
Be Window	.003" (.076 mm) Thick
Anode	Copper body with the target material attached
Standard Target Materials	Rhodium, Palladium, Tungsten, Titanium, Moly, Copper, Silver, Chrome
Target Angle	90° from the central ray
Focal Spot	1 mm x 1 mm square
Maximum Anode Dissipation with 10 cfm forced air cooling	50 Watts Titanium - 20 Watts Chrome - 40 Watts
Filament Characteristics	3.3 Amps and 2.5 Volts maximum
Maximum Anode Potential	50 kVp Maximum D.C. (Titanium - 20 kV)
Maximum Tube Current	Refer to Emission and Rating Chart
Cooling Method	Forced air convection
Weight	2 lbs (1.2 kg)

6128 Rev E 01/06 Manufactured by Varian Medical Systems Specifications subject to change without notice.

X-RAY Sources

50kV MAGNUM®
X-ray Tubes

NEW!

The MAGNUM® x-ray tube is now available in a 50kV package. The MAGNUM 50kV x-ray tube is a low power, miniature x-ray tube used for a variety of applications including handheld and benchtop instrumentation. MAGNUM x-ray tubes are small, lightweight, and can be packaged into custom enclosures.

Features	Benefits
Small, compact design	Close coupling of source to detector
Lightweight	Portable, versatile
Close coupling of collimator & target	Efficient utilization of x-rays
Stable output	Low detection limit
Low power consumption	Long battery life
Low spectral contamination	No unwanted peaks
High x-ray output	Short sampling time
Customizable configurations	Flexible form factor

Applications

Portable XRF
- RoHS/WEEE
- Alloy sorting
- Soil analysis
- Environmental
- Lead in paint
- Plastics analysis
- Material ID
- Security

Handheld Imaging
- Medical/Dental
- Material ID
- Security

Bench top EDXRF

Instrument Calibration

Micro-Fluorescence

Micro-Diffraction

Standard Package Includes:
- Transmission Target (End Window)
- MAGNUM tube potted in a brass shield
- High voltage power supply
- High voltage wire length is 11.5 inches

Customizable Options:
- Target materials and thickness
- Tube shield design
- Power supply packaging
- High voltage wiring length
- Integrated tube and power supply

MOXTEK®
452 West 1260 North
Orem, UT 84057
P 801.225.0930
F 801.221.1121
www.moxtek.com

Modern Handheld, Portable XRF Analyzer

Main Features

- ***Ergonomically designed, ideal form factor***
- ***Silicon "p-i-n" detector, < 200 eV***
- ***40 kV, 50 uA transmission anode low power x-ray source***
- *Lightweight*
  - 3 lbs (1.36 kg)
- ***Long, 12+ hours battery use***
- ***Large touch screen LC display***
  - 2.25" x 3" (57 mm x 76 mm)
- ***4096 channels MCA***
- ***optimized for speed ASIC based DSP***
- ***Integrated touch screen***
- ***Integrated bar code scanner***
- ***Integrated wireless communication link***
- ***Fastest FP***
- ***FP not sensitive to shape and surface irregularities***
- ***No transport restrictions***